Patch Migmatites from Västervik, Sweden: Subsolidus or Supersolidus?

Reactions, P-T Conditions and Trace Element Distributions

MSc thesis for Earth Structure and Dynamics, Utrecht University
Stijn Wansink, September 2023 - July 2024
Supervisor: dr. Leo Kriegsman; Second supervisor: Prof. dr. Paul Mason

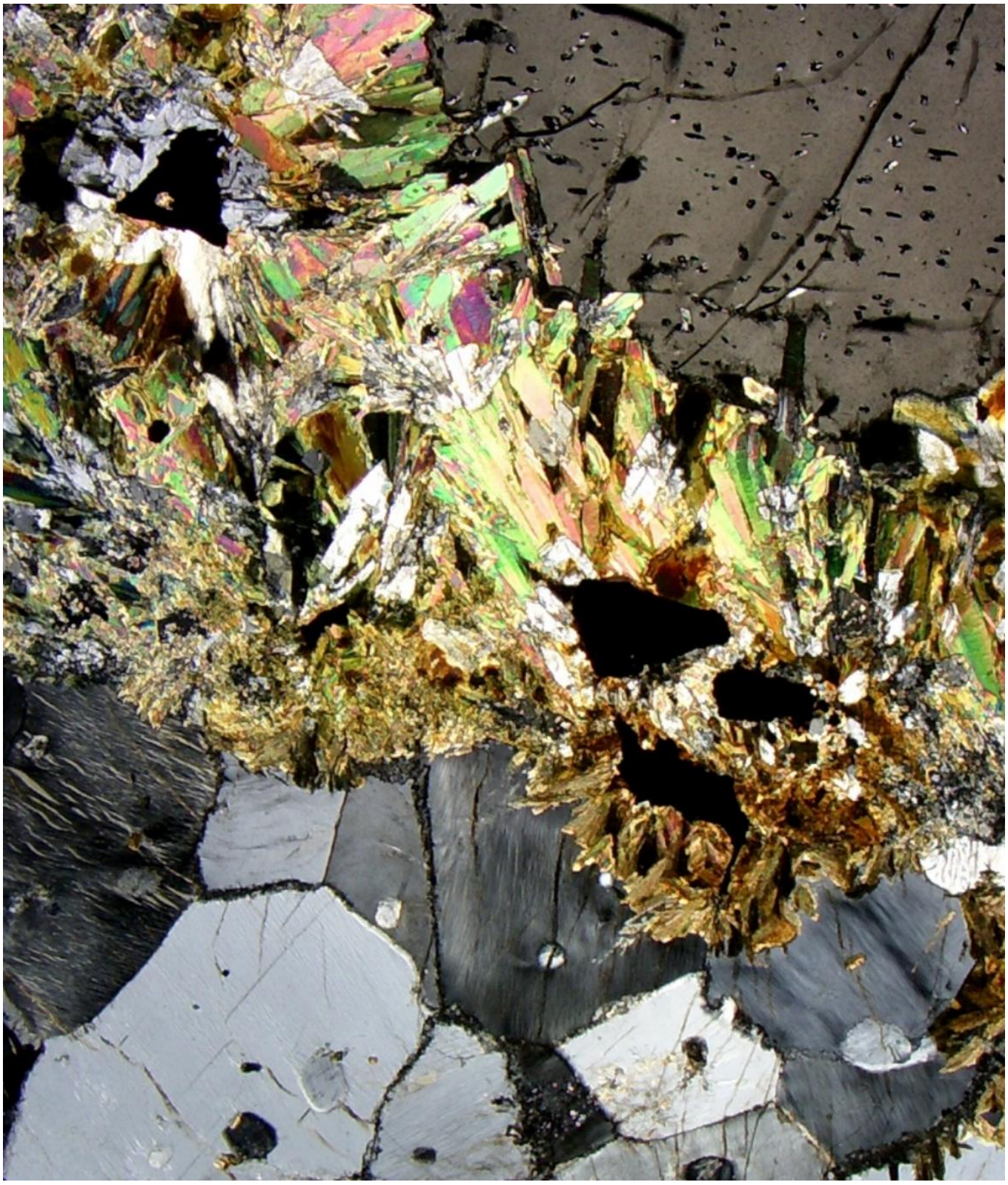

Abstract

The Flecky Gneiss from Västervik, south Sweden, contains a mafic and a felsic mineral segregation, composed of cordierite, biotite, andalusite and sillimanite, and alkali feldspar, plagioclase and quartz, respectively. Despite its similarity to a migmatite, this lithology has always been described as a metamorphic, subsolidus segregation. In this thesis, 38 thin sections of the Flecky Gneiss have been analysed structurally (petrographic microscope) and chemically (Electron Probe Microanalyser) to determine if melting has taken place. These thin sections cover a large part of the Västervik metamorphic region. Major and trace element segregation and zoning were measured for cordierite, alkali feldspar, plagioclase and biotite. Additionally, pressure-temperature conditions were modelled with Perple_X. In multiple thin sections, this investigation resulted in convincing structural indications for melting including phenocrysts, eutectic melt crystallisation and mafic selvedges in the leucosome as well as plagioclase melt remnants in the mesosome. These structural observations vary between thin sections and were not universally observed. Chemical zoning of Ba and Sr indicates a former melt presence during mineral growth and simultaneous growth of the melanosome and the leucosome. This was also observed in thin sections that were structurally less convincing of melt having taken place. Mineralogical assemblages and modelling in Perple_X concluded on two phases of contact metamorphism. Firstly during burial at 200 MPa and 680 - 730 °C and secondly at 300 MPa and 730 °C. These are distinguished by a phase of cooling and cordierite recrystallisation at 300 MPa and 630 °C. This implies a maximum burial depth of 11 km. This concludes that the Västervik Flecky Gneiss locally experienced melt in both heating events and should therefore be regarded as a patchy migmatite. Metamorphic conditions in the Västervik region vary widely on a small spatial scale resulting in a diversity of metamorphic facies offering more opportunities for mineralogical research. Additional research and data collection is yet required to reliably distinguish between other and similar sub- and supersolidus mineral reactions.

Acknowledgements

I would like to thank those who have supported me throughout the completion of this thesis. Firstly I would like to thank dr. Leo Kriegsman for his quick replies and feedback, adequate tips and offering me the opportunity to figure things out myself. The process and development of the thesis was equally insightful as the outcome. I am also grateful to Utrecht University, for providing the facilities and resources, and the tectonics department for welcoming me at the HPT laboratory. Finally, I would like to thank my family, friends and roommates for supporting me and allowing me to bother them with the same topics during the last year.

Cover image: Overview of the core and mantle of one of the flecks in thin section 11506. A cordierite remnant is located in the centre of the fleck core, surrounded by a retrograde reaction rim of andalusite and biotite, which is in turn surrounded by alkali feldspar and plagioclase. Image in cross polarised light. The size of the image is approximately 3.0 by 2.5 cm.

Table of contents

1, Introduction 5
1.1 Sub- Versus Supersolidus Differentiation 6
2, Geological Setting 8
3, Methodology 10
3.1 Structural and Mineralogical Analysis 10
3.2 Chemical Analysis 10
3.3 Data Processing 11
4, Results and Interpretations 12
4.1 Structural and Mineralogical Results 12
4.1.1 Summary 12
4.1.2 Individual Thin Sections 14
4.1.3 Group 1 15
4.2 Chemical Results 18
4.2.1 Bulk Rock Composition 18
4.2.2 Cordierite 20
4.2.3 Green Biotite 21
4.2.4 Feldspars 22
4.2.5 Opaques 24
4.3 Interpretations on Melting 25
4.3.1 Sequential Development in 11507 and 11535 25
4.3.2 Grain Boundaries 25
5, Modelling in Perple_X 27
6, Discussion 29
6.1 Prograde Development 29
6.1.1 Mesosome 29
6.1.2 Melanosome 30
6.1.3 Leucosome 31
6.2 Retrograde Development 31
6.3 Sequential Development and P-T Conditions 32
6.4 Limitations of This Study 33
6.5 Future Research 33
7, Conclusions 34
8, References 35
Appendix A, Images 37
Appendix B, Numerical Data 52

1. Introduction

In the south of Sweden, in the county of Kalmar, the town of Västervik is surrounded by metasedimentary rocks which are located in a region dominated by magmatic lithologies (mostly granites and granitoids). These metasediments consist of meta-arenites, various gneisses and migmatites (Kleinhanns et al., 2015). They occur in various types and stages of deformation and metamorphism, ranging from slightly metamorphosed quartzites with cross bedding, to raft migmatites (Kresten, 1971). Among these metasediments is a rock that has been called a 'Flecky Gneiss' (Swedish: fläckgnejs) which is a grey-pinkish, massive, rock of arkosic composition with a minor foliation (Svenonius, 1907). It contains many, cm-sized, oval-shaped spots called 'flecks'. These are composed of a black core which is surrounded by lighter, pink mantles of variable thickness. The core is mostly composed of cordierite (Crd), green biotite (green Bt), andalusite (And), sillimanite (Sil) and magnetite (Mag). The mantle is mostly composed of alkali feldspar (Afs), plagioclase (Pl) and quartz (Qz). Mineral abbreviations will be used according to Whitney & Evans (2009). The mantle can be of roughly the same surface area (in cross section) as the cores or can be almost absent. Alternatively, the mantles of multiple flecks may be connected together, forming a continuous region of felsic material. The cores are rarely connected. The fleck structures frequently, but not always, lie in a planar orientation, unrelated to the foliation orientation (Fig. 1.1, 1.2) (Loberg, 1963; Russell, 1969).

This compositional zoning therefore results in three distinct domains. The cores will be referred to as melanosome (Mela), the mantles and felsic material will be referred to as leucosome (Leu) and the non-fleck parts of the rock will be referred to as mesosome (Meso). These terms are generally reserved for migmatites and are used with a genetic meaning. For this research, however, it is convenient to use these three terms as they indicate compositional differences, and they are only used in a descriptive manner. Hence, they only refer to the observed compositional domains of the rocks and do not imply any formation processes as that will be concluded on separately in the conclusions.

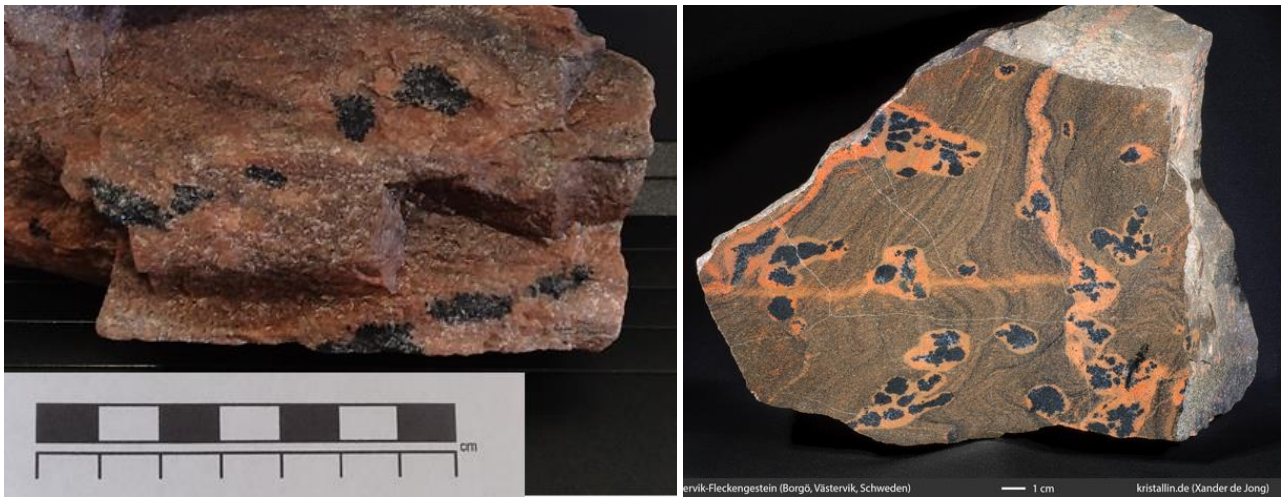

Figure 1.1 (left): Provided hand specimen of the Västervik Flecky Gneiss.
Figure 1.2 (right): Västervik Flecky Gneiss (cut and polished) showing connected leucosomes. This hand specimen is from near location 4 (Fig. 2.1) just like thin section 11507 (Torbohm, 2023).

Since the first detailed descriptions of this lithology, a lot of research has been carried out on the metamorphic history of the Flecky Gneiss and the Västervik region. Because the structure and composition resemble the mafic and felsic separation of a migmatite, many authors have focussed on unravelling which clues may be decisive in discriminating between melt-present and melt-absent metamorphic processes.

Most of them have concluded that the Västervik Flecky Gneiss, as well as similar phenomena, have only been the result of metamorphic processes, such as porphyroblastic growth, rejecting the inclusion with other migmatite rocks (Loberg, 1963; Russell, 1969; Kresten, 1971; Trumbull, 1988).

A renewed investigation will be made into the sub- or supersolidus processes involved with the Västervik Flecky Gneiss. In this research, 38 thin sections of the Västervik Flecky Gneiss will be investigated with various microscopy techniques (optical petrographic, SEM, EPMA) to further specify its metamorphic history and to determine whether the investigated material should be characterised as a (patchy) migmatite or remain as an unmolten metamorphic denomination (gneiss). Additionally, pressure-temperature modelling using Perple_X will be carried out.

1.1 Sub- Versus Supersolidus Differentiation

The formation of cordierite, together with felsic reaction products, may not only be formed by porphyroblastic growth, but can, at higher temperatures, also be produced at supersolidus conditions. A few formulae are derived as potential reactions that enable the formation of the observed mineralogy (Ashworth 1976; Pattison & Tracy, 1991; Kriegsman & Álvarez-Valero, 2010; Waters, 2001)

Subsolidus Crd formation:

And or *Sil + Bt + Qz* → *Afs + Crd + H_2O* (1)

Bt + Ms + Qz → *Afs + Crd + H_2O* (2)

Supersolidus Crd formation:

And or *Sil + Bt + Qz* → *Afs + Crd + Melt* (3)

Melt → *Afs + Pl + Qz* (4)

To be able to distinguish between sub- and supersolidus processes may therefore be dependent on the different textural and chemical characteristics of porphyroblastic segregation and melt crystallisation. Reactions (1), (2) and (3) provide a mechanism for creating the observed domains but imply a different role for water and also involve different chemical mobility for major and trace elements. Because Afs or melt is created simultaneously with Crd, the production and composition of the leucosome is regarded as prograde development despite the subsequent cooling required to crystallise a melt. Otherwise in this thesis, temperature is indicative of prograde or retrograde development. To start interpreting observations, a short list of distinctive melt characteristics must be reviewed. Many textural and chemical observations are rather unique to migmatites as reaction (4) unfolds.

Sawyer (2008) has summarised the current literature on migmatites listing, among many other factors, the following generally present aspects of migmatites.

1) Migmatisation (melting) generally but not always occurs at deviatoric stress (non-lithostatic pressure), resulting in preferred mineral orientations and material segregation along foliations.
2) Grain size generally decreases in the order Leu - Mela - Meso.
3) Grain size increases with metamorphic grade.
4) Melt will generate first at triple point grain boundaries of reactant minerals where melt relicts may still be observed.
5) Melt relicts may be present as intergranular material as films or as glass.
6) Melt crystallisation will form euhedral, felsic phenocrysts, usually Afs or Pl.
7) Leucosome Fsp is more sodic than mesosome Fsp.
8) Remaining melt can form a eutectic composition where it will crystallise after the phenocrysts.
9) Melt droplet inclusions may be present inside of other minerals.

10) During crystallisation, mobile elements partition into the remaining melt while the opposite is true for immobile elements.
11) Migmatite leucosome margins may produces a mafic selvedge at the interface with the mesosome.

As for characteristics indicative of subsolidus segregations, the following is compiled (Trumbull, 1988; Sawyer, 2008).

1) Metamorphic fleck structures don't necessarily follow foliation.
2) Grain size generally decreases in the order Leu - Mela - Meso.
3) Leucosomes may be Qz rich in the core but Fsp rich towards the margins due to successive growth during an increasing metamorphic grade and higher mobility of Fsp.
4) Higher metamorphic conditions will produce leucosome with a higher Fsp fraction.
5) The leucosome structure is equigranular and metamorphic in texture.
6) The segregated domains in subsolidus differentiation, are in chemical balance with the mesosome.
7) Mafic selvedges are the result of less mobile minerals remaining at the leucosome interface, forming a sort of restite.
8) Selvedges have preferred orientations and are partly composed of tabular Pl and Qz.

Numerous characteristics between sub- and supersolidus segregation overlap or are otherwise inconclusive but this sets some guidelines to structure observations and it will be dependent on a combination of these qualifications to determine which metamorphic conditions were present. Additionally, during supersolidus conditions, subsolidus processes will still take place but to negligible effect as the mobility of melt and the speed of those reactions is orders of magnitude more relevant (Sawyer, 2008).

2. Geological Setting

The Västervik metamorphic region lies on the interface of two major geological domains. It lies on the boundary of what is known as the 'Svecofennian Domain' (SD) to the NE and the 'Transscandinavian Igneous Belt' (TIB) to the SW (Fig. 2.1). The SD forms the majority of the Swedish upper crust and is composed of exposed intrusions (mainly granites, granitoids and some mafic intrusions) and some slivers of meta sediments. This was accreted and deformed during 1950 - 1860 Ma (Sundblad et al., 2021). The TIB is a 1000+ km long lithological zone stretching through Sweden and Norway and is almost entirely composed of granites, granitoids and some mafic lithologies that intruded during the 1850 - 1650 Ma timespan (Andersson et al., 2004). The TIB formed during a different tectonic setting and period of magmatism than the SD and is for a large part the result of (back-)arc volcanics during eastward dipping subduction (Stephens & Andersson, 2015). The many intrusions and magmatic accretions around Västervik that formed during the TIB continental cycle are all dated at more than 1500 Ma.

The Västervik region was part of a sedimentary basin, on the margin of the SD which is emphasised by the variety and detail of sedimentological structures such as wave ripples, erosional channels, mud cracks and cross bedding that are preserved in quartzites and the depositional environment was interpreted to be near shore deltaic with a tidal influence with cross bedding indicating a SW flow (Gavelin & Russell, 1967; Sultan & Plink-Björklund, 2006). The depositional area formed a back arc basin and the main period of sedimentation was determined to have been 1882 - 1850 Ma with zircon ages indicating a sediment provenance not quite resembling other granites in the SD and Baltic Shield but rather parts of the Ukrainian Shield (Sultan et al., 2005). The stratigraphic thickness is estimated to be 3000 - 5000 m although the true sedimentological thickness is likely less due to tectonic repetition (Gavelin & Russell, 1967; Russell, 1969).

Sometime after deposition, possibly as part of the converging subduction and related TIB lithologies, the Västervik region was caught up in extension, burial and magmatism which led to nearby intrusions and migmatisation in the timespan 1819 - 1795 Ma although previously the migmatisation phase was estimated to be older at 1830 - 1820 Ma (Beunk & Page, 2001; Kleinhanns et al., 2015). The SD and the TIB are bounded by the Loftahammar-Linköping Deformation Zone (LLDZ). This is a major transpressional shear zone that largely follows the interface between the TIB and the SD (Beunk et al., 1996; Beunk & Page, 2001). The LLDZ was active mostly during 1800 - 1780 Ma with fluids from subduction or dehydrating intrusions being guided along this shear zone (Beunk & Page, 2001). Lithologically, the Västervik metasediments are part of the SD but the LLDZ cuts through the same region which sometimes results in its inclusion within the TIB (Kleinhanns et al., 2015; Stephens & Andersson, 2015).

Peak pressure-temperature conditions have previously been estimated at 350 MPa and 580 °C, 350 - 450 MPa, and 250 MPa (Russell, 1969; van Tuyl, 1977; Rieffe et al. 1993). This geological history led to a unique region of mixed lithologies among which the Flecky Gneiss. The region forms a dominantly East-West trending synclinal orientation but is locally rather undeformed as evidenced by the sedimentary features observed (Russell, 1969). Additional, local intense folding during multiple deformation events is recognised but the thin sections investigated will not be linked to any structural events due to lacking local information of the thin sections investigated (Beunk & Page, 2001).

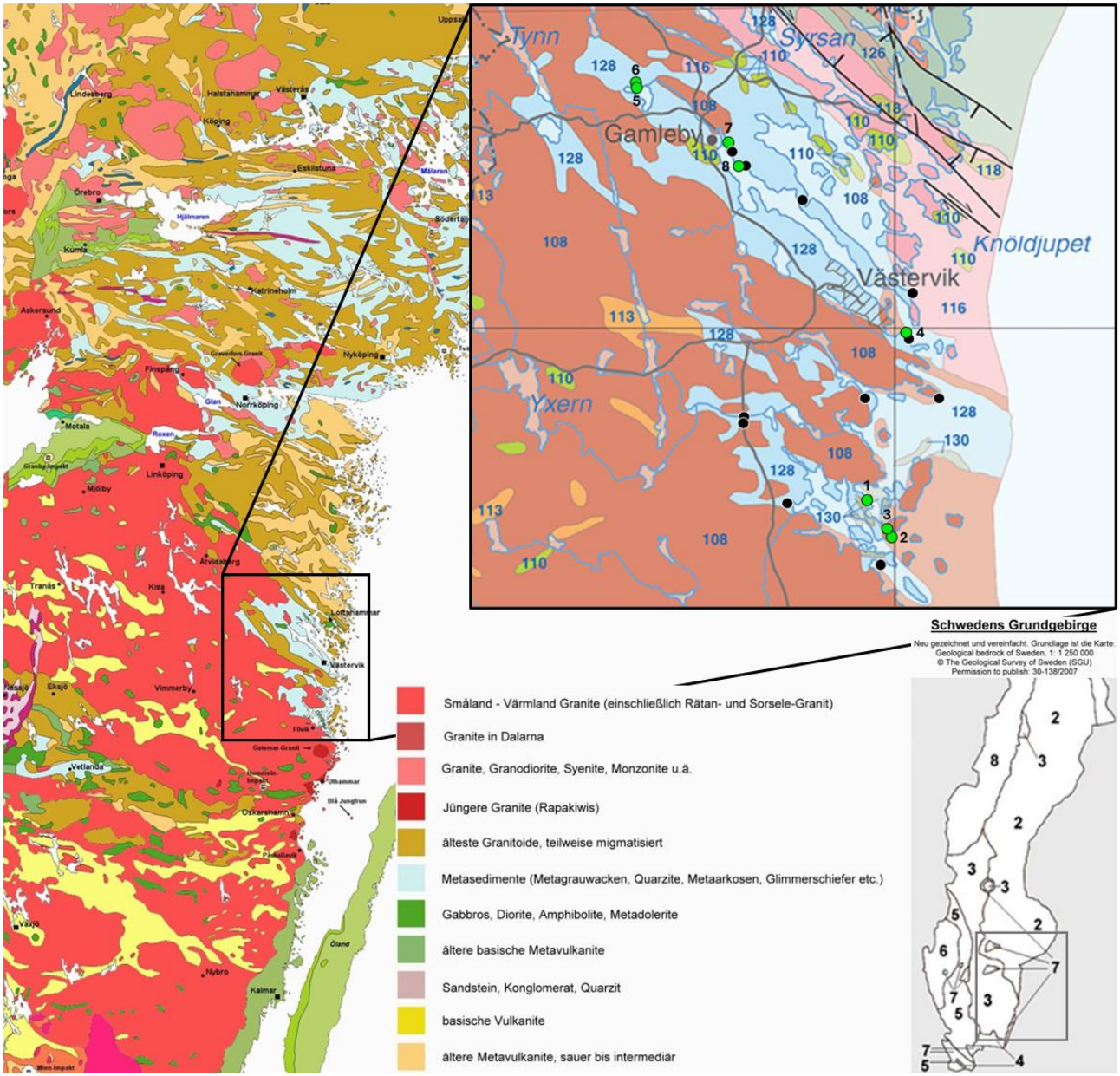

Figure 2.1: Lithological map of SE Sweden indicating the SD in the north (2, mostly brown) and the TIB in the south (3, mostly red). Almost everything coloured brown, red, yellow and green (except blue and regions indicated with 7 in the national map) are magmatic lithologies. Blue is metasediments. The sample map indicates similar colours where blue is metasediments and everything else is of magmatic origin. 1 - 8 (green) are the known thin section locations in this research and the other thin sections are derived from any of the other marked locations (black). Maps after Geological Survey of Sweden (2007) and Torbohm (2023).

3, Methodology

For this thesis, 38 thin sections and one hand specimen from the Västervik metasediments were provided (Fig. A1). They were collected in 2000 as part of a PhD fieldwork by Annika Nyström, supervised by dr. Leo Kriegsman, on migmatisation in Fennoscandia. The 38 thin sections were derived from an unknown amount of sample locations but 20 of them are from 8 known locations (Fig. 2.1). The other 18 thin sections were from any of the other mentioned locations from the fieldwork around Västervik but no specific attention will be paid to regional differences of the thin sections related to the sample locations. The thin sections contained both a serial number (e.g. 11530), as well as a research specific numbering from the research in 2000 (e.g. AIN-00-68b). Because of simplicity and consistency, only the serial numbers will be used in this thesis. All serial numbers higher than 11520 as well as 11498, 11503, 11504 and 11505 are from unknown locations. All data was gathered at Utrecht University, partly at the High Pressure and Temperature Lab.

3.1 Structural and Mineralogical Analysis

To start of the investigation of the 38 thin sections, a general description of the mineral compositions, structures and relationships was made since there is great variety among the thin sections provided. For the structural and mineralogical investigations, a petrographic microscope (Zeiss Primo Star) with cross polarising filters was used. From this, a selection was determined to be representative for the Flecky Gneiss and the reactions investigated as well as coarse grained enough to be analysed. These are described in detail in the results. Some of the otherwise less relevant thin sections are shortly mentioned and are included in the general summary (4.1.1). From this, three thin sections, called group 1, were selected to be chemically analysed (11506, 11507, 11534). A subsequent analysis with three more thin sections, group 2, was not realised. Thin sections 11506 (AIN-00-6), 11507 (AIN-00-27) and 11534 (AIN-00-76) thus form the bulk of the information gathered and they provide all the chemical data for this research. Only three thin sections have been investigated chemically.

3.2 Chemical Analysis

Only 11506 was shortly analysed with a tabletop Scanning Electron Microscope (JEOL JCM-6000). This was done to acquire some initial data in preparation for the following steps. Both chemical data and images were acquired of all the domains in 11506. Varying elements were analysed, depending on the minerals measured. This chemical data was combined with chemical data from subsequent methods. For some minerals or features, this was the only chemical data acquired.

Subsequently, the three group 1 thin sections were analysed with an Electron Probe Microanalyzer (EPMA) (JEOL JXA-8530F). Across the three thin sections, a total of 109, 1 - 10 µm electron spot analyses were made for the following 16 elements: Al, Ba, Ca, Cl, F, Fe, K, Mg, Mn, Na, P, S, Si, Sr, Ti and Zr. These spots were used for the following minerals: Afs, Bt, Chl, Crd, Ms, Opq (Hem, Mag, Ilm) and Pl. And, Sil and Qz were not investigated as they were regarded to be less chemically versatile and not analytically interesting. The spots were roughly equally spread out over the thin sections and the respective domains. Additionally, some manual spot traces (4 or 5 spots) were made across larger minerals of Afs, Crd and Bt.

With the EPMA, chemical maps of a selection of regions were made. This was done for the elements Al, Ba, Ca, Fe, K, Mg, Mn, Na, P, Si and Ti. The locations for the maps chosen were mostly the interfaces of the domains. This should give insight into potential chemical interactions or differences between the three domains as well as within the domains themselves. The chemical maps were of varying sizes and resolutions. The colour scaling of the EPMA maps is a gradient in the order of increasing chemical abundance: black, blue, green, red, pink, white. This colour scheme has no absolute value and is modified for every map individually.

3.3 Data Processing

All chemical data was processed via Microsoft Excel. For most analyses, weight percent (wt.%) is used to compare similar minerals in the domains or thin sections but also molar percent (mol%) is used to specify zoning or chemical exchange. The three thin sections are handled completely separately when dealing with bulk rock compositions but for individual mineral populations, the measurements are generally grouped. Specification on differences between the thin sections is given where required. Volume percentages (vol.%) of the thin section were determined with point counting on petrographic microscope images. This was subsequently normalised to wt.% per domain. The amount of water present in the minerals was only calculated from the EPMA data for Bt, Chl and Crd during cation calculation. Therefore, the water content of the thin sections is entirely derived from their measurements.

4, Results and Interpretations

4.1 Structural and Mineralogical Results

The 38 thin sections show considerable variation in their mineralogy and structure, but multiple thin sections are very similar, leading to the recognition of recurring assemblages. A common trend is the varying stages of retrogression and recrystallization which is apparent in all three domains. Some thin sections are too fine grained, recrystallised or weathered to interpret meaningful mineral relationships so not all will be discussed in detail equally. The following comprises a summary all thin sections and an overview of the thin sections and observations that were regarded as especially relevant.

4.1.1 Summary

Mesosome

The Mesosome is relatively similar throughout all thin sections. On average, it consists roughly of equal parts Afs, Bt, Pl, and Qz, but the Bt fraction varies significantly. Bt always has a preferred mineral orientation but to varying extent and sometimes it forms more dominant foliation. Fsp grains frequently contain multiple tiny Qz inclusions but in those thin sections, the same is true in the leucosome. Some thin sections have relatively interlocking grains but others have more anhedral minerals. Multiple thin sections also contain significant abundances of Ms or Sil. Sil occurs both as single, euhedral grains and as fibrolite clusters which can be found both on grain boundaries as well as inside of other minerals. In multiple thin sections, similar intergranular material was found in the mesosome as in the leucosome. Few thin sections have a mesosome which consists mostly of Qz where Fsp is only present as tiny, rounded or cuspate grains which mostly occur on Qz grain boundaries (Fig. A2). Some thin sections have a mesosome consisting only of Qz, Opq and Ser and coarse Ms (Fig. A3). However, the structure and geometry of their Qz grains still resemble other mesosomes so presumably Fsp and Bt are completely reacted during metamorphism or fluid reactions. Ser is a prevalent mineral in many thin sections and is interpreted as a locally retrograde constituent.

Melanosome

The melanosome is by definition composed of more mafic minerals (Crd, Bt, Opq). A few different recurring geometries and assemblages are recognised, leading to the distinction of four types of melanosome.

1) Type 1 melanosome consists of Crd grains or recrystallised pseudomorphs of Crd. This occurs in two shapes, massive or round Crd crystals filled with tiny Opq grains or large Crd poikiloblasts with sometimes large (10 - 1000 μm) Qz inclusions. These Crd occur in varying states of recrystallisation, both for the massive and poikiloblastic grains (Fig. A4). Their similar structure however, indicates the retrogressive reactions and a common formation history. The varying retrogression defines the sub types a, b and c.
    a) Crd is entirely intact and does not show signs of recrystallisation. Crd is in direct contact with the leucosome. Some thin sections are also observed with And as part of the poikiloblast or have And in parts of the leucosome. No clear correlation or interpretation could be made for the differences between the poikiloblasts and the massive Crd grains.
    b) Crd pseudomorphs that are partially or wholly recrystallised into And + Bt sometimes with some chlorite. The grain size varies widely. And and Bt are intergrown and frequently radiate away from Qz or Opq grains. Sometimes And + Bt forms a rim around some intact Crd but usually the entirety of Crd is recrystallised. Bt is intergrown with Qz and is usually rather green coloured. The former poikiloblast structure of Crd is usually strongly recognisable relative to melanosome1a. No dominant mineral orientation appears to be present among the And + Bt but this was not quantified. Sil is also commonly present in melanosome1b but usually in combination with And.

c) Crd pseudomorphs that are completely recrystallised into extremely small Ser or green Bt sometimes with coarser Ms. Crd pseudomorphs indicate the common origin as former Crd but almost no structural information can be derived from the mineralogy. Ser is frequently present in all domains. Sometimes Ms can form large, euhedral minerals.

2) Type 2 melanosome consists of intergrown Bt + Sil but without any rounded fleck shapes (Fig. A5). This usually forms tabular or massive aggregates. Melanosome2 can be located between the mesosome and the leucosome and can form rather voluminous formations. There is a strong preferred mineral orientation among both Bt and Sil. Melanosome2 mostly contains browner Bt relative to melanosome1b.

Leucosome

The leucosomes consist for the majority of Afs and Pl with some Qz. Afs ranges from 50 % to 90 % and Qz and Pl can account for fractions of up to tens of percent. Some less clear fleck thin sections have a majority Qz leucosome composition. Additionally, Opq is usually minorly present in the leucosome as well as occasionally some Bt. Two types of leucosome are recognised based on structural observations, mostly the grain size distribution and composition.

1) Type 1 leucosome is mainly composed of coarse (>1000 µm) grains with an unequal grain size distribution. The majority of the largest grains are Afs with sometimes large Pl or Qz grains. The grain size is rather similar between these large grains but apart from them, many smaller grain clusters are present (Fig. A6). Most grains have some intergranular material which is composed of Pl or Qz but locally, the large grains are interlocking. Qz usually has lobate grain boundaries, mostly expressing the lobate side whereas Afs or Pl are frequently more cuspate in shape. This is also observed between two Qz grains. Afs almost always has albite exsolution and in many, coarser leucosome, microcline twinning. The margins of the leucosome are sometimes more abundant in Afs but other times more abundant in Qz. Large Afs grains are sometimes poikiloblastic in texture. Occasionally some Bt or some Opq is present in leucosome1 but this differs per thin section.
2) Type 2 leucosome is composed of equigranular and mostly interlocking Afs with some Pl and Qz. The grain size is much smaller than type 1 at around 100 - 500 µm (Fig. A7). Afs forms the great majority, around 50 - 90 %, with the remaining part composed of Pl and Qz. The Qz abundance highly varies and is in a few thin sections observed up to 50 %. Qz also forms as inclusions in Afs or Pl. Intergranular material is rarely similar to leucosome1 but in multiple thin sections, the grain boundaries are abundant in microcrystalline Qz + Sil needles (±10 µm). The same intergranular material in leucosome2 is present in the mesosome in these thin sections.

During this thesis, in the context of the migmatite hypothesis, the large Fsp grains were referred to as 'phenocrysts' and the smaller Fsp grains were referred to as 'eutectic' grains. However, these are only used as pragmatic and descriptive terminology and don't have any migmatitic or metamorphic meaning until the conclusions and this will be used only to specify this crystallographic difference.

Accessory minerals

Accessory minerals among the thin sections include chlorite (Chl), ilmenite (Ilm), monazite (Mnz), muscovite (Ms), Rutile (Rt), sillimanite (frequently as fibrolite) (Sil) and tourmaline (Tur). These were not all observed simultaneously. Chlorite is observed in a few thin sections as part of melanosome1b. Ilm is measured once in the leucosome but its abundance among Opq is otherwise unknown. Mnz is frequently observed as tiny grains (usually ±10 µm) associated with Bt and is more common in melanosome2 and leucosome1 i.e. higher grade assemblages. In multiple thin sections Ms formed a significant percentage of the mineralogy.

It is common in some mesosomes and in some melanosomes. In most thin sections, Ms was minorly present but in varying abundances. Rt is only observed in two or three thin sections and only as tiny, singular grains. Sil is in the melanosome more often than not a significant constituent but is also very common in other domains as few grains or bundles of fibrolite. Tur is only observed with And and only in three thin sections (11515, 11516, 11517) and without any clear fleck structures.

4.1.2 Individual Thin Sections

11504, 11505, 11506 These thin sections have almost identical leucosome2. 11506 will be described in much detail later. The leucosome is very equigranular, consisting almost entirely of Afs with a very minor part Pl and almost no Qz. The grains are entirely interlocking apart from some microcrystalline Qz + Sil which is also observed in the mesosome. Towards the flecks the grain size reduces and the Pl fraction increases somewhat. These thin sections have clearly defined fleck cores and are all type 1b. 11504 and 11505 contain poikiloblast pseudomorphs but 11506 contains massive Crd remnants in the core. The melanosome of 11506 also contains a few clusters of large Sil grains as well as some tiny Sil grains in Fsp in the mesosome. This is interpreted as retrograde recrystallisation close to Sil stability conditions. 11506 is from sample location 2.

11502, 11529, 11533 These thin sections don't have clear fleck structures but they have clusters of only Sil and clusters of Bt + Sil and have a strongly layered structure. There is no clear melanosome. Some parts of leucosome are rather distinct, which is coarse, located between the layers of Bt + Sil with some intergranular material. Some parts in 11502 consist of Sil surrounded by only Qz. Ser is common at grain boundaries. One part in 11529 strongly resembles a migmatite (Fig. A8). 11502 is from sample location 3.

11509, 11511 These thin sections contain a melanosome1b core in 11509 and a melanosome1a, intact Crd poikiloblastic core in 11511. Parts of the poikiloblasts are composed of And, indicating a prograde formation in Crd-And stability conditions. The leucosome2 consists of very equigranular Afs with minor Pl and Qz and much intergranular Pl or Qz (Fig. A9). Every third grain boundary has intergranular material. The leucosome is only slightly coarser than the mesosome. All Afs and Pl grains have Qz inclusions but this is also the case in the mesosome. Few fibrolite clusters are present among other minerals. 11511 is from sample location 7.

11512, 11514, 11515, 11516, 11517 These thin sections don't contain clear fleck shapes and the darker, more mafic parts only consist of Bt + Ms and And poikiloblasts with locally some Tur. And is present in all domains of this thin section and the apparent leucosome domains consist of only And surrounded by Ser or equigranular, interlocking Pl + Qz grains which are equally fine grained as the mesosome. These four do not resemble other thin sections. They are all from sample location 7.

11527, 11528, 11530, 11531 These thin sections all contain massive Crd grains, sometimes with a poikiloblastic centre as well as a homogeneous margin. One Crd grain is observed with sector zoning. The leucosome1 is very coarse grained with large Afs and Pl phenocrysts (Fig. A10) as well as intergranular material and clusters of eutectics (Fig. A11). The leucosome in these thin sections strongly resembles a migmatite. The leucosome also contains some Bt and Ms is more abundant than in other thin sections, mostly at the margins of the leucosome. The Pl content is much higher than in other leucosomes. The mesosome Fsp contains similar exsolution and twinning as the leucosome but have a three times smaller grain size. Additionally, the leucosome1 of 11527 contains a thin margin of Bt between the leucosome and mesosome which resembles a migmatite selvedge (Fig. A12).

11534, 11535, 11536 These thin sections are very similar and they stand out as they all contain both melanosome1b as well as melanosome2, leucosome1 and no recognisable portion of mesosome. 11534 and 11535 will be described in more detail later. The melanosome1b domains are characterized by green Bt and melanosome2 is characterized by the lack of fleck shapes and brown Bt + Sil. In 11535 melanosome1b transitions into melanosome2, suggesting a similar origin (Fig. A13). Sil is prominently present in melanosome2 and sometimes but not consistently in melanosome1b.

Sil is more abundant in 11535 and 11536. In 11535, Bt with varying Qz intergrowth patterns is observed (Fig. A14). In 11535, the leucosome is mostly type leucosome1 but local differences in the leucosome are apparent and there is a coarsening towards the centre of the leucosome. This leucosome change is rather distinct and the grain size increases from ±500 µm to >2000 µm (Fig. A15). Mostly the grain size and abundance of Qz vary. All parts of the leucosome have some intergranular material albeit rather narrow. The grain size reduces towards melanosome2. Two Afs grains in the coarsest part of the leucosome in 11535 show Carlsbad twinning. Some clusters of fibrolite are recrystallised into And. 11507 is similar to these thin sections but will be discussed in much detail later.

4.1.3 Group 1

With a general analysis completed, a selection of three thin sections was made for further chemical analysis which was named group 1: 11506, 11507 and 11534 (Fig. 4.1). Group 1 was selected based on their coarse mineralogy, clear separation of domains (except no mesosome in 11534), different types of melanosome, varying states of Crd recrystallisation and different types of leucosome (Table 4.1). Crd is assumed to be relevant in the fleck formations so varying states of retrogression played a role in the selection. Images of the domains of the group 1 thin sections are provided (Fig. A16 - A25). This section will describe the minerals and structures in group 1 in great detail.

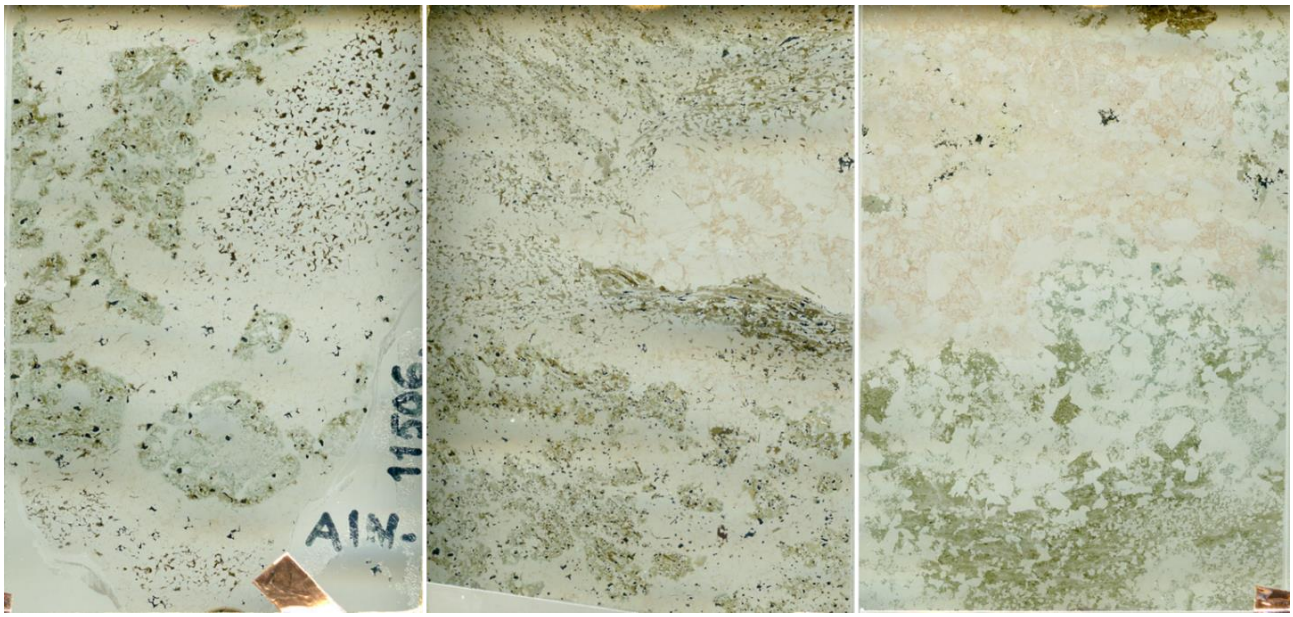

Figure 4.1: Group 1 thin sections. From left to right: 11506, 11507, 11534. Picture taken by non-polarised light before going into the EPMA. The thin sections have dimensions of 25 by 45 mm.

Thin section	State of Crd retrogression (estimate)	Melanosome type	Leucosome type
11506	60 %	1b	2
11507	90 %	1b & 2	1 & 2
11534	100 %	1b & 2	1

Table 4.1: Overview of the characteristic melanosome and leucosome types of the group 1 thin sections.

A photographic surface area measurement and point count analysis was made to determine the proportions of the domains (Table 4.2) and their mineral abundances (Table 4.3). This resulted in rather different values for the domains of the three thin sections but this is partially what they were selected for. A reliable Mela/Leu ratio is difficult to establish as the leucosome is of inconsistent thickness or distribution with regards to the melanosome as specified in the introduction (Fig. 1.2).

vol.% domains	Mesosome	Density	Melanosome	Density	Leucosome	Density
11506	25.74 %	2.79 g/cm^3	31.87 %	3.05 g/cm^3	42.39 %	2.63 g/cm^3
11507	8.41 %	2.79 g/cm^3	56.37 %	3.04 g/cm^3	35.22 %	2.64 g/cm^3
11534	0	-	58.22 %	3.02 g/cm^3	41.78 %	2.63 g/cm^3

Table 4.2: Volumetric distribution and approximated densities of mesosome, melanosome and leucosome in the three analysed thin sections.

Minerals per domain (wt.%)		Qz	Pl	Bt	And or Sil	Opq	Crd	Afs
11506	**Mesosome**	23.72 %	28.79 %	22.13 %	2.82 %	3.98 %		18.55 %
11507	**Mesosome**	3.04 %		37.96 %	11.87 %	14.58 %	32.56 %	
11506	**Melanosome**	9.08 %	14.79 %			1.69 %		74.44 %
11507	**Melanosome**	10.46 %	37.51 %	22.73 %	1.13 %	3.99 %		24.17 %
11534	**Melanosome**	15.26 %		27.96 %	33.17 %	8.79 %	14.82 %	
11506	**Leucosome**	28.56 %	20.78 %			1.68 %		48.98 %
11507	**Leucosome**	19.33 %		42.01 %	38.65 %			
11534	**Leucosome**	33.78 %	20.39 %					45.83 %

Table 4.3 : Mineral abundance of all domains of the group 1 thin sections.

11506

11506 has the best domain demarcations, some of the most euhedral minerals and some of the most homogeneous Crd out of all thin sections. Overall it is the most comprehensive and non-weathered thin section. More importantly, the flecks have clear cores and rims which contain some intact as well as recrystallised Crd. This thin section and a few like it, indicate the recrystallisation of Crd. The interface between the mesosome and the leucosome is very sharp. The mesosome consists of Afs, Pl, Qz, Bt, Opq and some Sil. The fraction Afs/Pl was estimated to be 40/60 vol.%. Afs, Pl and Qz and are mostly interlocking. Albite twinning is common in Pl and microcline twinning is sometimes present in Afs.

Bt grains are relatively elongated and express a preferred orientation but are otherwise spaced apart and don't create any recognisable foliation. They are subhedral and have rounded and thin edges and appear to be affected by metamorphic processes. They also appear to be partially replaced by Qz or Fsp. Bt slivers are frequently present as intergranular material, forming a single slender brown grain or tiny rounded grains. Sil occurs both as larger, euhedral minerals and as tiny fibrolite clusters, present among all other minerals and domains. Fibrolite orientations appear to be random but this is unspecified. The grain boundaries, most recognisable between Fsp or Qz grains, are mainly filled with microcrystalline Qz + Sil needles or thin Bt. Bt and Sil form the least euhedral minerals in the mesosome.

The melanosome type 1b consists of very round fleck cores composed of a single Crd grain in the centre with a margin composed of And + Bt. The melanosome contains round Qz and Opq grains as well as a few clusters of rather coarse Sil. This And + Bt intergrowth sometimes radiates away from Qz or Opq grains which is interpreted to be growth directions. Since these round Qz and Opq grains are also present within the intact Crd, they are interpreted to be part of the prograde mineralisation. Bt is generally very green but located towards Opq grains, it is much browner. Additionally, Bt grains themselves are usually intergrown with Qz. The interface of the melanosome and the leucosome is characterized by a haze of microcrystalline Qz + Sil needles as well as an increase of And towards the melanosome-leucosome interface. The grain size reduces somewhat towards the leucosome interface.

The leucosome type 2 consists for the great majority of Afs. The Afs is equigranular, interlocking and generally shows narrow perthite exsolution and rarely microcline twinning. Albite twinning in Pl is rare. The Pl abundance was not precisely determined but was estimated at 15 vol.% of all Fsp. Qz is present as smaller grains as well as inclusions in Afs or Pl. The grain boundaries are almost all populated by microcrystalline Qz + Sil needles. Rare fibrolite grains are also present among other, much coarser minerals. Additionally, myrmekite patterns are observed in Pl. Occasionally, some Opq minerals are present.

11507

11507 has less distinct but greater variation of domains as well as some mesosome. The flecks and cores are poorly defined but there is some melanosome1b present although much smaller than in 11506. Even some Crd remnants seem to be present but this was in fact Chl. Additionally, there is a significant section of melanosome2. Both types of leucosome are present. Leucosome1 as a coarse, pink section in the centre and a finer leucosome2 that forms some spaced foliation with melanosome1b.

The mesosome consists of almost the same components and abundances as 11506 but the structures are somewhat different. Afs and Pl are much more abundant at the expense of Qz. Additionally, the grain size of Afs, Pl and Qz is around two times smaller compared to 11506. Afs, Pl, Qz and Bt are all anhedral. Afs usually shows microcline twinning or perthite exsolution. Albite twinning in Pl is rare. Bt is about the same as in 11506 where many appear to be partly cut off, intruded or otherwise replaced by Afs, Pl or Qz. They also form some foliation which is folded within the mesosome domain. Bundles of fibrolite are incorporated among other minerals. Grain boundaries are commonly occupied with Pl or Qz.

The melanosome is composed of multiple assemblages in this thin section (Fig. 4.1). There is a clear patch of melanosome2, Bt + Sil, located next to leucosome1, as well as melanosome1b located throughout the rest of the thin section (outside of the mesosome) that alternates between melanosome1b and leucosome2. Melanosome2 is more prominently present but in a single section. Melanosome1b is more linear and arguably more heterogeneous. Melanosome1b consists of rounded blobs, rather similar to 11506 but many times smaller, composed of an intergrowth of And, Bt, Sil, Opq, Qz and some Chl. Compared to 11506, the melanosome1b is less round and essentially forms the foliation. Additionally, all components are more intergrown. What is mostly remarkable, is the abundance and co-occurrence of And as well as Sil. Sil forms a significant part of melanosome1b and is frequently intergrown with browner Bt, resembling melanosome2. And is very euhedral and surrounded by green Bt.

In certain parts of melanosome1b, it is observed that Sil has grown over all other minerals in melanosome1b as well as overgrown And (Fig. A26). This is interpreted as a later crystallisation of Sil.

The leucosome is, like the melanosome, composed of two types in the same thin section. Centrally, next to the patch of melanosome2, leucosome1 is present but in between the structures of melanosome1b, leucosome2 is present. Leucosome1 is coarse with >1000 µm grains of Afs or Qz with patches of smaller grains of mostly Qz as well as Afs and Pl. Macroscopically, leucosome1 is rather pink and this is observed as a haze of small, red points, in Fsp and in grain cracks. Leucosome1 narrows in the direction of the mesosome and the Bt grains align in a curve around a part of leucosome1. Some large grains in leucosome1 are interlocking but many other grains have some intergranular material of Pl or Qz. Afs, Pl or Qz are all seen with some lobate or curvy grain boundaries which do not appear to relate to other structures in the leucosome. Additionally, myrmekite patterns are observed in smaller Pl grains at the margin of the leucosome. The leucosome grain size reduces and Qz becomes more abundant towards the margins. Leucosome2 is composed for the majority of equigranular Afs and Pl and is about a third of the grain size of leucosome1. Afs contains extensive perthite exsolution. Leucosome2 contains a significant amount of Opq whereas leucosome1 doesn't contain any Opq. Essentially all grains in leucosome2 have intergranular Pl or Qz.

11534

11534 is somewhat different as it doesn't contain any mesosome and essentially no Opq. The melanosome presents a gradient from very green to browner Bt. The melanosome1b forms around very large Qz grains similar to other Crd pseudomorphs but much larger. The leucosome1 is some of the coarsest of all thin sections and is some of the most macroscopically pink coloured as well as the most fractured.

The melanosome type1b is composed of the same And + Bt intergrowth and it surrounds equally voluminous, >1000 µm Qz grains. These Qz all have a similar mineral orientation which is interpreted as congruent growth. Some parts of the pseudomorph framework are almost only And and some parts are almost only Bt. Bt gradually colours browner away from the leucosome1. There, Sil is more present although a great part is recrystallised into And. However, even the brownest Bt still does not reach the composition of common or mesosome Bt and remains rather green.

The leucosome type 1 in 11534 is very coarse and very fractured. The largest grains are composed of euhedral Afs and Pl as well as numerous large Qz grains or Qz clusters. Afs and Pl contain numerous inclusions. Most grains are interlocking. Qz has less lobate grain boundaries than in other thin sections. Leucosome1 contains almost no Opq.

4.2 Chemical Results

4.2.1 Bulk Rock Composition

The bulk rock composition was calculated for the group 1 thin sections with mineral abundances and average compositions of the minerals of each respective domain per thin section (Table B1, B2 & B3). Not enough measurements were made for Opq to support a reliable composition for each domain. For And, Qz and Sil, their basic mineral formulae were used. Composition of the domains themselves was calculated with their own normalised mineral abundances.

If the melanosome and leucosome are partitioned material from the mesosome, it is hypothesised that during porphyroblastic growth, this takes place in a chemically closed system and the reacted domains are in chemical equilibrium with the mesosome (Loberg, 1963; Russell, 1969; Trumbull, 1988). Therefore, the following should be true.

$$Melanosome + Leucosome = Mesosome \quad (5)$$

And so;

$$Melanosome * wt.\%_{Mela} + Leucosome * wt.\%_{Leu} - Mesosome = 0 \quad (6)$$

In a chemically closed system with a complete segregation from the mesosome, reaction (6) should result in a sum of 0 (Table 4.4). For the calculation of 11534, the average of the mesosomes of 11506 and 11507 was used as 11534 does not contain a mesosome. The mesosome is rather constant in composition so this will give some approximation for 11534.

Al_2O_3 is the only element which is significantly enriched in the group 1 thin sections. 11506 isn't majorly (>1 wt.%) enriched in any element. 11506 is minorly (<1 wt.%) enriched in seven elements. 11507 is majorly enriched in Al_2O_3 and minorly in FeO. 11534 is only majorly enriched in Al_2O_3. The reacted domains of these thin sections are all majorly depleted in SiO_2, Na_2O, CaO and minorly in TiO_2. The depletion of FeO in 11534 is expected as the entire thin section is almost devoid of Opq. Water does not vary much between the reacted domains and the mesosome.

Along the numerical order of the thin sections, The melanosome is progressively abundant in SiO_2 and Al_2O_3, poor in FeO and the leucosome is progressively abundant in SiO_2 and poor in Al_2O_3 and Na_2O. From the domain balancing, it is interpreted that SiO_2, or Qz, is not in chemical equilibrium and the (near) general depletion of K, Na and Ca indicates a significant role for mobile element migration.

Bulk rock (wt.%)	11506	11507	11534	Mela + Leu - Meso	11506	11507	11534 (Approx)
SiO_2	54.32 %	50.43 %	54.07 %	SiO_2	-22.16 %	-12.79 %	-13.07 %
Al_2O_3	20.89 %	29.94 %	31.60 %	Al_2O_3	-0.54 %	10.74 %	7.66 %
FeO	10.53 %	8.89 %	3.73 %	FeO	0.09 %	0.40 %	-5.52 %
K_2O	7.26 %	4.54 %	5.42 %	K_2O	0.26 %	-1.68 %	-0.87 %
MgO	3.07 %	2.12 %	2.38 %	MgO	0.71 %	-0.27 %	-0.30 %
Na_2O	1.81 %	1.24 %	0.77 %	Na_2O	-1.52 %	-3.01 %	-2.55 %
F	0.16 %	0.19 %	0.18 %	F	<0.005 %	-0.04 %	-0.02 %
CaO	0.59 %	0.41 %	0.25 %	CaO	-1.71 %	-1.48 %	-1.56 %
TiO_2	0.38 %	0.37 %	0.26 %	TiO_2	-0.68 %	-0.44 %	-0.60 %
Cl	0.07 %	0.04 %	0.15 %	Cl	-0.14 %	-0.09 %	-0.02 %
BaO	0.15 %	0.09 %	0.09 %	BaO	0.10 %	-0.06 %	-<0.005 %
ZnO	0.07 %	0.05 %	0.04 %	ZnO	-<0.005 %	-0.03 %	-0.03 %
SrO	0.07 %	0.03 %	0.04 %	SrO	0.02 %	-0.04 %	-0.02 %
MnO	0.03 %	0.02 %	0.02 %	MnO	<0.005 %	-<0.005 %	-<0.005 %
P_2O_5	0.08 %	0.05 %	0.04 %	P_2O_5	0.02 %	-0.05 %	-0.03 %
SO_3	0.02 %	0.02 %	0.02 %	SO_3	-0.01 %	-0.01 %	-0.01 %
H_2O	0.50 %	1.58 %	0.93 %	H_2O	-0.07 %	0.07 %	-0.12 %

Table 4.4: Bulk rock composition (left) of the group 1 thin sections and net enrichment or depletions of the flecks relative to the mesosome (right). Enrichments or depletions >1 wt.% are marked in green or red respectively.

4.2.2 Cordierite

Cordierite plays an important role in the processes investigated in this research and was intended to be compared between 11506 and 11507. However, the presumed Crd remnants in 11507 are all Chl as the shapes much resembled other Crd remnants. EPMA spot traces were made over the radii of the Crd and Chl grains to measure trace elements and growth zoning (Fig. 4.2). This indicated an Sr increase of 108.0 mol% and 129.9 mol% and a Ba decrease of 8.4 mol% and 81.4 mol% for 11506 and 11507 respectively, towards the margin relative to the core. Both thin sections show comparable results for Ba and Sr even though they are different minerals. This indicates similar growth conditions for 11506 and 11507. The decrease of Ba during growth indicates that Ba was less likely to partition into Crd during growth which indicates an increasing Ba partitioning in nearby melt and similarly, Sr increases towards the margin as it partitions into Crd. The Si, Al, Fe and Mg concentrations of the minerals are vastly different and vary within the trace, ruling out individual changes to the minerals having a significant effect on Ba or Sr.

Additionally, EPMA chemical maps were made for Crd and Chl. Both showed cracks which were enriched in Ca, K and Na and in 11506, these cracks were depleted in Mg in 11506 but in 11507 they were enriched in Mg. These zones in 11507 additionally showed high concentrations of Al and K.

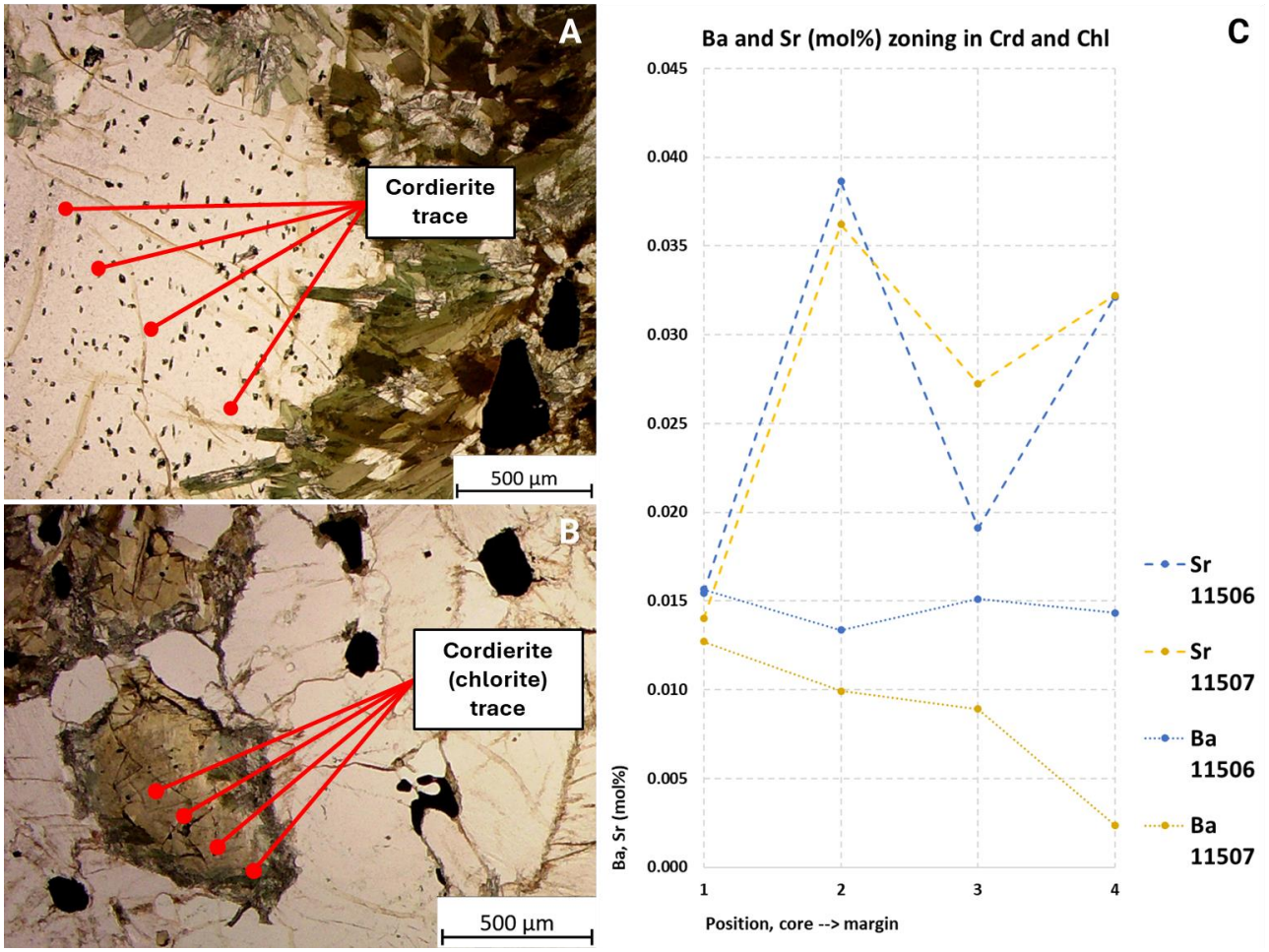

Figure 4.2: A; EPMA spot trace on a Crd grain in 11506. B; EPMA spot trace on a Chl grain in 11507. C; Ba and Sr zoning of both spot traces.

4.2.3 Green Biotite

Biotite has one clearly distinct characteristic in many thin sections which is its highly green colour in melanosome1b. This is visible macroscopically as well as in PPL through the microscope. In melanosome2, all Bt is rather brown so Bt may indicate differences in origin between melanosome1b and melanosome2. This green colour was thought to be caused by a chemical difference so all Bt measurements of all domains were graphed for Fe and Ti (Fig. 4.3). During EPMA spot measurements, Bt was distinguished as green, regular (=other), brown and mesosome Bt.

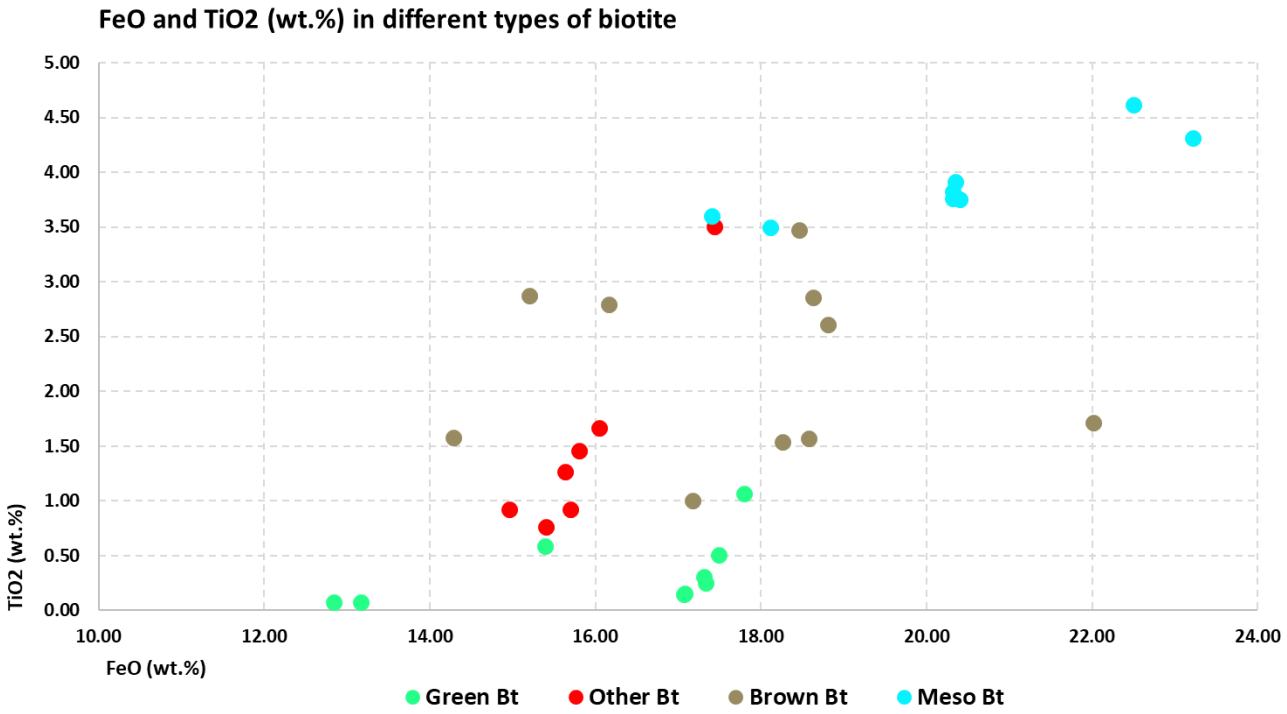

Figure 4.3: Correlation of FeO and TiO_2 in melanosome Bt (green Bt, regular (=other) Bt, very brown Bt) and mesosome Bt.

This indicates that the colour differences in Bt are mainly caused by a depletion of Ti and somewhat of Fe. The distinction between the Bt types is not marked by an abrupt, chemical change between any of the types. It does however indicate that essentially all Bt, also in the different melanosome types, is depleted in Ti and Fe with respect to the mesosome. Mesosome Bt is on average 19.3 wt.% more abundant in FeO and 237.7 wt.% more abundant in TiO_2 relative to the melanosome average. Additionally, Bt in the melanosome is on average 26.7 wt.% more abundant in MgO relative to the mesosome which is interpreted to be of similar origin relative to Crd.

To also verify the relationship between the brown Bt and the oxides in melanosome2b, a singular, 5-spot trace was made over a long, around 500 µm, radial Bt grain in 11506. As it radiates away from Opq, Ti is depleted by 54.2 mol% and Fe by 4.4 mol%. Adjacent to the Opq, TiO_2 is even more concentrated in Bt than in Opq itself with 0.8 wt.% in Opq and 1.17 wt.% in Bt. This same region was imaged with an EPMA Ti map which confirms the observations (Fig. A27).

4.2.4 Feldspars

Feldspar has been distinguished and analysed for Afs and Pl in both the mesosome and the leucosome. The leucosome is a reaction product of the mesosome so Fsp may have different compositions and trace element characteristics. The mesosome Afs is generally similar to the leucosome Afs which are both of sanidine composition. Pl in the mesosome is of andesine composition and Pl in the leucosome is generally more sodic, reaching oligoclase composition (Fig. A28). No majority calcic Pl has been observed anywhere.

The mesosomes were analysed with chemical maps. This indicates the Afs/Pl ratio which was estimated at about 40/60 vol.% respectively. A Ba map was made which indicated that Ba is concentrated mostly in Afs and in those, Ba is slightly but not consistently enriched towards the grain margins (Fig. 4.12). Additionally, Ba is more abundant in smaller Afs grains. In the mesosome of 11507, this pattern is similar.

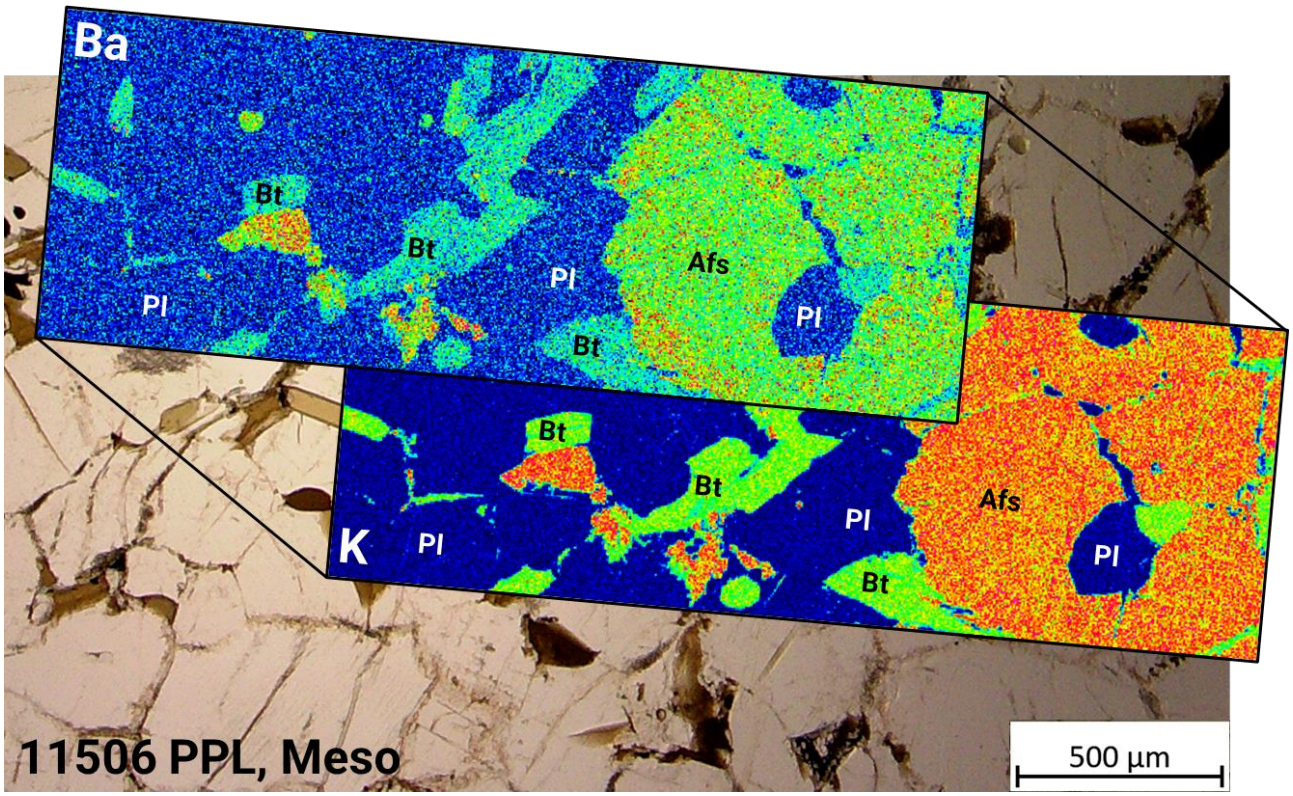

Figure 4.4: PPL photograph of the mesosome of 11506 with two chemical maps overlain. K map (lower) showing Afs (orange), Pl (blue) and Bt (green). This map is superimposed on the PPL picture. The Ba map (upper) shows Ba concentrations in the same minerals indicating mostly Ba enrichment in Afs (green) instead of Pl (blue).

The Pl abundance of the leucosome was estimated at 15 vol.% in 11506 and 30 vol.% for 11507 and 11534. No Pl composition was precisely measured for the leucosome of 11507 during the chemical analysis so the leucosome Pl composition of 11534 was also used for 11507. 11534 was chosen instead of 11506 because of the greater mineralogical similarity between the two.

A section of leucosome in 11534 was analysed with chemical maps (Fig. 4.5). This section contains large Afs grains, a large Qz grain and finer grained Pl between all larger grains. This indicates that Pl is regularly present as intergranular material as well as less euhedral than Afs or Qz. Additionally, larger Afs have a depletion of Na towards the grain margins and Pl have an enrichment of Na towards the grain margins. This is not observed in other chemical maps of the leucosome where albite exsolution is more common than here in 11534. In Pl, in the same enriched Na margins, Ca is depleted.

Ba is observed to be more concentrated in Afs grain boundaries as well as more enriched in smaller Afs grains than in large ones. A similar pattern of Pl presence and Ba enrichment is observed for leucosome2 in 11507 (Fig. A29). On average the BaO concentrations in Afs are 15.9 % higher in the leucosome than in the mesosome.

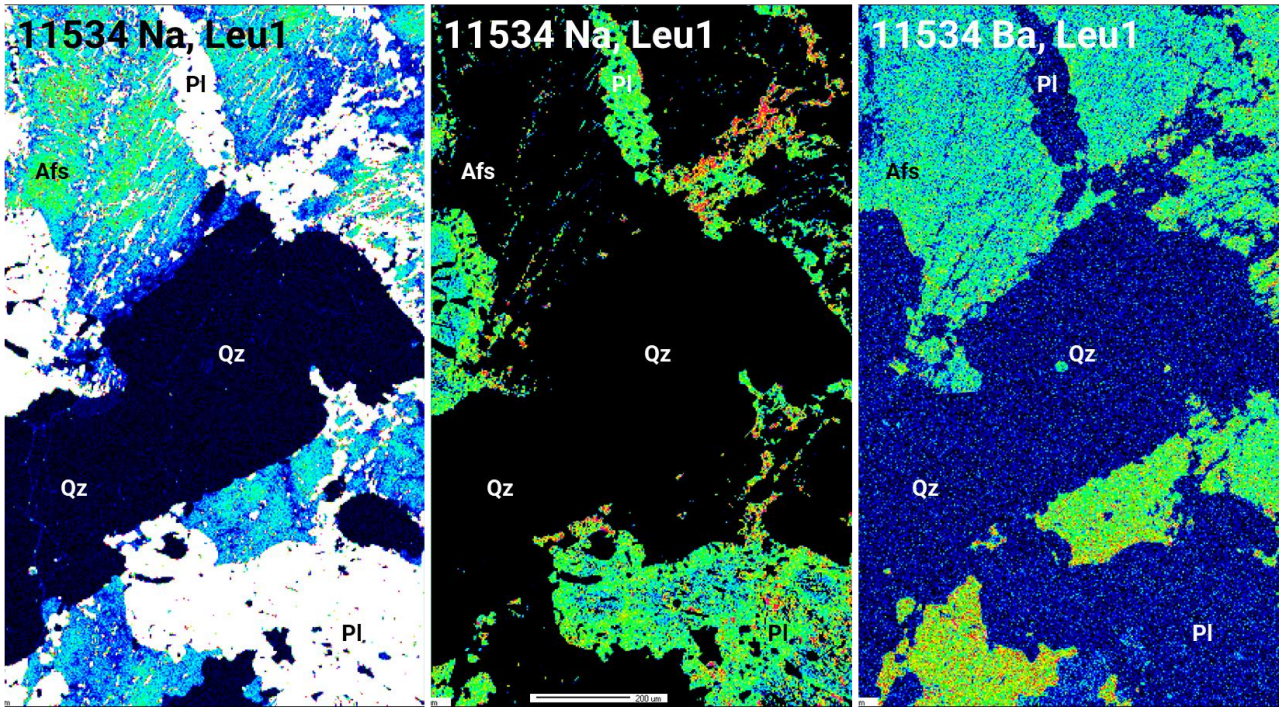

Figure 4.5: EPMA map for Na (left and central), at different colour settings, and for Ba (right) in part of the leucosome of 11534. Ba is clearly concentrated in Afs and shows enrichment towards grain boundaries as well as in smaller grains. The large central black grain is Qz.

Due to the crystallographic differences between phenocrystic and eutectic Fsp grains in the leucosome, extensive attention was paid to their chemical variations and trace elements. Spot traces were made for two large Afs grains in each thin section (6 total) (Fig. 4.6A). This indicated a Ba enrichment towards the margins in 4/6 traces with an average increase of 19.7 mol% compared to the centre (Fig. 4.6C). The highest enrichment was in 11507-1 with 84.8 mol%. On average the phenocrysts in 11506 contain the most BaO with an average concentration of 0.41 wt.%. This indicates that Ba concentrations increased as the phenocrysts crystallised which is congruent with mobile element partitioning in melt during phenocrystic growth. Similarly, Sr somewhat decreases towards the margins of the phenocrysts which indicates the same as the immobile Sr partitioned into Fsp during initial growth (Fig. 4.6D).

Subsequently, the BaO and SrO concentrations were compared between the eutectics and phenocrysts. To make a valid comparison with the (entirely Afs) phenocrysts, only the Afs eutectics will be considered as 8/10 measured grains were Afs. This indicated that eutectic Afs have a 17.1 wt.% higher BaO concentration and a 9.3 wt.% lower SrO concentration than the average of the phenocrysts (Fig. 4.6B). The average eutectic BaO concentration is higher than 12/16 measured values for the phenocrysts. Strangely, the BaO/SrO forms a rather linear relationship for the phenocrysts but not for the eutectics. The eutectic Sr concentration is expected to decrease while Ba increases similar to the phenocryst margins. This is not correlated to K, Na or Ca. If the eutectic grains would all have crystallised simultaneously, they are expected to share the same BaO as well as SrO concentration but this appears to be untrue for Sr. This means that the BaO values of the eutectics support late crystallisation from a melt but SrO values don't match equally well.

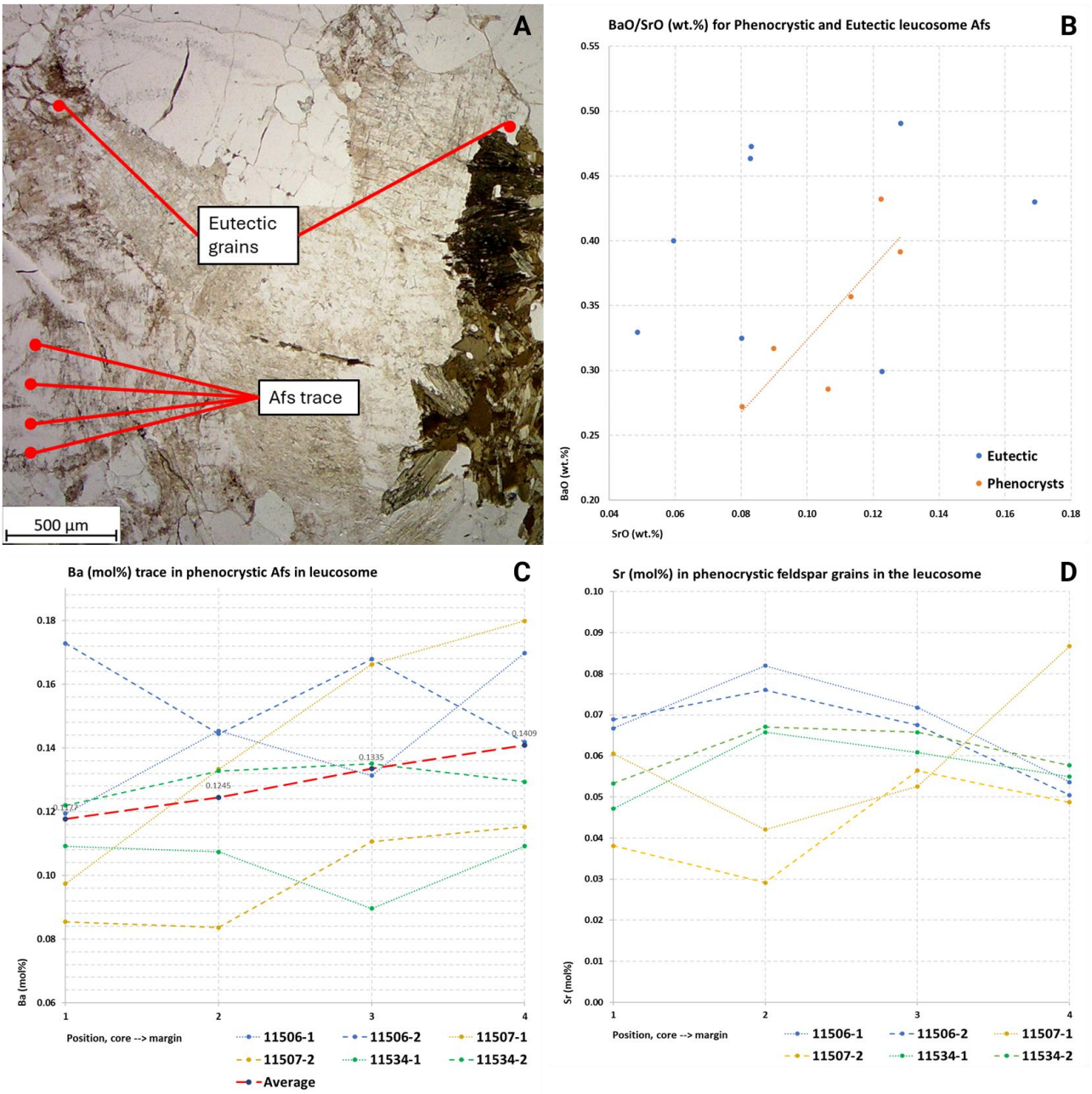

Figure 4.6: A; Interface of leucosome1 and melanosome2 in 11534 with the measurements for the trace of 11534-2 in a phenocryst as well as two eutectics. B; BaO plotted against SrO for the average of the phenocrysts and the eutectics. C; Ba concentrations in the traces of the phenocrysts. D; Sr concentrations in the traces of the phenocrysts.

4.2.5 Opaques

All measured opaque minerals are (iron) oxides, containing high amounts of Ti. They are sparsely measured and not in all thin sections in all domains. Opq in the mesosome consists entirely of magnetite, in the melanosome Opq consists for 7.9 % of hematite and in the leucosome for 14.4 % of hematite. Mag in the mesosome contains barely any TiO_2 (<0.1 wt.%) which is similar in the melanosome. In 11534 in the melanosome and the leucosome, two grains contain 13.4 and 23.1 wt.% TiO_2 which are therefore titanomagnetite. This is confirmed by an EPMA image, showing Ilm exsolution lamellae. Additionally, in 11507, one Ilm containing 61.6 wt.% TiO_2 was measured. Overall magnetite is the dominant oxide with Ti enrichment in the reacted domains.

4.3 Interpretations on Melting

4.3.1 Sequential Development in 11507 and 11535

Both intact and recrystallised Crd (melanosome1a, b and c) is observed both with leucosome1 and leucosome2. Melanosome2 is however only observed with leucosome1 nearby. Especially thin sections 11507 and 11535 may be indicative in clarifying the relationships between the different melanosome and leu types.

In 11507, the proximity of melanosome1b with leucosome2, and melanosome2 with leucosome1, suggests that these are genetically related. Melanosome2 is distinct because it contains brown Bt, because it doesn't or didn't contain any Crd and because it contains a large portion of Sil. Melanosome2 is therefore a higher grade metamorphic assemblage. Sil is however also observed in melanosome1b, even where it overprints And. This suggests that in 11507, melanosome2 and leucosome1 are the product of a secondary phase of metamorphism, overprinting an already present melanosome1b after retrogression. In 11507 this is further evidenced with part of the mesosome curving around a part of leucosome1, as if leucosome1 had intruded there into the lithology. The presence of melanosome2 is not a requirement for the presence of Sil as it is also observed in melanosome1b.

In 11535, a transition from melanosome1b to melanosome2 is observed (Fig. A13) as well as two times a sudden but adjacent coarsening in leucosome (Fig. A15). Whereas in 11507 the different melanosome and leucosome types are separated, in 11535 they are both connected in a gradual transition. This therefore questions the relationship with a multi-generational explanation such as in 11507 as a gradual change is expected to be the result of gradually changing conditions. Therefore, 11507 and 11535 both suggest an increase of metamorphic grade but 11507 expresses this as an overprinting and second phase whereas 11535 expresses a gradual increase of metamorphic grade. The sample location of 11535 is unknown but is expected to be not nearby 11507.

4.3.2 Grain Boundaries

With the EPMA maps, the grain boundary compositions could be verified. Maps were made for leucosome and mesosome which confirmed the two types of intergranular material observed. Thin sections either have a haze of microcrystalline Qz + Sil or thin sections have Pl (and sometimes Qz) films at the grain boundaries. This is then also observed in the respective mesosomes. Pl films are abundant in leucosome1 but notably in 11507, it is also present in leucosome2 as well as the mesosome (Fig. 4.7). Similar leucosome2 with intergranular material is observed in for example 11511 (Fig. A9). Additionally, the leucosome2 to leucosome1 transition in 11535 as well as in a few other thin sections, appear to show intergranular Pl in leucosome2 to decrease at distance from leucosome1.

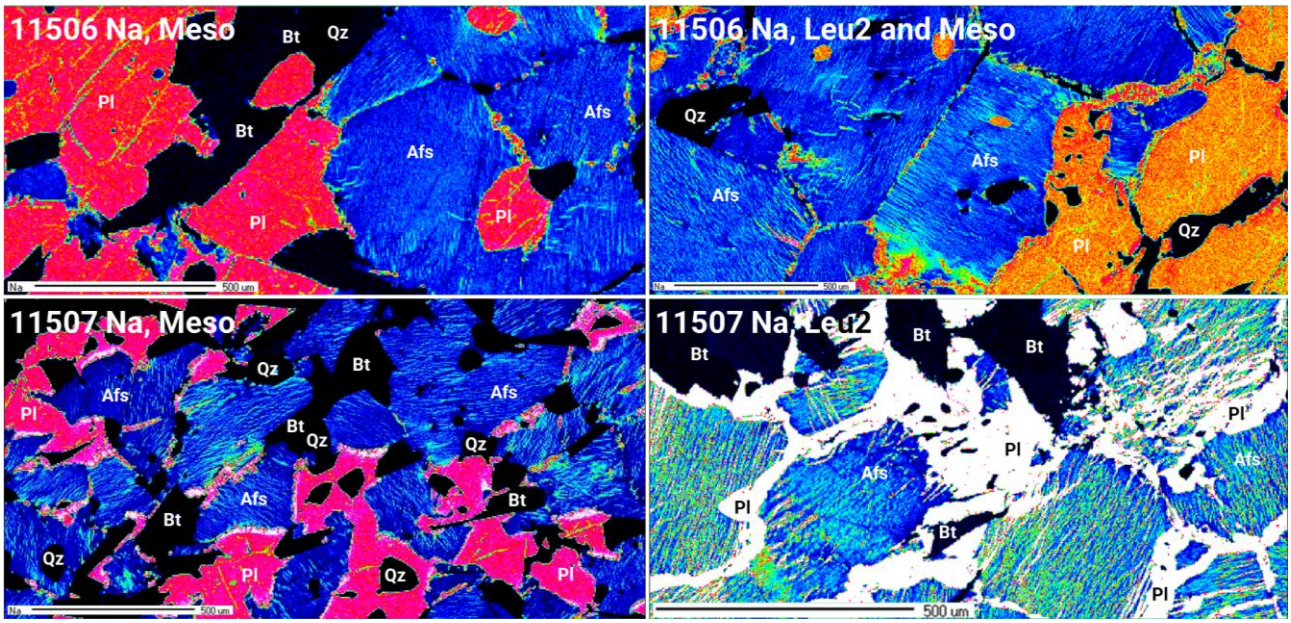

Figure 4.7: Na maps of the mesosome (left) and the leucosome2 (right) of 11506 (upper) and 11507 (lower). Coloured is Afs (blue) and Pl (red, pink, orange or white). This indicates the absence of intergranular Pl in 11506 and the abundance of intergranular Pl in 11507. Both in mesosome and in leucosome, Pl is present as films. In the mesosome this is visible as more Na rich sections, connected to larger Pl. Also visible is the more intense albite exsolution in 11507. Note the different scale bars. The leucosome in 11507 is much finer grained than in 11506.

From the combined mineralogical and geochemical data, it is interpreted that leucosome1 is consistently composed of not only structural but also chemical compositions that indicate melting (phenocrysts, eutectics, Ba zoning, intergranular Pl, selvedges). However, in many leucosome2, the structural elements are less indicative and convincing to be equally certain. With the intergranular material such as in 11507 and 11511, it is interpreted that leucosome2 with intergranular Pl in the leucosome as well as the mesosome are also the result of melting reactions. This therefore differs per thin sections based on the grain boundaries.

5, Modelling in Perple_X

Perple_X version 6.9.1 was used with thermodynamic data from hp62ver.dat (version 23-11-2023). The modelling largely followed Ex.12 on anatectic modelling from a student manual, version 29-01-2022, from Daniele Castelli and Chiara Groppo from the university of Turin, Italy, as provided on the Perple_X website. The modelled elements are Al, Ca, Fe, K, Mg, Na, Si, Ti and H2O. The other elements investigated were not modelled in Perple_X (accounting for ± 0.5 wt.% of the bulk rock). For Fe, the mol% of Fe + Mn was used. The pseudosections are SiO_2 (Qz) saturated in all mineral stability fields as Qz is observed in every domain. Due to prograde dehydration mineral reactions, the lithology is water saturated until melting (when H_2O partitions into melt). This was combined for the pseudosections here meaning that they are water saturated until the solidus. P-T pseudosections were made for the three group 1 thin sections according to their chemical compositions.

The modelled compositions and stability fields fit well for 11507 and 11534 but 11506 was modelled to have either garnet (Gt), orthopyroxene (Opx) or staurolite (St) in all stability fields (Fig. A30). 11506 was therefore imaged for only the fields that contain And, Crd or melt whereas 11507, 11534 and the average composition were imaged for all fields except the ones containing Gt, St, Opx or Ky. The final pseudosection was modelled for the average composition which was used to reconstruct the geological history of the Flecky Gneiss. The following indicative compositions are observed with interpretations from structural observations as well as pressure-temperature estimates resulting from Perple_X.

Prograde 1:

(a) And + Crd + Afs
Contact metamorphism increased the temperature but locally melting conditions were not reached.
200 MPa and ± 680 °C

(b) And + Crd + Melt
Elsewhere the temperature did reach melting in And-Crd stability conditions.
200 MPa and 730 °C

Retrograde:

(c) And or Sil + Bt
Cooling during burial lead to Crd recrystallisation close to Sil stability conditions, locally recrystallising most of the Crd cores.
300 MPa and 630 °C

Prograde 2:

(d) Bt + Sil + Melt
Secondary contact metamorphism led to (re)melting and formation of Bt + Sil.
300 MPa and 730 °C

Some thin sections are observed with only (b) (11531), some with only (c) (11505) and some with (c) as well as (d) (11507). No thin section was convincing in having had only (d). Multiple thin sections are observed with Sil but without melting such as in 11506. This indicates Crd recrystallisation close to Sil stability conditions as no other secondary deformation is observed in 11506 like in 11507.

Therefore, multiple P-T paths are interpreted which are dependent on locality specific conditions. (a) - (d) all fall withing a relatively confined high pressure low temperature (HPLT) field of 200 - 300 MPa and around 600 - 750 °C. To achieve melting conditions, a minimum of 700 °C must have been reached and the maximum pressure is around 300 MPa.

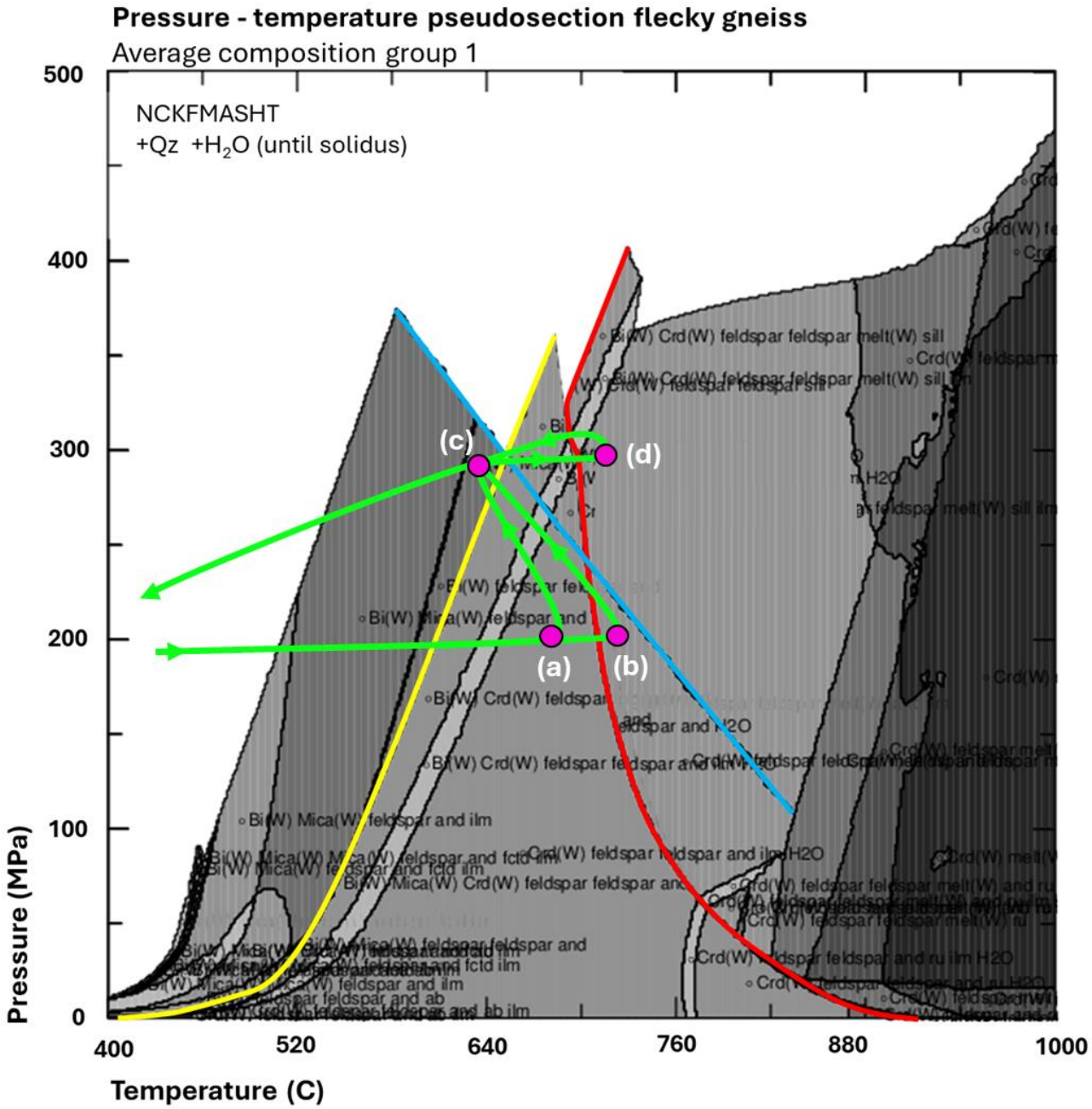

Figure 5.1: Pressure-temperature pseudosection indicating mineral stability fields for the average composition of the group 1 thin sections. Indicated are four indicative mineral assemblages (a, b, c, d) that are observed. Locally different temperatures are interpreted. Yellow indicates the stability curve of Crd (towards higher temperature), blue indicates the stability curve of And (towards lower temperature) and red indicates the melting curve (towards higher temperature). The stability field text is to be disregarded.

6, Discussion

Despite major differences in mineralogy and structures, varying assemblages of the Flecky Gneiss have revealed a complex geological history of the Västervik region. The more constant texture and composition of the mesosome has coupled the variety of the reacted domains. The different types of melanosome and leucosome indicate that multiple prograde assemblages are the result of different metamorphic conditions in a limited area. Similarly, other authors have mentioned significant local differences and varying compositions within their own regions (e.g. Russell, 1969; Kresten, 1971; Kleinhanns, 2015). Despite greatly varying observations and compositions, it is unambiguous that the same general phenomenon and rock type is analysed. This is to emphasize that some earlier publications on this region and the Flecky Gneiss have based their conclusions on a single locality whereas the samples of this thesis span almost 50 km apart and therefore, different observations and interpretations are to be expected.

The fleck shapes and alignment mostly don't follow the foliation which is used as argument that the Flecky Gneiss is a porphyroblastic product as most migmatites form under deviatoric stress where the melt collects in the foliation plane but this may as well be an indication that the Flecky Gneiss did form under lithostatic pressure and is produced by contact metamorphism (Loberg, 1963; Mehnert, 1968; Sawyer, 2008).

The thin sections analysed here show significant enrichment in Al_2O_3 and depletion in SiO_2, Na_2O, CaO and TiO_2 with respect to the mesosome meaning that the group 1 thin sections did not form a chemically closed system especially regarding the depletion of essentially all elements (except Al_2O_3) in two out of three thin sections. Additionally, the individual domains themselves present enrichment and depletion trends which may be due to their individual metamorphic grade or lateral differences in the composition of the metasediments. Trumbull (1988) noted similar elements involved in mobility namely enrichment in K_2O (and minor SiO_2 and Al_2O_3) and depletion in Na_2O and CaO, although much more minor than discussed here. Even though he investigated a different fleck composition, it is suspected that alkali elements are essential in facilitating chemical mobility to form fleck separations.

Loberg (1963) and Trumbull (1988) concluded based on the chemical equilibrium they measured between the domains, that the flecks were porphyroblastic products and they claimed the domain separation to be an expected outcome of diffusion controlled porphyroblasic growth. If the Flecky Gneiss would be a porphyroblasic product, how does reaction material segregate in this manner? Macroscopically, it can be observed that the leucosome material can aggregate and collect in large (semi planar) sections without any melanosome nearby (Fig. 1.2). Mass transport clearly covered great distances which may be impossible without a fluid phase present.

6.1 Prograde Development

6.1.1 Mesosome

The two mesosomes observed mostly express differences in grain shapes and grain boundaries but were otherwise the most consistent domain among the thin sections. It is interpreted that the protolith of the Flecky Gneiss was composed of a somewhat similar composition as the mesosome, forming a slightly pelitic arkose. This is however uncertain as in situ material separation (the flecks) has affected the mesosome composition and structure. This is most pronounced for Bt which are all anhedral, have thinned grain margins and are present as intergranular material. It may be possible that grain boundary diffusion was prevalent enough to affect Bt to the extent observed. Additionally, the intergranular Pl in 11507 strongly suggests melt remnants to be present in the mesosome. The role of the microcrystalline Qz + Sil in 11506 is less clear but this is not a convincing indication of melt. Additionally, alkali enrichment during regional metasomatism as well as local silicification of Fsp is recognized as a relevant factor in changing the lithologies around Västervik, complicating the certainty about the protolith (Mehnert, 1968, P. 149; Vollbrecht & Leiss, 2008).

The metamorphic grade of the mesosome is less indicative than in the other domains but the presence of Sil as large (>10 µm), grains within the mesosome, indicates that Sil conditions have been reached also in thin sections only following P-T path (a) - (c). As indicated by the melanosome1b, this is interpreted to be recrystallisation during burial, heading towards Sil stability conditions but may also be an effect of secondary heating.

Ba is observed to concentrate towards Afs grain margins in the mesosome, similar to what was measured for the leucosome. This may be a property of Ba in Afs but if the Ba concentration is unrelated to crystallising from melt, this should be considered for observations in the other domains. No trace data was acquired for mesosome minerals but this could have been compared.

6.1.2 Melanosome

Numerous observations support the formation of Crd as fleck cores with varying leucosome types in sub- and supersolidus conditions. Thus, Crd is formed both via reaction (1) or (2) as well as via (3) + (4) which is locality dependant. The Ba and Sr data for Crd support the presence of a melt phase and indicate simultaneous growth with phenocrystic Afs in the leucosome. The differences between the formation as poikiloblast or as massive grains is however not determined and both types of Crd are observed in what are concluded to be similar conditions (subsolidus). In 11534 the poikiloblastic structure contains Qz grains of >1000 µm where other poikiloblasts only have 50 µm Qz inclusions. Additionally, some Crd minerals become homogeneous towards their margin. This characteristic of Crd has not been understood although the structure in 11534 is potentially related to different mineral reactions (explained below).

Melanosome2 is different because of its composition of Bt + Sil. The browner Bt and the lack of fleck shapes indicates a significantly different origin. Reactions (1) and (2) which were focussed on so far are mostly interesting because of the formation of Crd and Afs but there are more reactions that can produce Crd as well as other mafic assemblages such as observed in melanosome2. This requires combining some other common phase equilibria that are relevant in melting (Pattison & Tracy, 1991).

$Ms + Chl \rightarrow And\ or\ Sil + Bt + Crd + H_2O$ (5)

$Ms + Chl \rightarrow And\ or\ Sil + Bt + Qz + H_2O$ (6)

$Ms + Qz \rightarrow And\ or\ Sil + Afs + H_2O\ or\ Melt$ (7)

These reactions all react simultaneously with Ms and combining them results in:

$Chl + Ms + Qz \rightarrow And\ or\ Sil \pm Crd + Bt + Afs + Melt$ (8)

Reaction (7) can therefore not only explain the presence of melanosome2 but combined with (5) it also provides an option for the simultaneous formation of Crd as well as Bt and Sil such as in 11535. This is somewhat problematic for the interpretation of And + Bt as retrograde products of Crd in melanosome1b but the green Bt still supports this distinction. To some extent reaction (8) also nuances the relevance of the second prograde deformation but more on that in 6.1.4. It can be concluded that multiple reactions took place in the thin sections observed. This could mean that the 'simple' Crd forming reactions (1) and (2) were involved with the more comprehensive fleck thin sections such as 11506 whereas in other thin sections a combination of (5), (6) and (7) is observed. For example in 11534, (6) and (7) could be relevant in the formation of the fleck like structures with the large Qz grains and the And + Bt intergrowth. This is supported by the similar mineral orientation of the large Qz grains. The melanosome increases in Bt concentration away from the leucosome, potentially indicating a relative dominance of reaction (6). Additionally, thin sections with aggregates of Sil + Qz (11502, 11529, 11533) may be the result of reaction (6).

Lastly, Bt + Sill aggregates are reported in numerous migmatites and are also mentioned to be a potential product of the reaction with Crd and Ms (Pattison & Tracy, 1991; Sawyer, 2008). Reaction (9) is not clearly observed and other thin sections with intact Crd lack Ms to facilitate this reaction. It is unclear if this would have been viable in the time and conditions of the Flecky Gneiss.

Crd + Ms → And or Sil + Bt + Qz + H_2O (9)

6.1.3 Leucosome

The leucosomes and their sub types have revealed the most convincing melt indications of all domains. It is concluded that all leucosome1 thin sections provided convincing structural (phenocrystic and eutectic mineralogy, mafic selvedges, intergranular melt remnants) and chemical (Ba and Sr zoning, Ba enrichment, intergranular Pl) indications that melting has taken place. However, many similar indications are also observed in leucosome2, obscuring the differences between leucosome1 and leucosome2. Even though the structural characteristics of leucosome1 are more in line with migmatite textures than leucosome2, the grain size (distribution) turned out to be an insufficient distinction by itself.

Although the bulk composition of leucosome1 in 11506 and leucosome2 in 11534 are similar (Table B3), leucosome2 is frequently almost devoid of Qz such as in 11504, 11505 and 11506. If leucosome1 and leucosome2 would be the result of the same processes, at least a similar composition is expected. This suggests a different origin for leucosome2. If the subsolidus reactions (1) or (2) only produce Afs, this means that leucosome2 is the product of subsolidus formation. The more sodic composition of leucosome Pl relative to the mesosome (Fig. A28) is in line with melting but this is also observed in the leucosome2 of subsolidus 11506 (Sawyer, 2008).

The Ba and Sr zoning in phenocrysts as well as in the Ba enrichment in the eutectics largely supports the presence of melt but the same signatures are observed for 11506 which is not interpreted to be molten. Perhaps very similar dynamics are present in subsolidus (porphyroblastic) segregation but this is not verified. Ba zoning appeared similar in the mesosome so this could be an Afs specific characteristic. Earlier research on this Flecky Gneiss has omitted Ba from their analysis, making it difficult to compare these observations. Many other relevant trace elements are likewise not included in this study such as Rare Earth Element (REE) distributions. These did not indicate convincing melt signatures albeit for a different Flecky Gneiss (Trumbull, 1988).

6.2 Retrograde Development

The main retrograde reaction that is observed is the recrystallisation of Crd reacting into And + Bt. This is essentially the reversal of reaction (1) except that it requires the influx of K rich water (Kresten, 1971; Pattison & Tracy, 1991; Waters, 2001).

Crd + H_2O (with K) → And or Sil + Bt + Qz (10)

The presence of free water is not unlikely as the region around Västervik is abundant in intrusions, releasing water from crystallising magma and affecting surrounding lithologies. The presence of alkali rich fluids has been discussed by multiple authors as important interactions around Västervik and the mobilisation of alkalis could be related to the depletions and anhedral Fsp that is observed (Mehnert, 1968, P. 149; Vollbrecht & Leiss, 2008). Additionally, the Flecky Gneiss were subject to dynamic recrystallisation which is observed as lobate and anhedral grain boundaries, mostly in the leucosome (Vollbrecht & Leiss, 2008). Lastly, the Sil observed in some subsolidus melanosome1b did not clearly take part in the second metamorphism, is interpreted to be the result of retrograde recrystallisation close to Sil stability conditions.

Russell (1969) concluded that the Mg abundance in green Bt is derived from the recrystallised Crd. Similarly, the remaining Fe and Ti has formed the Opq grains in the melanosome as Crd could not integrate all Fe and Ti. During retrogression, Crd does not contain enough FeO and TiO_2 and the diffusion from prograde Opq is not sufficient to form retrograde brown Bt. The lack of green Bt or Opq in some thin sections (such as in 11534) further argues for a significant role for reactions (5) and (7) where Bt is not involved.

Lastly, the leucosome of some thin sections colours (macroscopically) rather pink among fractured Fsp. This is not quantified but it occurs more in coarser, melt derived leucosome1. It may be possible that as nearby melt crystallised and water went out of solution, this free water affected Fsp in the leucosome as well as aided the recrystallisation of Crd (Kriegsman, 2010). This is not observed in all leucosome1 especially not in the thin sections with melanosome1a, meaning that the pink leucosome colouring is more likely to be a general retrograde artefact, not directly related to melt water.

6.3 Sequential Development and P-T Conditions

The interpreted P-T path and the secondary heating event are not based on all thin sections but a small selection that may indicate a multistage deformation. Evidence for this is found in 11507, 11511 and 11535. 11507 is the most convincing as it contains the two main types of melanosome and leucosome next to each other as well as indications of Sil overprinting and leucosome1 that 'intrudes' the mesosome. This raises the question if it's possible that the intergranular Pl in leucosome2 in 11507 is the result of remelting during the generation of leucosome1 and melanosome2. This may explain why the otherwise Afs, equigranular and fine grained leucosome2 in 11507 contains Pl films at all Afs grains (Fig. 4.7). The same is observed in the leucosome2 of 11511 which otherwise does not have a convincing melt structure. The sudden coarsening of the leucosome in 11535 is different to the rest of the thin sections and the leucosome and melanosome are not as segregated as in 11507. Perhaps this thin section indicates that a subsolidus reaction got overtaken by a supersolidus reaction or the intergranular material in the finer part of the leucosome indicates a similar remelting as in 11507 but this must have been in very close succession. Apart from 11507, other thin sections like 11535 could potentially be resolved without a second deformation phase and with for example reaction (8). This means that the P-T paths reconstructed in chapter 5 still includes a high and a low pressure contact metamorphism where locally Sil as well as And conditions were reached.

In this research, no chemical P-T approximations were made based on specific mineral interactions or equilibria such as may be done with Bt + Gt or Crd + Gt (Thomas & Rana, 2019; Thomas et al., 2020). Therefore, only bulk mineral assemblages were analysed and thermodynamic modelling with Perple_X was carried out to approximate P-T conditions. The pressures reached on either of the prograde steps could vary significantly but the interpretation that leucosome2 is not resulting from melt, but is observed with at least some Sil, narrows the peak pressure window to 250 - 300 MPa. The lower end could be much less however but is impossible to further constrain here. Considering a geothermal gradient around 50 °C/km, a pressure of ±300 MPa is realistic at 600 - 700 °C. Previous P-T estimations range from 350 MPa and 580 °C to 250 MPa and 350 - 450 MPa and temperature estimates of 400 °C and 725 °C with a similar geothermal gradient (Russell, 1969; Rieffe et al., 1993; van Tuyl, 1977). Magmatic intrusions have been abundant around Västervik and contact metamorphism played a major role in recrystalising and melting lithologies in the vicinity as well as burial at 8 - 12 km depth. This means that from the Perple_X derived model, a similar pressure and a higher temperature estimate is made relative to earlier research. This may be related to an underestimation of the water content of the thin sections investigated as well as the fact that other publications have avoided concluding on melting conditions.

6.4 Limitations of This Study

At every analytical step the results would have significantly improved from doubling the dataset. Additionally, more chemical datapoints would have contributed to more reliable data as some minerals only had a few datapoints to base interpretations on. For this reason, domain balancing and bulk rock composition analysis is likely to be the least reliable part of the chemical analysis in this research. Especially the point counting was problematic for the mineral abundances as not enough images or points were used and the volume of Qz measured in the melanosome of 11506 is certainly an underestimation.

Furthermore, almost no field data was available for the thin sections investigated which denies contextual interpretations regarding the thin section differences. Trends, patterns and interpretations made are perhaps not quite reliable as thin sections may be unrelated.

The water content of the thin sections was only determined for Bt, Chl and Crd. This means that the leucosome is now concluded to have 0 wt.% water which is unlikely. This could differ significantly from realistic values as water was presumably present as intergranular fluids especially under different P-T conditions. This could have a big influence on melting conditions that were now modelled differently and at a minimum estimate.

6.5 Future Research

This research has added to the knowledge and information of the Västervik region and specifically the Flecky Gneiss found in multiple locations. Not everything about the Flecky Gneiss is yet resolved and mostly questions remain about the shapes and interactions of different mineral reactions. The potential for different minerals to react is well established and their viability can be calculated but every locality has different specific conditions and compositions meaning that not only descriptions of rocks need to be shared but also more images on rare lithologies such as Flecky Gneiss so they can be easily compared via online databases. Typical assemblages are well studied and published but microscopic mineral textures for rare or transitional lithologies appear to be undervalued. Similarly, the petrographic analysis could have been more conclusive if a few thin sections of a confirmed patchy gneiss were available for comparison.

Specifically this Flecky Gneiss would benefit from an expansion of detailed fieldwork information. Since the sub- and supersolidus textures are this closely related, other aspects of the metamorphic conditions such as macroscopic geometry need to be observed on an outcrop scale. Clearly the local differences in Västervik are large so options for mineralogical research remain.

Additionally, the analysis of this Flecky Gneiss would be improved by including more mobile elements. In the analysis. REE analysis is a good indicator for analysing melt but that was not analysed in this research.

7, Conclusions

Structural and chemical investigations into the material separation and mineral reactions of the Västervik Flecky Gneiss have revealed a variety of processes of which some have resulted in partial melting by contact metamorphism. Crd has been at the core of fleck generation and mineralogical compositions show that melting has taken place in And stability conditions as well as in Sil stability conditions at varying pressures but similar temperatures. Despite other research, the segregation of the melanosome and the leucosome is calculated to not be in chemical equilibrium with the mesosome and both melt and water played a significant role in metamorphism. Subsolidus reactions creating similar Crd fleck formation by porphyroblastic growth are also interpreted but the chemical evidence for subsolidus Crd formation is less conclusive as many similarities with supersolidus structures are present.

Structural and compositional assemblages of the leucosome distinguish two types which are concluded to be related to sub- and supersolidus reactions. Leucosome1 contains convincing migmatite structures including large euhedral Afs and Pl phenocrysts, Afs, Pl and Qz eutectics, intergranular Pl and Qz melt remnants and a Bt selvedge. This is concluded to be the result of melting. Leucosome2 is equigranular, consists for the majority of interlocking Afs and is sometimes barely coarser than the mesosome. Some leucosome2 also contains intergranular Pl. This is concluded to be the result of subsolidus segregation but similarities between leucosome1 and leucosome2 are observed, potentially because of remelting of leucosome2. Ba and Sr zoning in Afs phenocrysts and Ba enrichment in eutectics supports the presence of melt during growth in the leucosomes. This data is however similar for leucosome2 which also supports melting.

The varying stages of retrograde recrystallization of Crd into And or Bt + Sil indicates the similarity and formation of Crd in both sub- and supersolidus conditions. The intimate relationship between And and Sil proves that most reactions took place close to the transition of And and Sil stability conditions. Ba and Sr zoning in Crd supports a melt presence and indicates simultaneous growth with leucosome phenocrysts. This potentially also supports melting for leucosome2. Other melanosome consists of Bt + Sil which is concluded to be a secondary phase of contact metamorphism leading to melting in Sil stability conditions after retrograde Crd recrystallization during burial.

The mesosome is affected by metamorphism and despite a large fraction of Bt remaining, it is clearly involved in prograde mineral reactions. The mesosome supports melting having taken place as indicated by intergranular Bt and Pl melt remnants. Ba zoning in Afs in the mesosome contains similar patters as Afs in the leucosome which makes Ba zoning inconclusive for phenocrystic growth in a melt.

Reconstructed pressure-temperature conditions to achieve melting with the observed mineralogy are estimated at 200 MPa and 680 - 730 °C and at 300 MPa and 730 °C distinguished by a phase of cooling and cordierite recrystallisation at 300 MPa and 630 °C. This means the Flecky Gneiss was buried to around 11 km depth. To achieve melting by contact metamorphism in both the And and later in the Sil stability conditions, a secondary heating is estimated to have reached a similar temperature at higher pressure.

Summarising, the Västervik metamorphic region and the Flecky Gneiss has endured varying conditions and is concluded to have reached melting conditions during HTLP contact metamorphism in multiple locations, potentially during multiple events. The flecks in the Flecky Gneiss are the product of both sub- and supersolidus Crd formation, resulting in a segregated region of more mafic and more felsic minerals. The sub- and supersolidus lithology are difficult to tell apart, melting definitely has taken place locally although not on a pervasive level as seen in other migmatites. The Västervik region is lithologically and metamorphically diverse and apart from numerous subsolidus processes in the region, the Flecky Gneiss should be considered to be a patchy migmatite instead.

8, References

Andersson, U., Gorbatschev, R., Wikström, A., Högdahl, K., Ahl, M., Nyström, J.-O., Sjöström, H., Bergman, S., Eklund, O., Claeson, D., Mansfeld, J., Stephens, M., Wahlgren, C.-H., Lundqvist, T., Smeds, S.-A., Sundblad, K., & Öhlander, B. (2004). *The Transscandinavian Igneous Belt in Sweden: A review of its character and evolution*. Geological Survey of Finland.

Ashworth, J. R. (1976). Petrogenesis of migmatites in the Huntly–Portsoy area, northeast Scotland. *Mineralogical Magazine*, 40(1), 661–682.

Beunk, F. F., Page, L. M., Wijbrans, J. R., & Barling, J. (1996). Deformational, metamorphic and geochronological constraints from the Loftahammar-Linköping Deformational Zone (LLDZ) in SE Sweden: Implications for the development of the Svecofennian Orogen. *GFF*, 118(sup004), 9.

Beunk, F. F., & Page, L. (2001). Structural evolution of the accretional continental margin of the Paleoproterozoic Svecofennian orogen in Southern Sweden. *Tectonophysics*, 339(1), 67–92.

Gavelin, S., & Russell, R. V. (1967). Primary sedimentary structures from the Precambrian of southeastern Sweden. *Geologiska Föreningen i Stockholm Förhandlingar*, 89(1), 74–104.

Geological Survey of Sweden (SGU) (2007). Schwedens grundgebirge.

Kleinhanns, I. C., Whitehouse, M. J., Nolte, N., Baero, W., Wilsky, F., Hansen, B. T., & Schoenberg, R. (2015). Mode and timing of granitoid magmatism in the Västervik area (SE Sweden, Baltic Shield): Sr–Nd isotope and SIMS U–Pb age constraints. *Lithos*, 212-215, 321–337.

Kresten, P. (1971). Metamorphism and migmatization in the Västervik area, SE Sweden. *Geologiska Föreningen i Stockholm Förhandlingar*, 93(4), 743–764.

Kriegsman, L. M. (2001). Partial melting, partial melt extraction and partial back reaction in anatectic migmatites. *Lithos*, 56(1), 75–96.

Kriegsman, L. M., & Álvarez-Valero, A. M. (2010). Melt-producing versus melt-consuming reactions in pelitic xenoliths and migmatites. *Lithos*, 116(3-4), 310–320.

Loberg, B. (1963). The Formation of a Flecky Gneiss and Similar Phenomena in Relation to the Migmatite and Vein Gneiss Problem. *Geologiska Föreningen i Stockholm Förhandlingar*, 85(1), 3–109.

Mehnert, K. R. (1968). *Migmatites and the origin of granitic rocks.* Elsevier.

Pattison, D. R. M., Tracy, R. J. (1991). Phase equilibria and thermobarometry of metapelites. In: Kerrick, D. M. (ed), Contact Metamorphism. *Mineralogical Society of America Reviews in Mineralogy,* 26, 105-206.

Rieffe, E. C., van Lil, R., Verweij, P. M., & Beunk, F. F. (1993). Preliminary data from the Loftahammar Shear Zone, southeastern Sweden. In M. B. Stephens & C.-H. Wahlgren (Eds.), Ductile shear zones in the Swedish segment of the Baltic Shield. Abstracts and excursion guide. *Sveriges Geol. Undersökning, Rapp. och Meddel*, 76, p. 16.

Russell, R. V. (1967). Paleocurrent analysis in deltaic Precambrian meta-sedimentary rocks from Västervik, Sweden. *Geologiska Föreningen i Stockholm Förhandlingar*, 89(1), 105–115.

Russell, R. V. (1969). Porphyroblastic differentiation in fleck gneiss from Västervik, Sweden. *Geologiska Föreningen i Stockholm Förhandlingar*, 91(2), 217–282.

Sawyer, E. W. (2008). *Atlas of Migmatites.* The Canadian Mineralogist Special Publication 9. NRC Research Press.

Stephens, M. B., & Andersson, J. (2015). Migmatization related to mafic underplating and intra- or back-arc spreading above a subduction boundary in a 2.0–1.8 Ga accretionary orogen, Sweden. *Precambrian Research*, 264, 235–257.

Sultan, L., Claesson, S., & Plink-Björklund, P. (2005). Proterozoic and Archaean ages of detrital zircon from the Palaeoproterozoic Västervik Basin, SE Sweden: Implications for provenance and timing of deposition. *GFF*, 127(1), 17–24.

Sultan, L., & Plink-Björklund, P. (2006). Depositional environments at a Palaeoproterozoic continental margin, Västervik Basin, SE Sweden. *Precambrian Research*, 145(3-4), 243–271.

Sundblad, K., Salin, E., Claesson, S., Gyllencreutz, R., & Billström, K. (2021). The Precambrian of Gotland, a key for understanding the Proterozoic evolution in southern Fennoscandia. *Precambrian Research*, 363, 106321.

Svenonius, F. (1907). *Beskrifning till kartbladet Vastervik.* Sveriges Geologiska Undersökning (SCU), Ser. Aa, No. 137.

Thomas, H., & Rana, H. (2019). Valid garnet-biotite thermometer: A comparative study. *Journal of Nepal Geological Society*, 58, 61–68.

Thomas, H., Rana, H., & Mishra, A. (2020). APPLicability of garnet-cordierite (Gt-Crd) geothermometer. *Journal of Nepal Geological Society*, 60, 147-161.

Torbohm, M., (2023, August 23). *Västervik Fleckengestein.* Kristallin. https://www.kristallin.de/Schweden/Vaestervik-Fleckengestein/Vaestervik-Fleckengestein.html

Trumbull, R. B. (1988). Petrology of flecked gneisses in the northern Wet Mountains, Fremont County, Colorado. *Geological Society of America Bulletin*, 100(2), 247–256.

van Tuyl, M. M. (1977). Petrographic and mineral chemical investigations on pelitic xenoliths in the Grundemar Massif, Västervik area, SE Sweden. *Unpublished internal report. Vrije Universiteit, Amsterdam.*

Vollbrecht, A., & Leiss, B. (2008). Complex fabric development in Paleoproterozoic meta-quartzites of the Västervik Basin, SE Sweden. *GFF*, 130(1), 41–45.

Waters, D. J. (2001). The significance of prograde and retrograde quartz-bearing intergrowth microstructures in partially melted granulite-facies rocks. *Lithos*, 56(1), 97–110.

Whitney, D. L., & Evans, B. W. (2009). Abbreviations for names of rock-forming minerals. *American Mineralogist*, 95(1), 185–187.

Perplex data

Manual:
D. Castelli, C. Groppo (29-1-2022). PERPLE_X TUTORIALS. *Dipartimento di Scienze della Terra, Università di Torino.* https://www.perplex.ethz.ch/perplex/tutorial/Castelli_Groppo_Torino_Tutorial/previous_versions/

Thermodynamic dataset:
hp62ver.dat
https://www.perplex.ethz.ch/perplex/datafiles/

Version:
Perple_X 6.9.1
https://www.perplex.ethz.ch/perplex/ibm_and_mac_archives/WINDOWS/previous_version/

Appendix A, Images

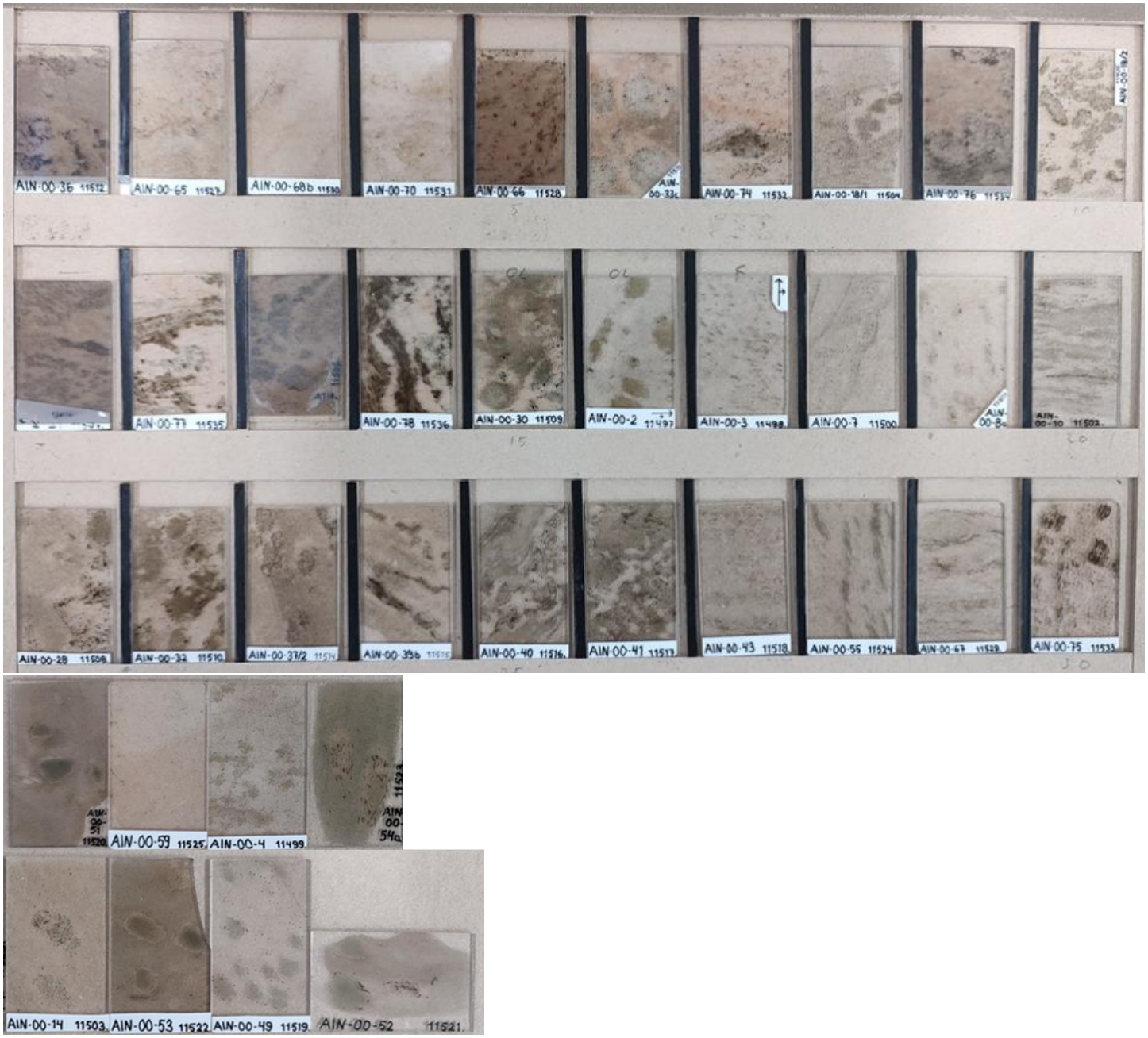

Figure A1: Overview of the thin sections analysed.

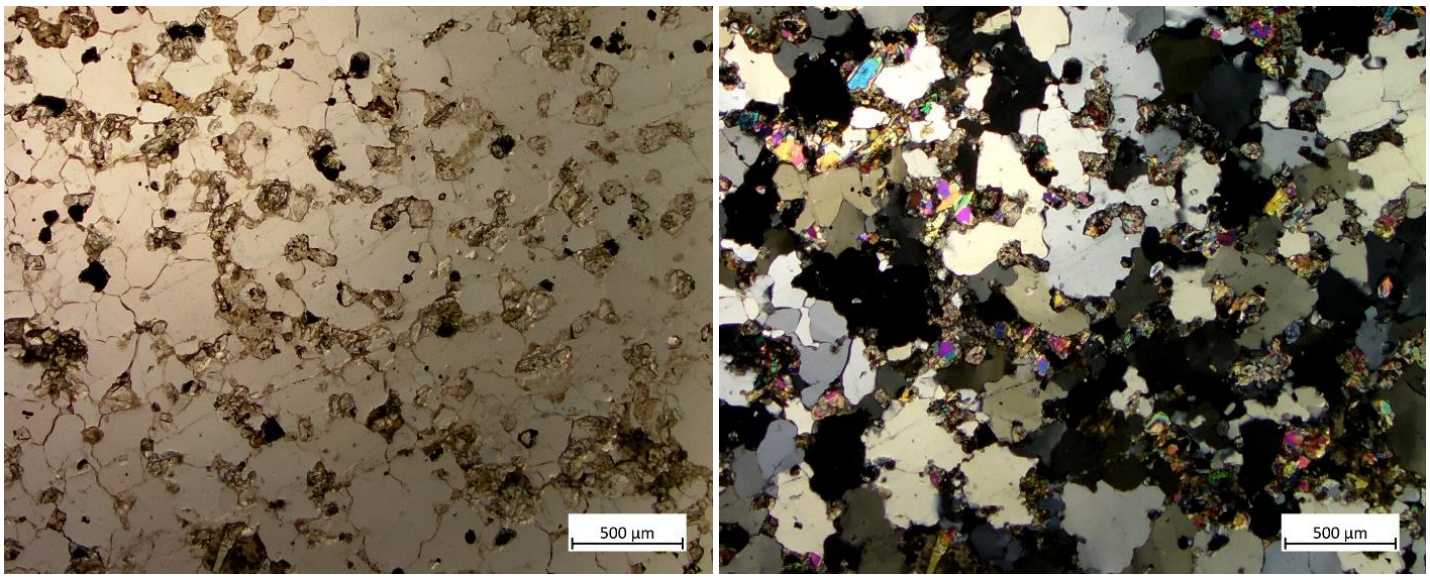

Figure A2: Leucosome in 11500. In PPL and XPL. Note the scarcity of feldspars.

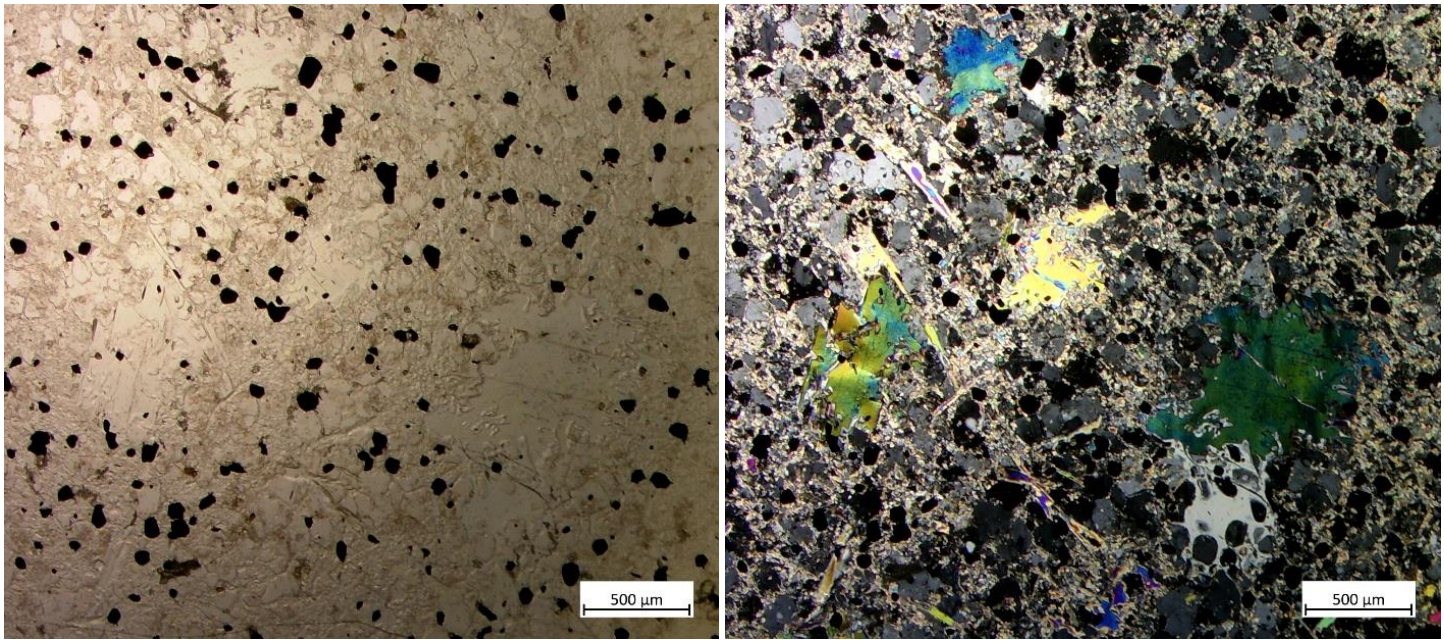

Figure A3: Mesosome in 11497. In PPL and XPL. Not the absence of biotite, the coarse muscovite and feldspar replaced by sericite.

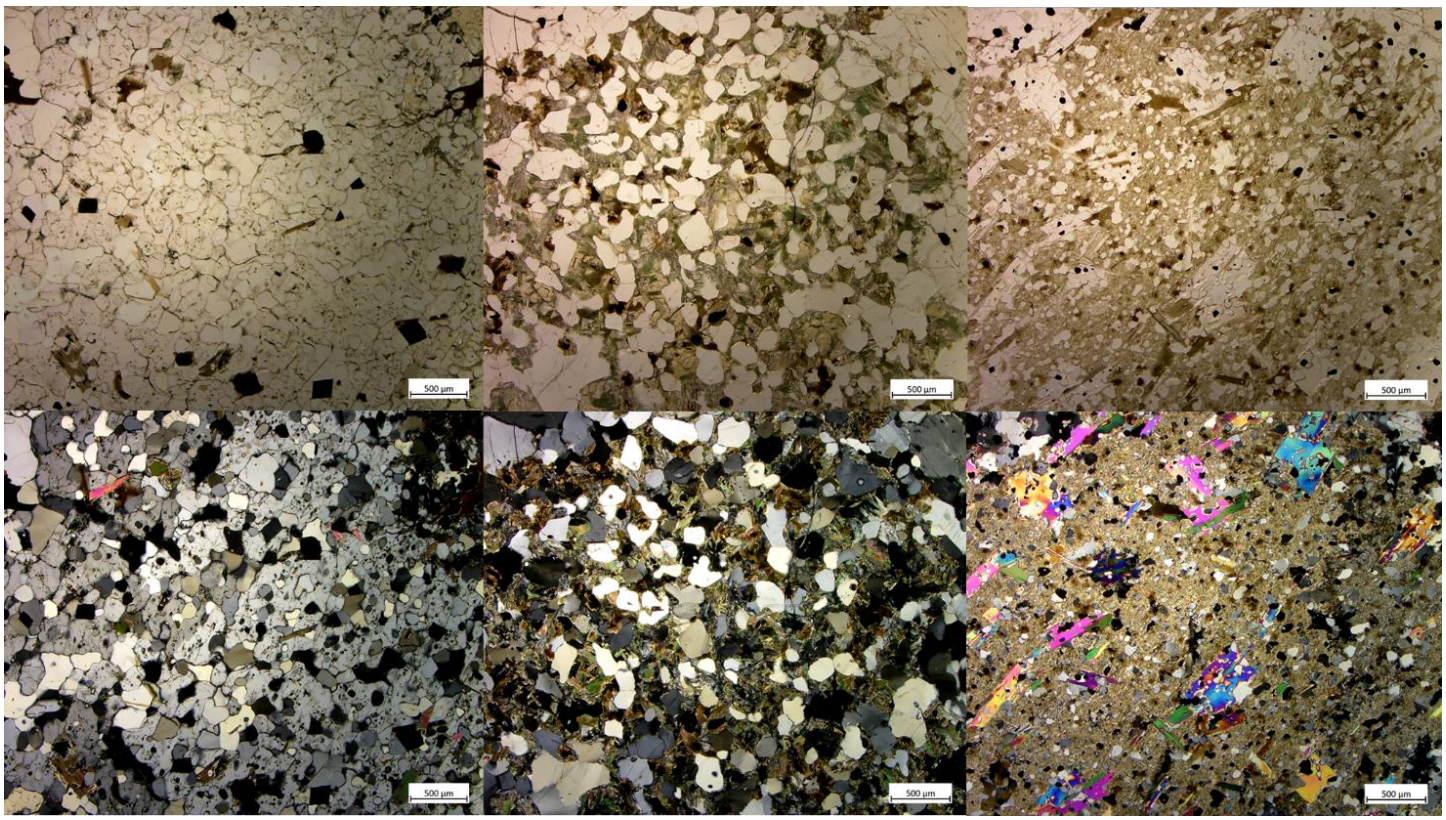

Figure A4: Overview of the recrystallization of cordierite poikiloblasts in PPL (upper) and XPL (lower). 11511 (left) is composed of cordierite and andalusite, 11504 (centre) is composed of andalusite, biotite and chlorite and 11497 (right) is composed of sericite, biotite and muscovite. This defines the melanosome types a, b and c.

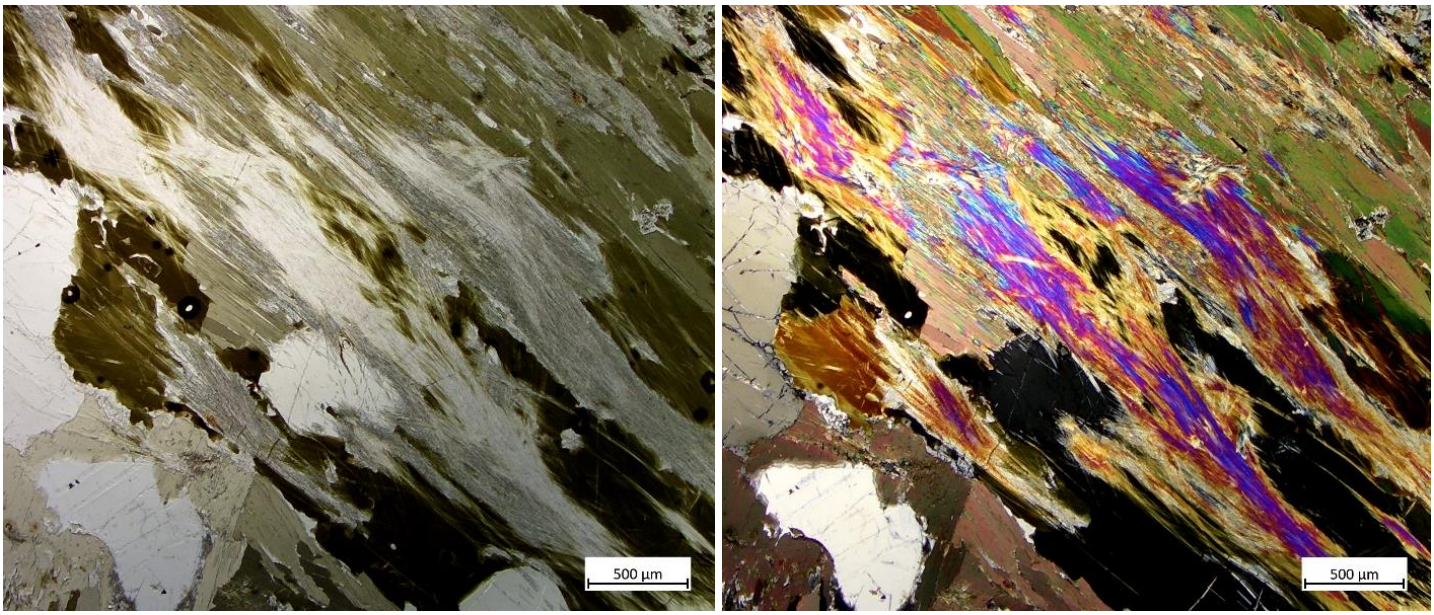

Figure A5: Typical example of melanosome2 in 11533. In PPL and XPL.

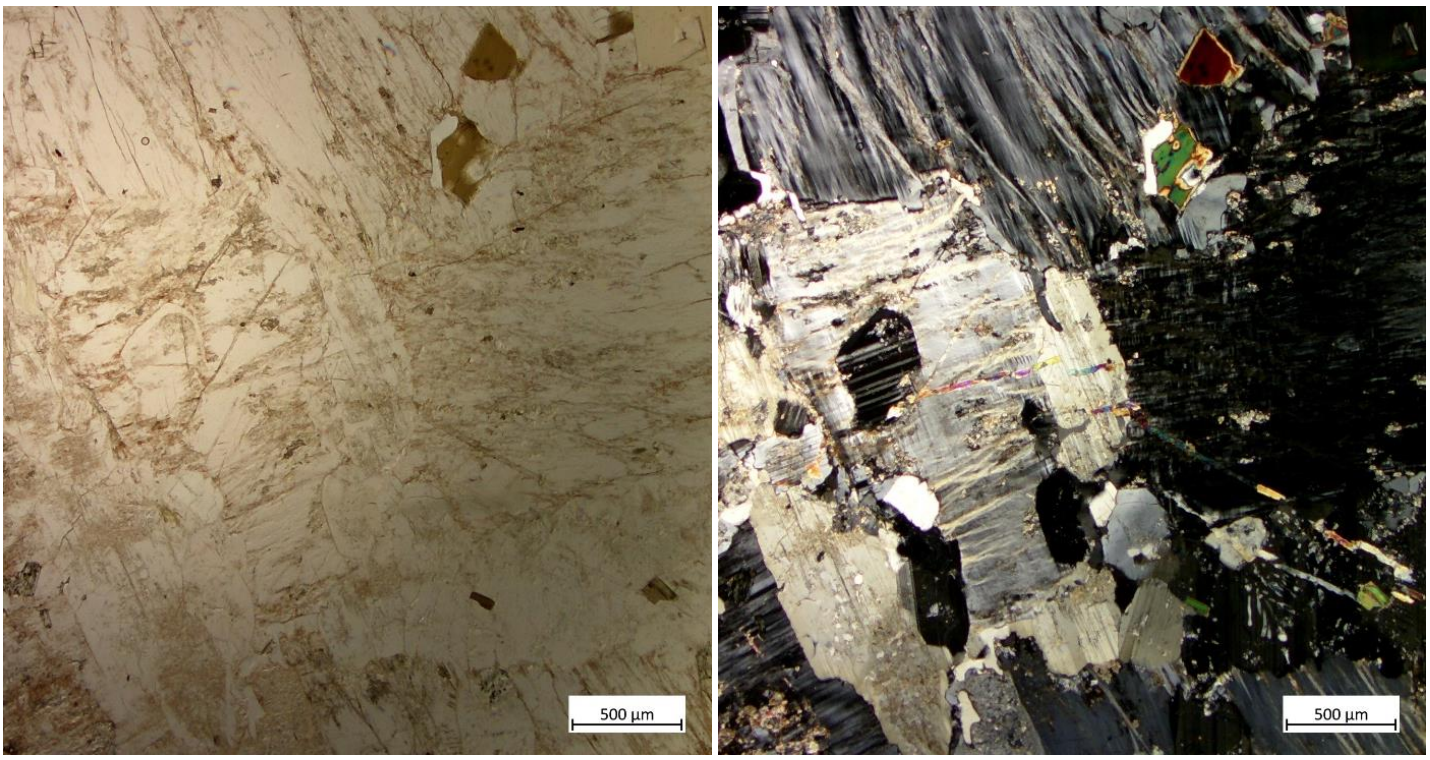

Figure A6: Typical example of Leucosome1 in 11528. In PPL and XPL.

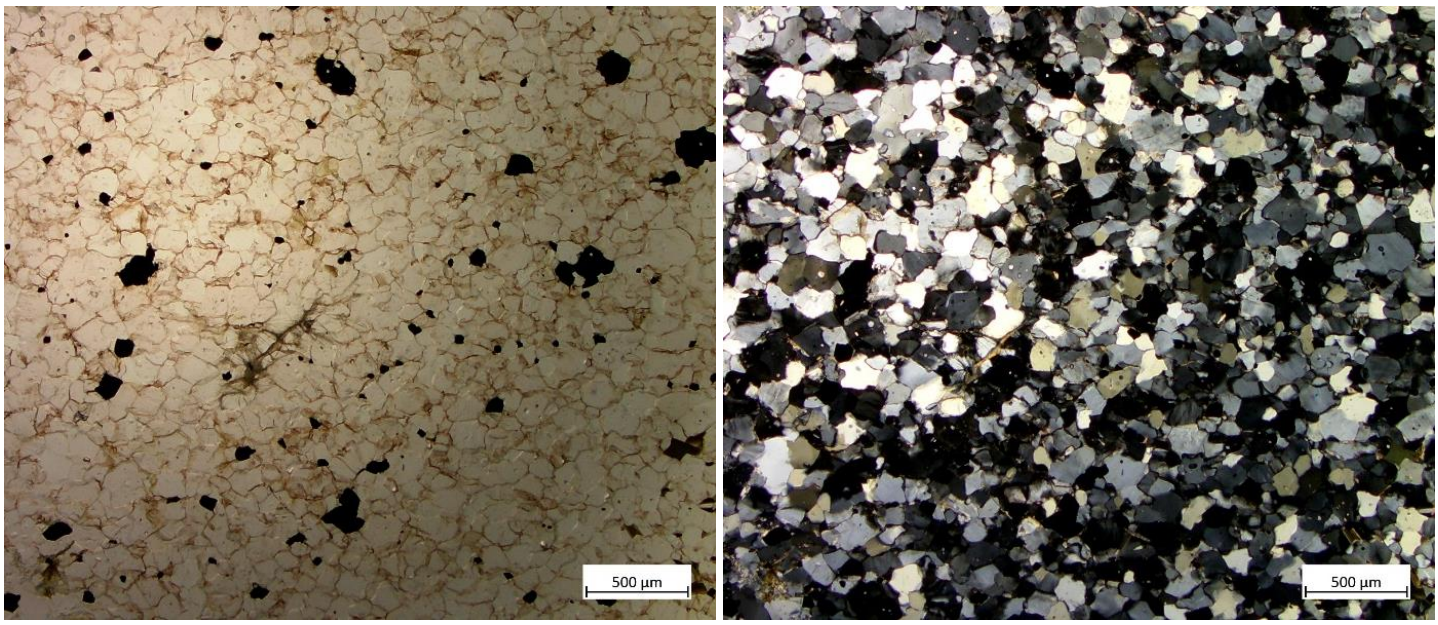

Figure A7: Typical example of Leucosome2 in 11515. In PPL and XPL.

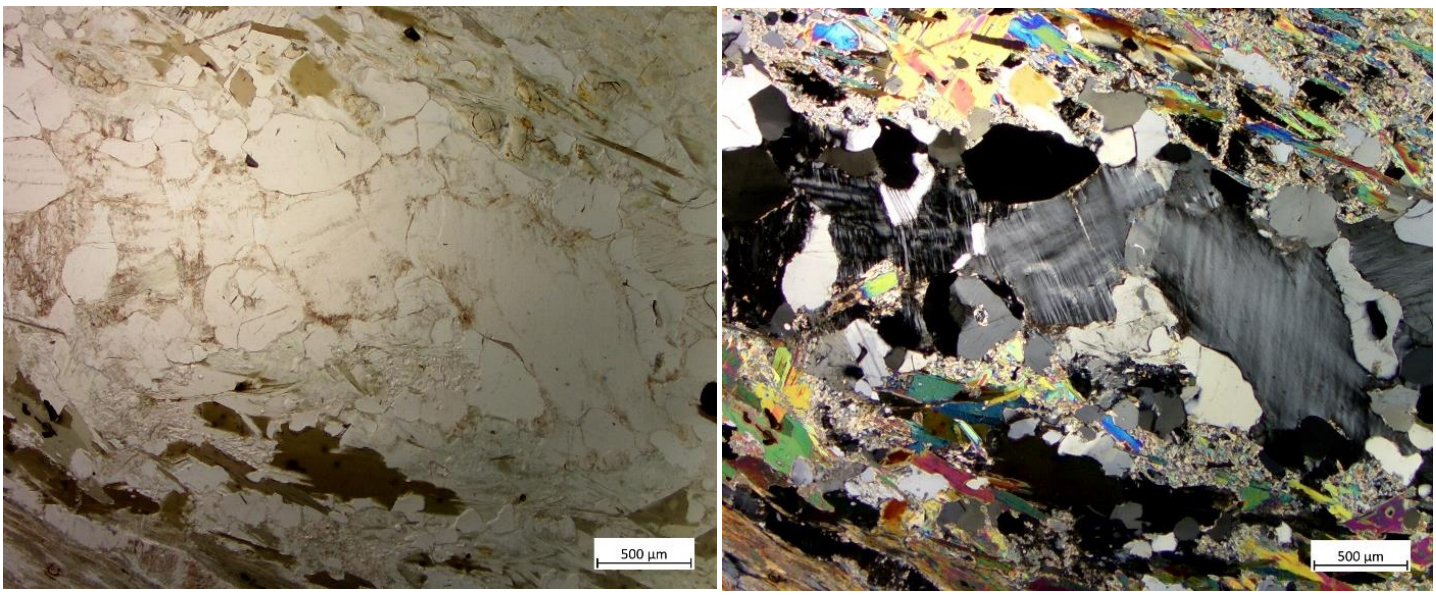

Figure A8: Leucosome1 lense in 11529. In PPL and XPL.

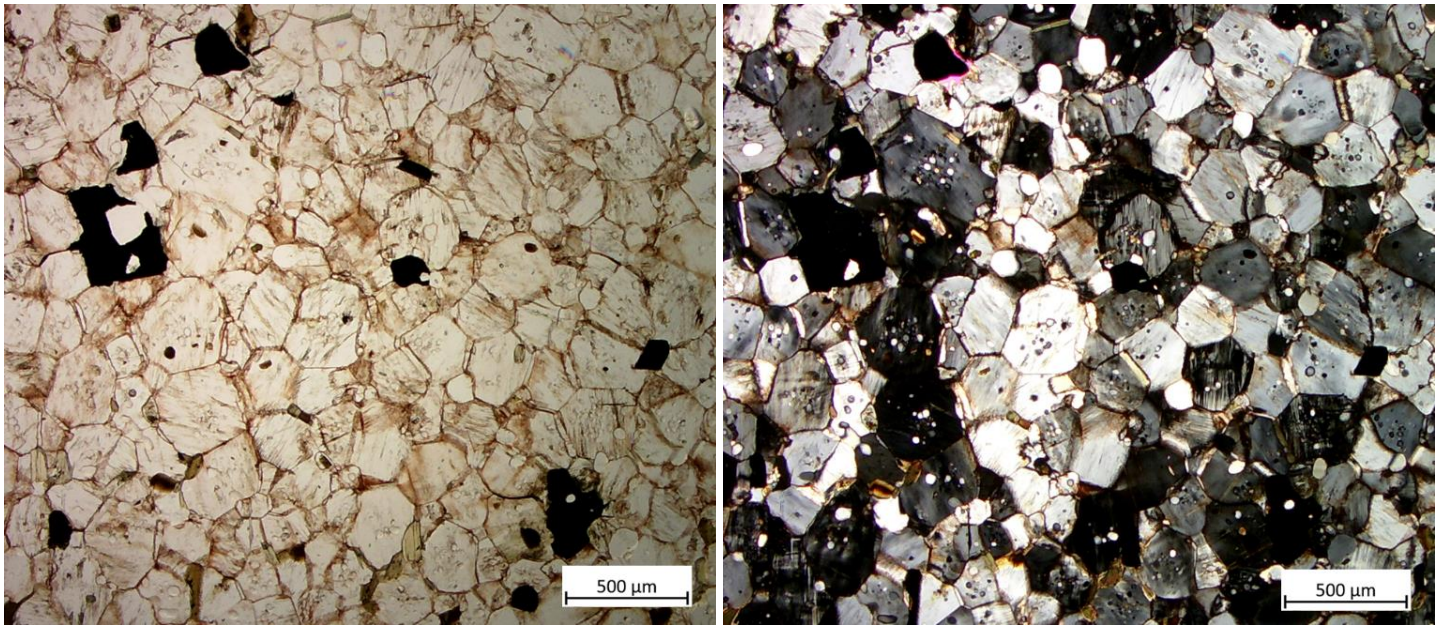

Figure A9: Leucosome2 in 11511. In PPL and XPL. Note the intergranular minerals.

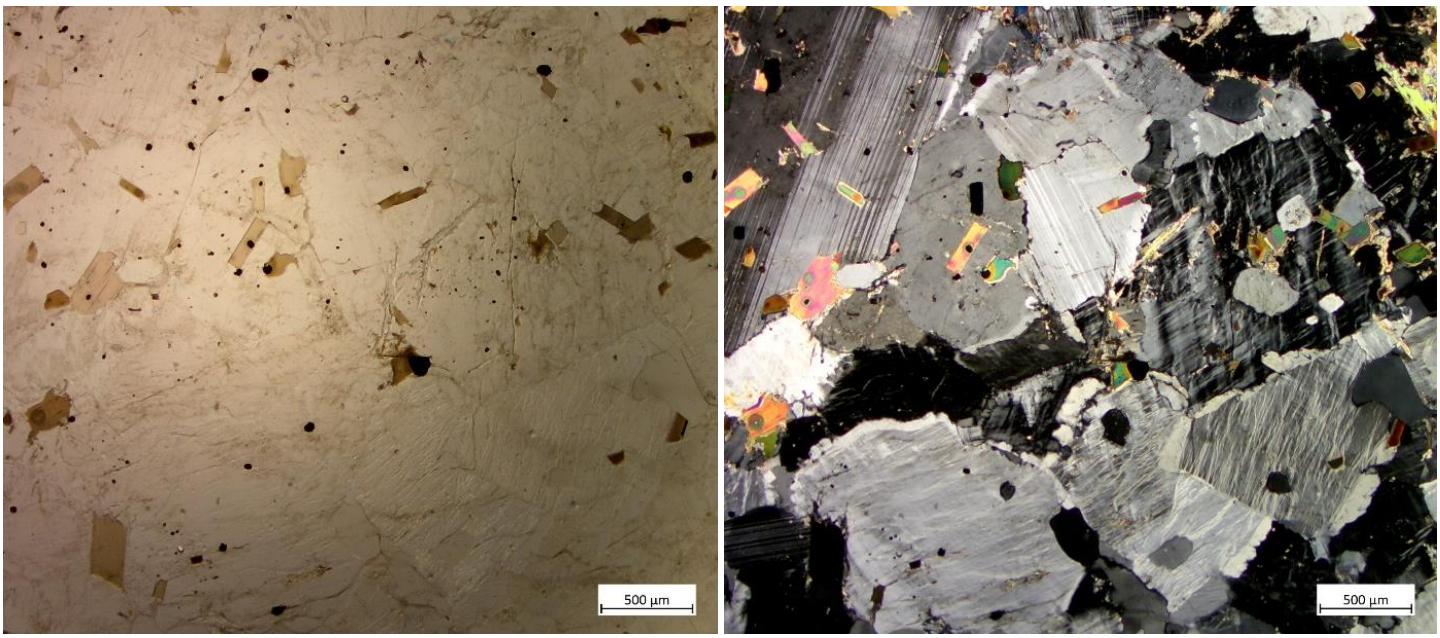

Figure A10: Leucosome1 in 11531. In PPL and XPL. Note the alkali feldspar and plagioclase phenocrysts and intergranular plagioclase.

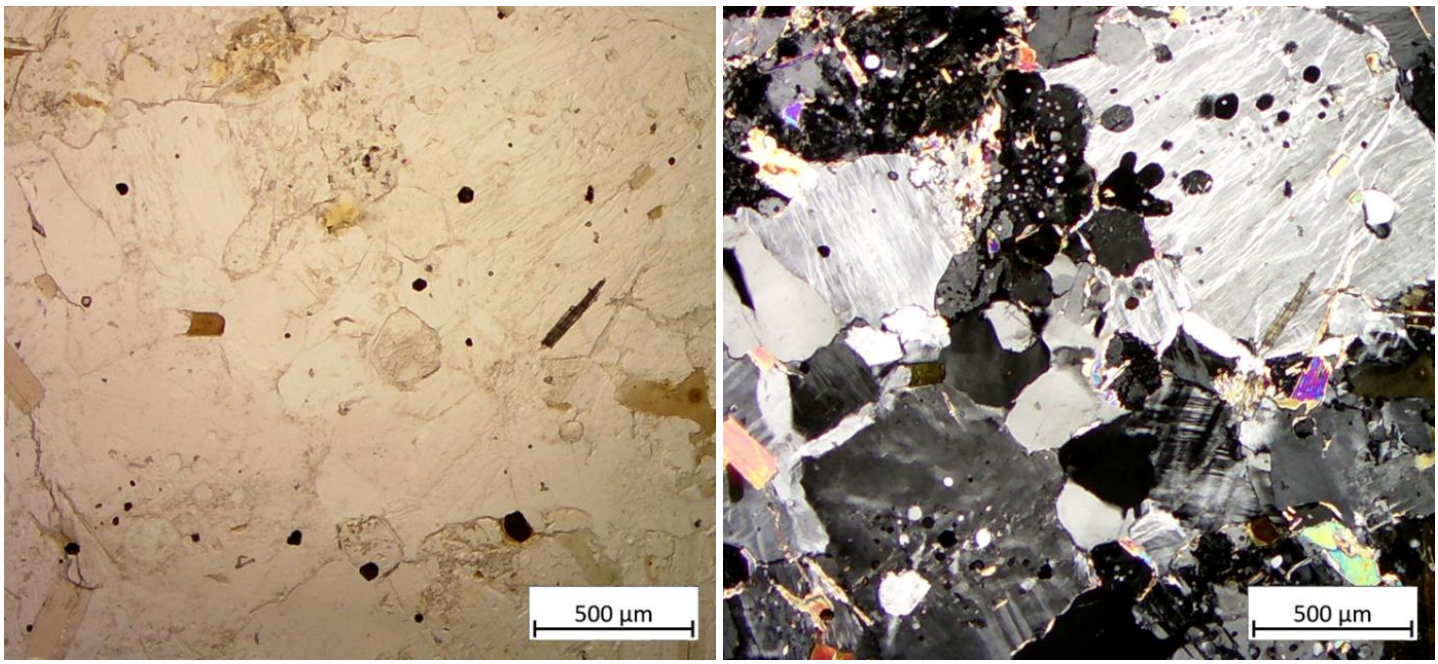

Figure A11: Leucosome1 in 11531. In PPL and XPL. Note the feldspar poikiloblasts.

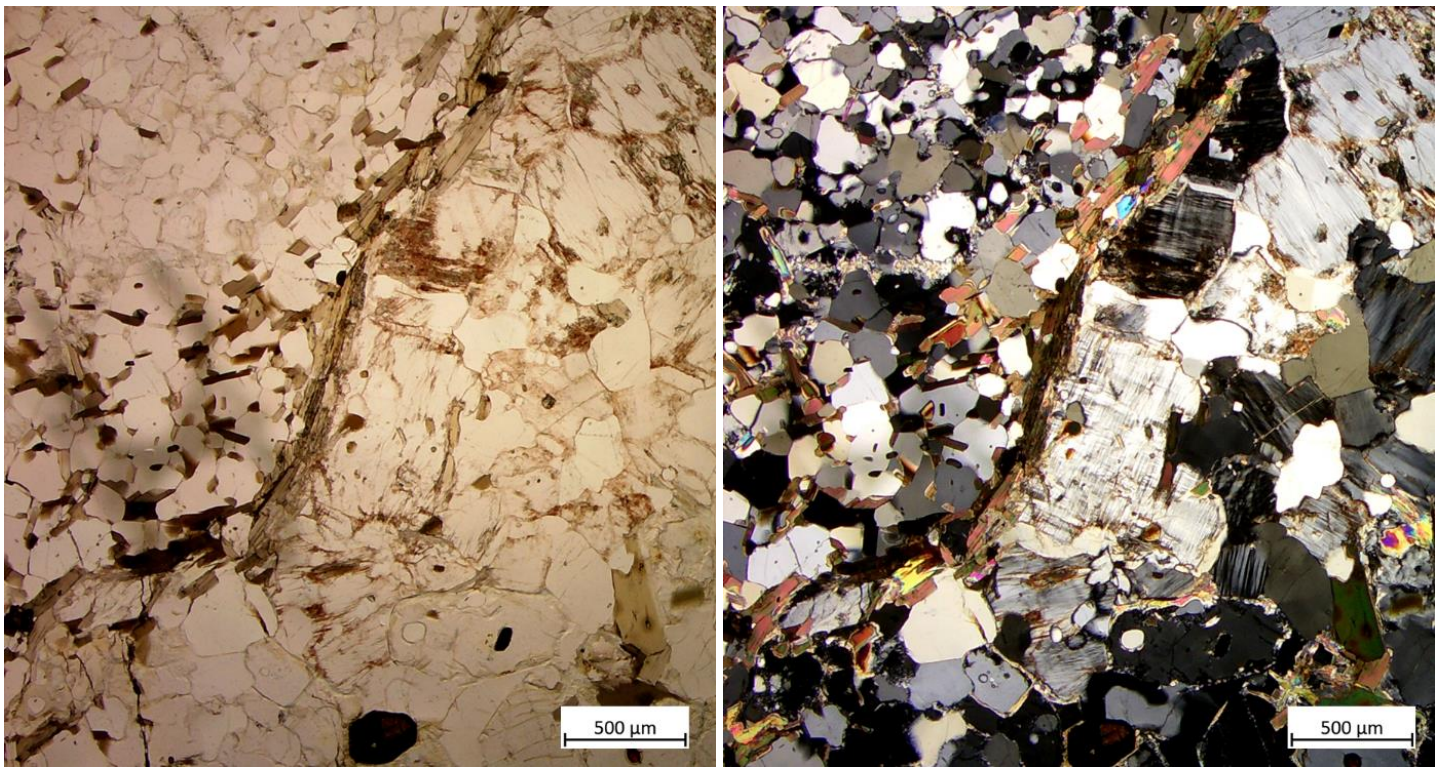

Figure A12: Biotite selvedge on the interface of the mesosome (left) and leucosome (right) in 11527. In PPL and XPL.

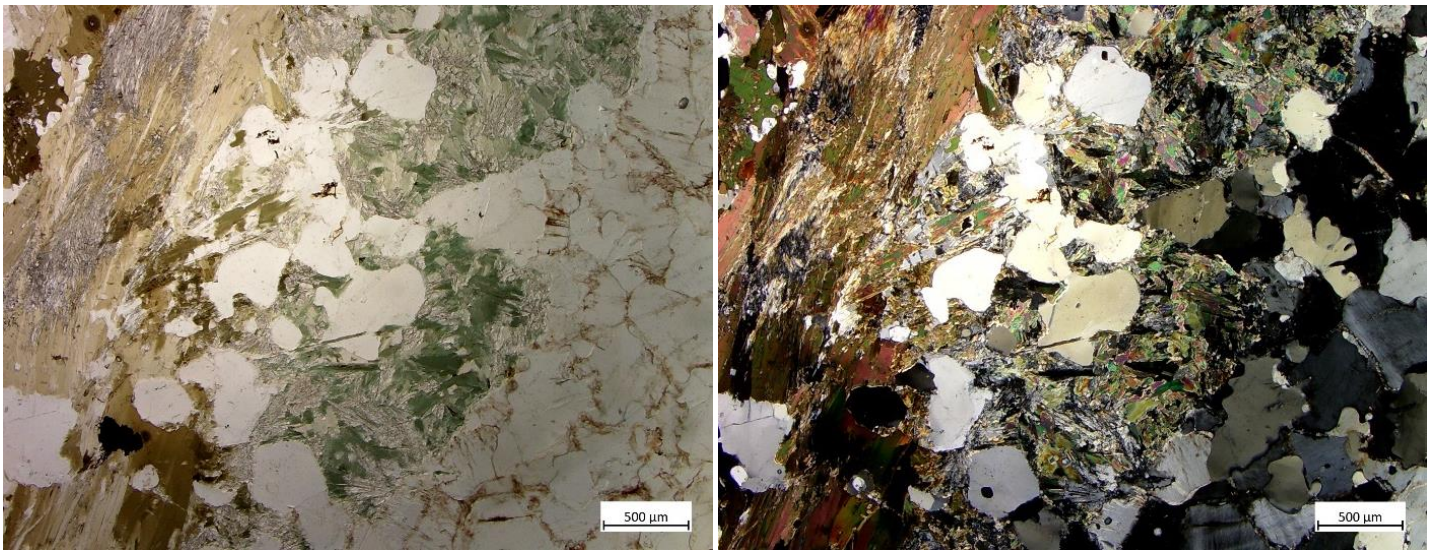

Figure A13: Melanosome1b (green) and melanosome1 (brown) in 11535. In PPL and XPL. Note the connectivity and transition between the melanosome types and respective abundance in andalusite or sillimanite.

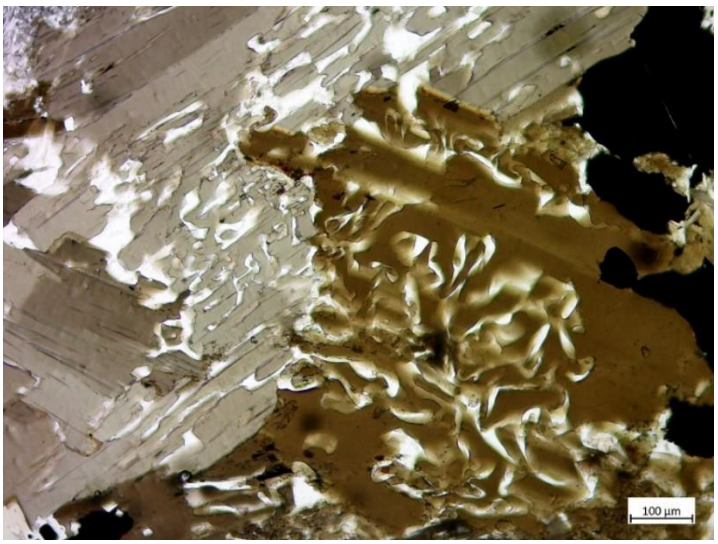

Figure A14: Intergrowth of biotite with quartz in 11535. In PPL and XPL.

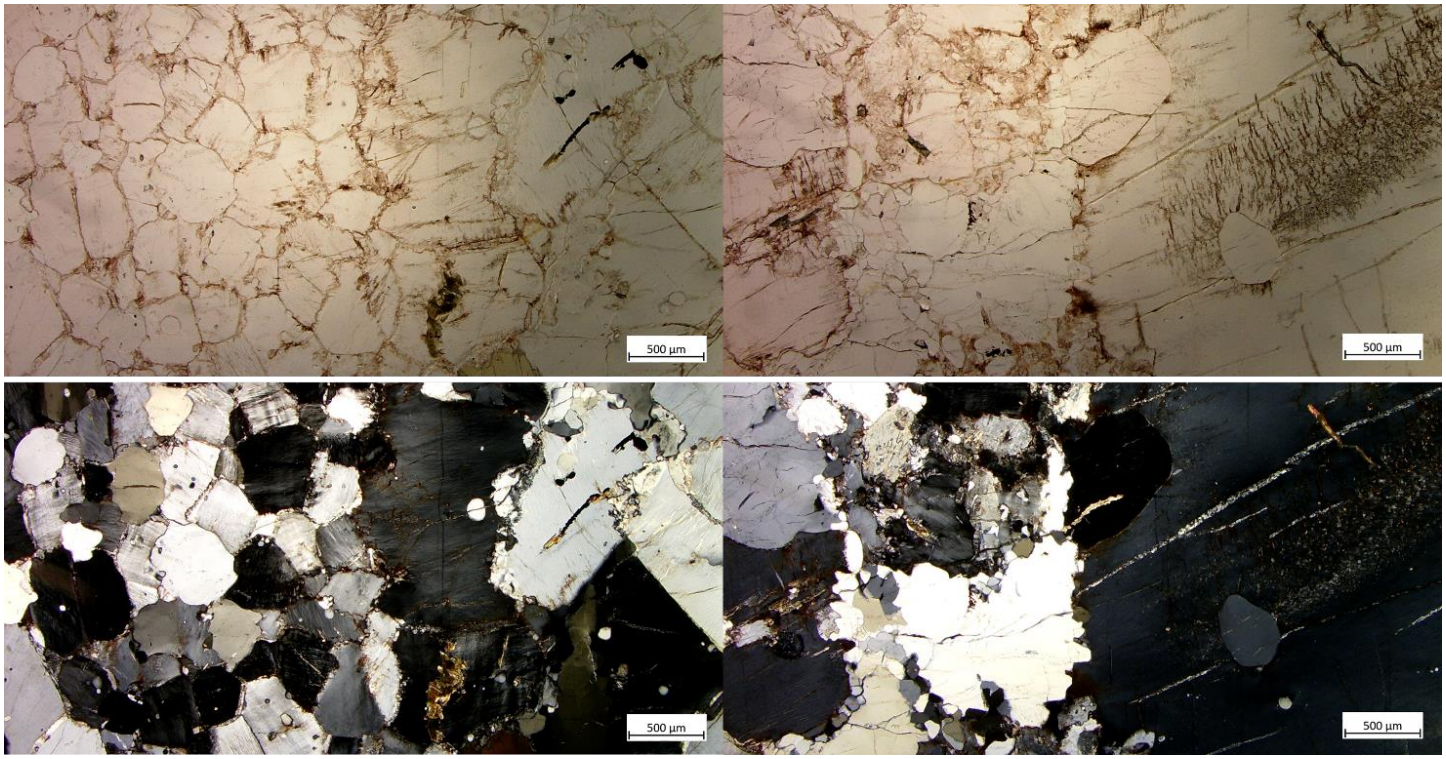

Figure A15: Coarsening of the leucosome from left to right. Three grain sizes are observed with twice a distinctive interface (left and right image). In 11535. In PPL (upper) and XPL (lower).

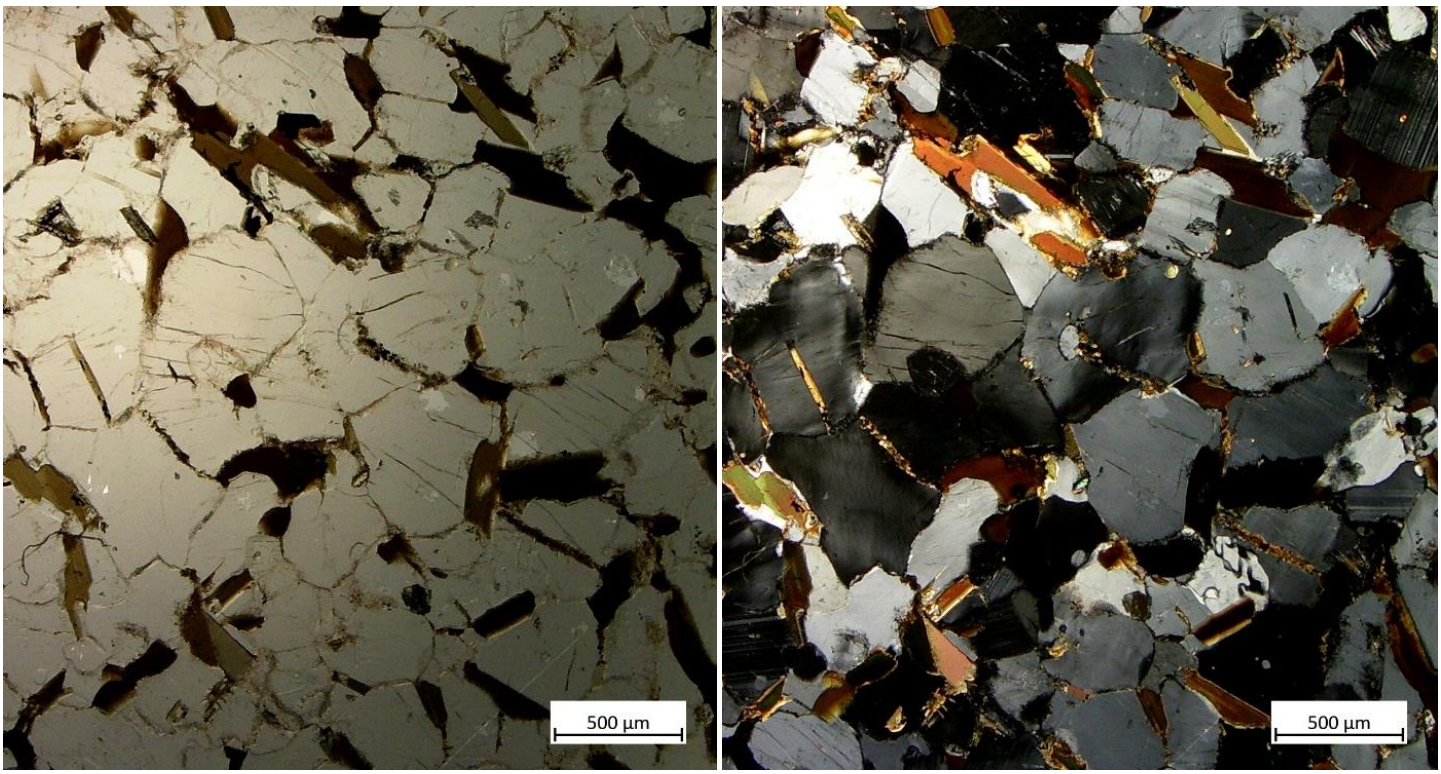

Figure A16: Typical overview of the mesosome in 11506. In PPL and XPL.

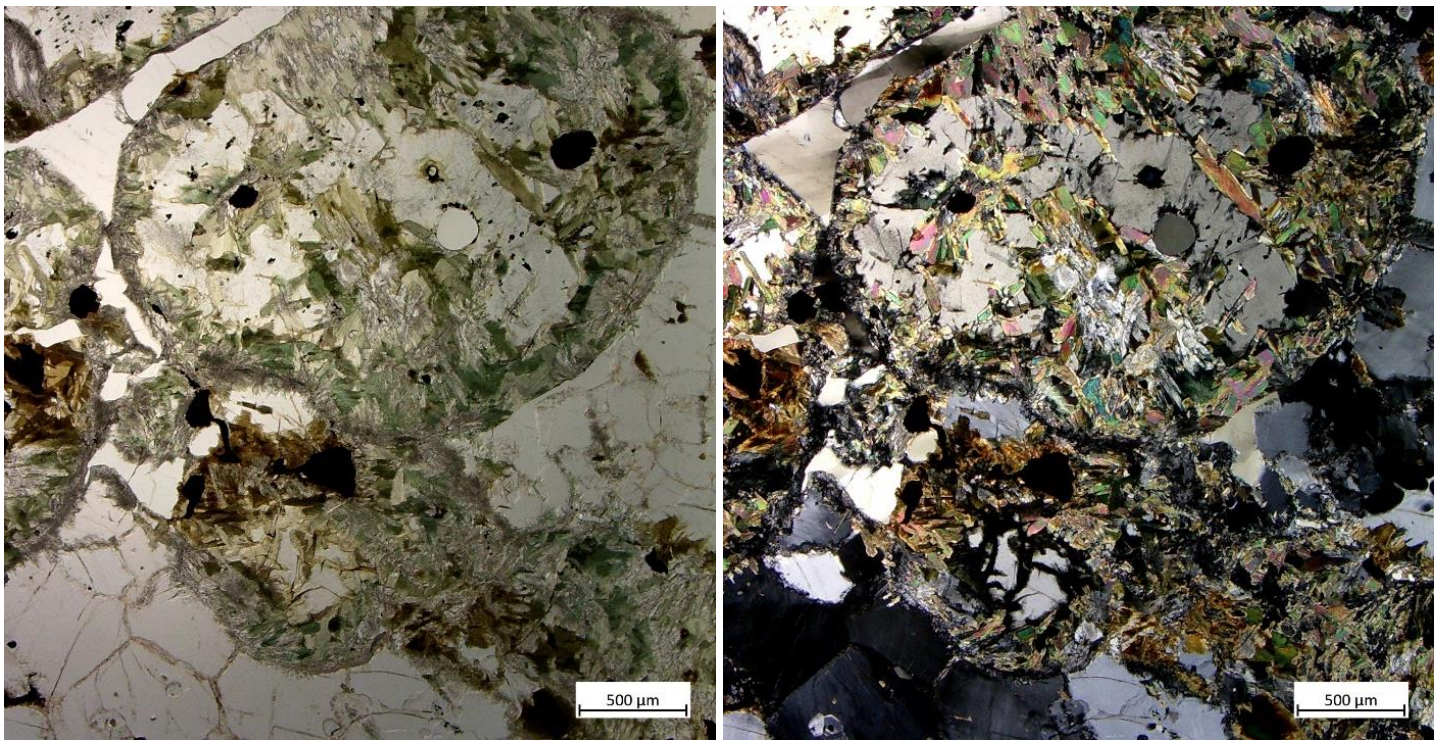

Figure A17: Typical overview of the melanosome in 11506. In PPL and XPL.

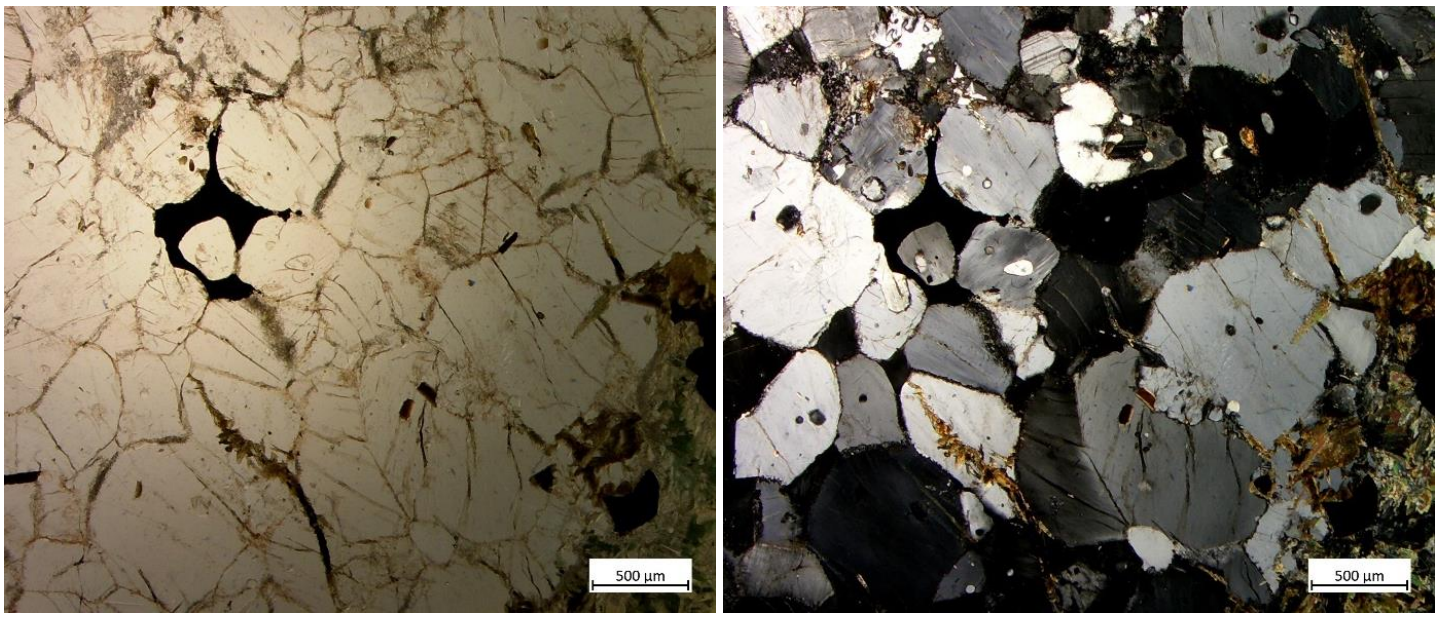

Figure A18: Typical overview of the leucosome in 11506. In PPL and XPL.

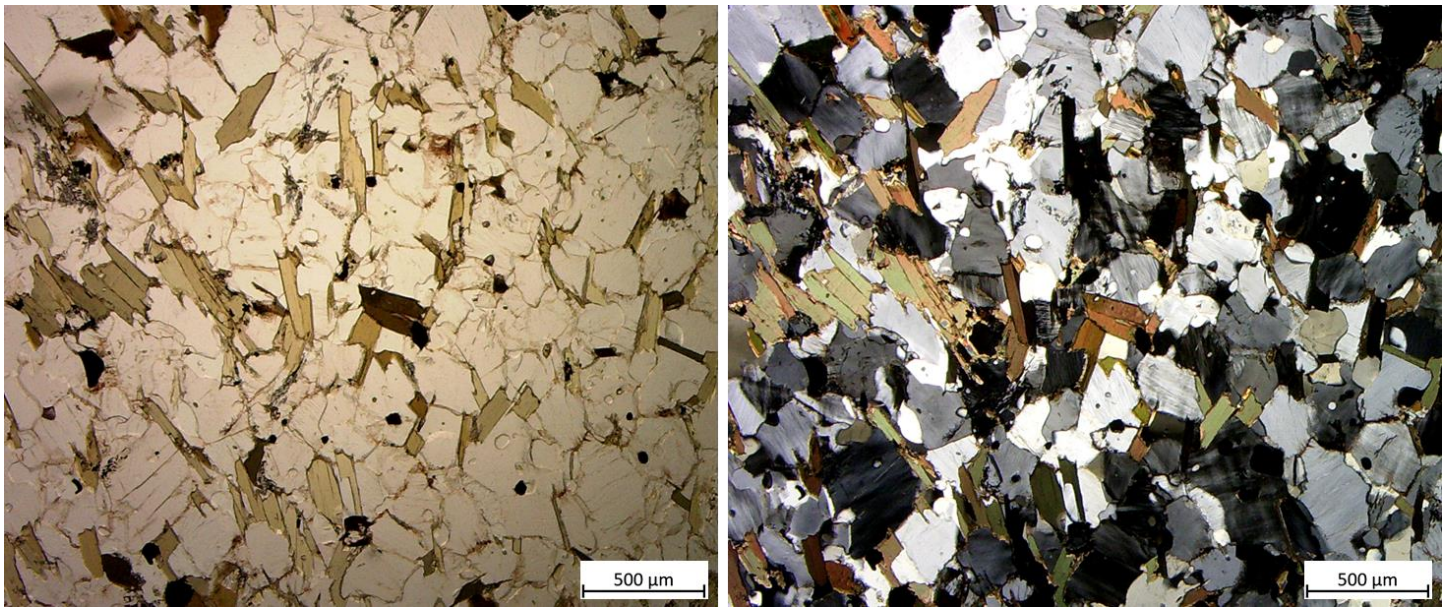

Figure A19: Typical overview of the mesosome in 11507. In PPL and XPL.

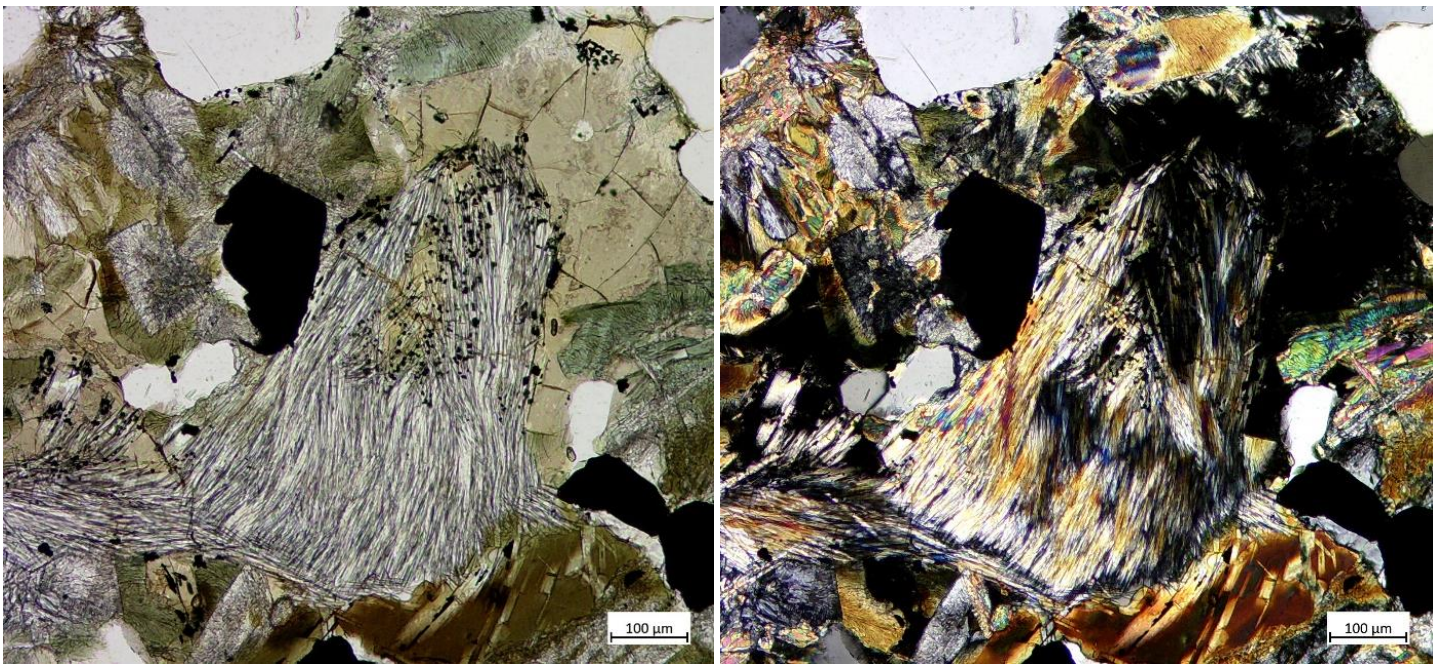

Figure A20: Typical overview of the melanosome1b in 11507. In PPL and XPL.

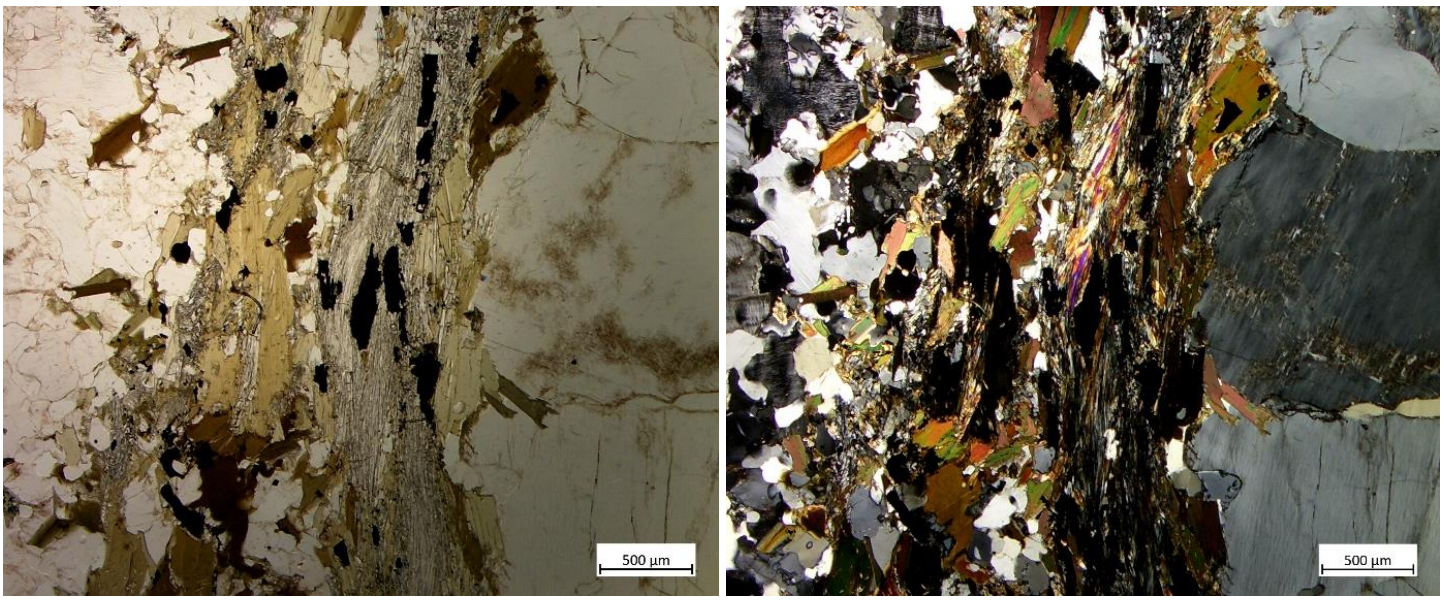

Figure A21: Typical overview of the melanosome2 as well as leucosome1 and leucosome2 on either side of it, in 11507. In PPL and XPL.

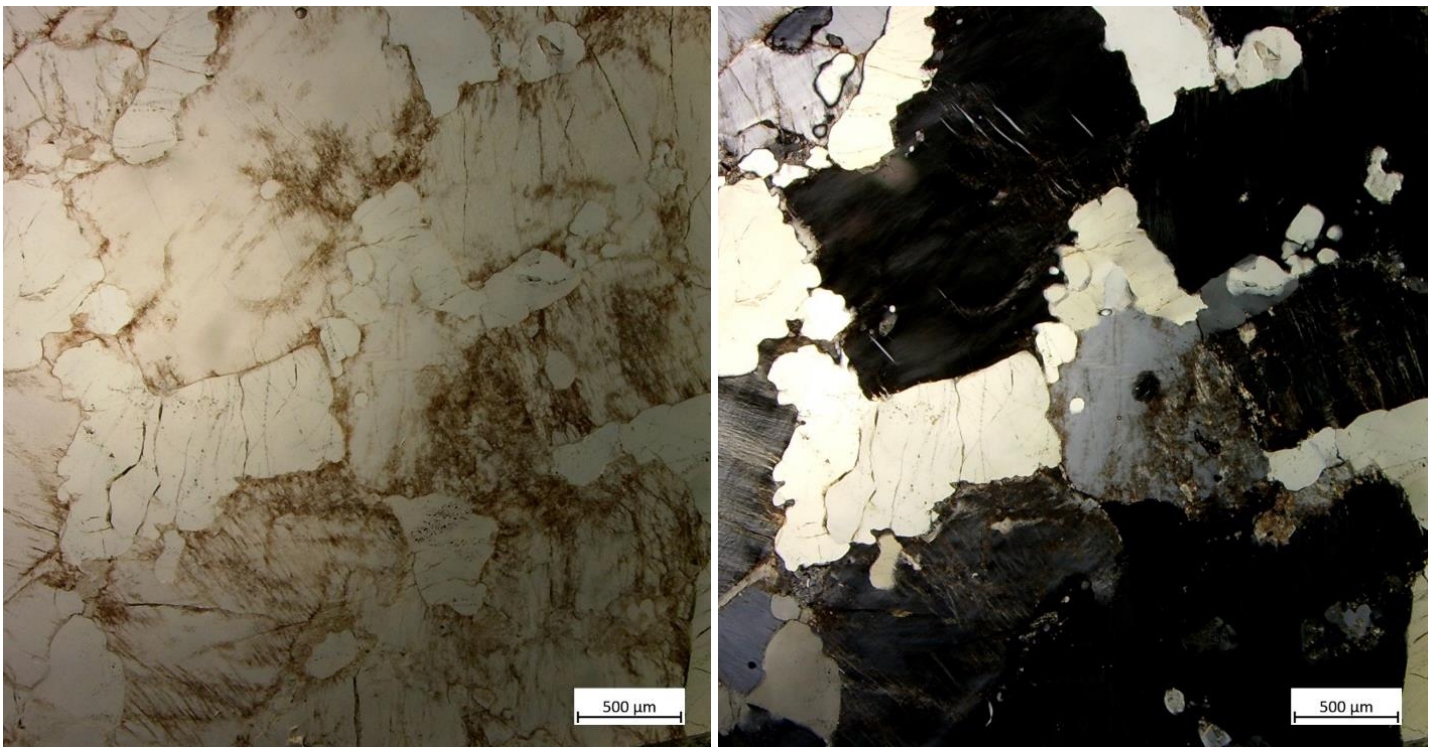

Figure A22: Typical overview of the leucosome1 in 11507. In PPL and XPL.

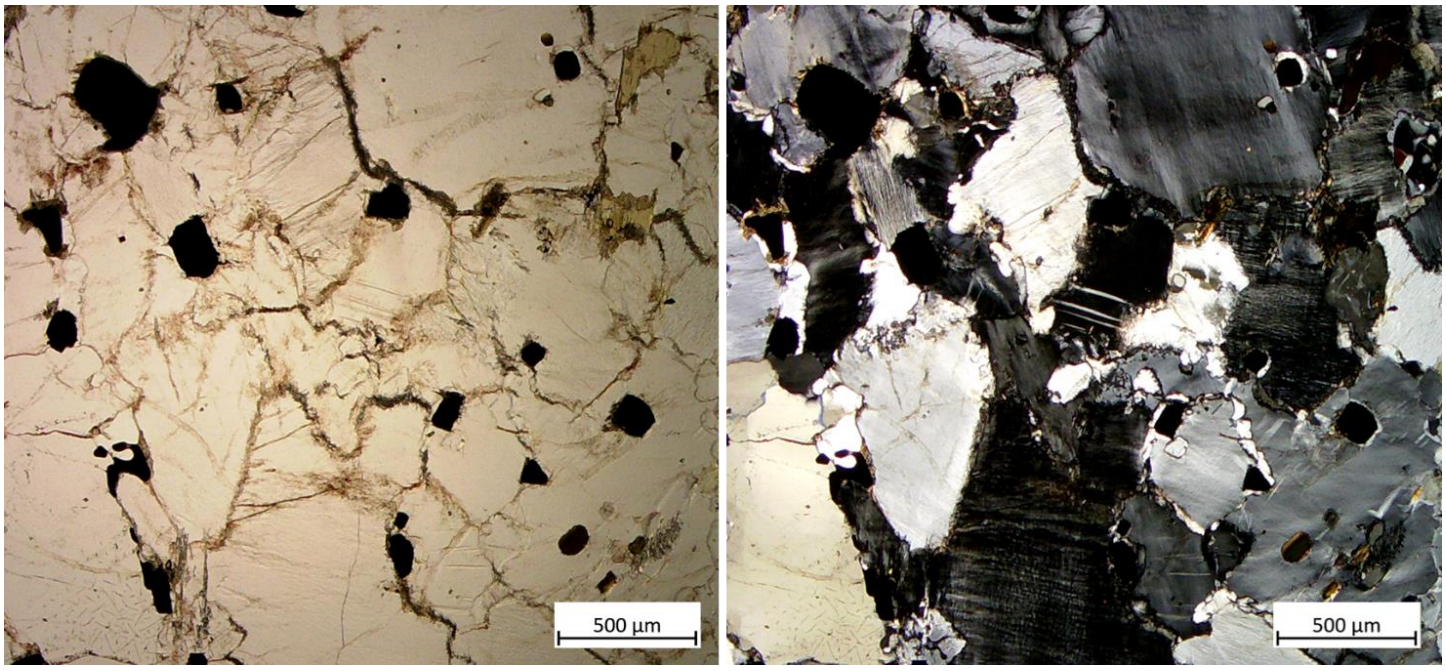

Figure A23: Typical overview of the leucosome2 in 11507. In PPL and XPL.

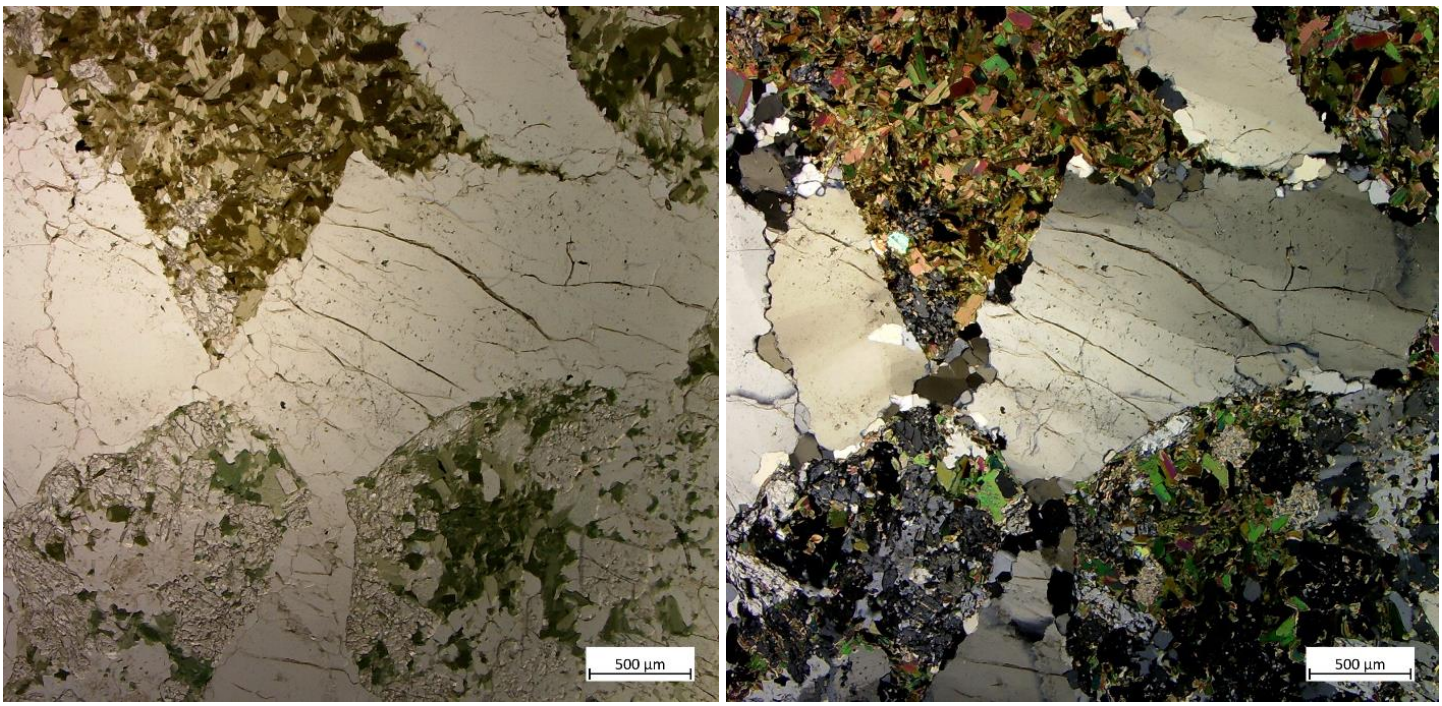

Figure A24: Typical overview of the melanosome1b in 11534. In PPL and XPL. Note the varying composition of the melanosome segments ranging from mostly andalusite to mostly biotite.

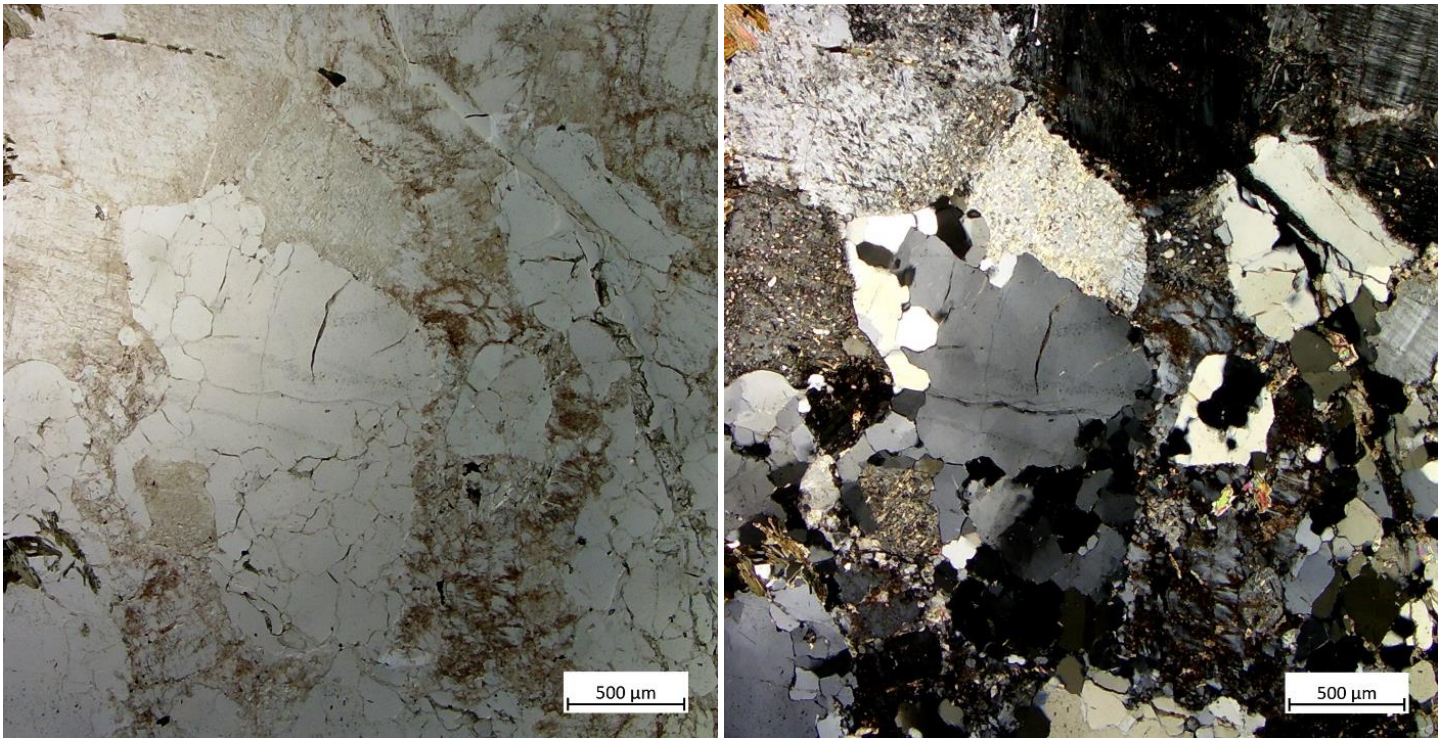

Figure A25: Typical overview of the leucosome1 in 11534. In PPL and XPL.

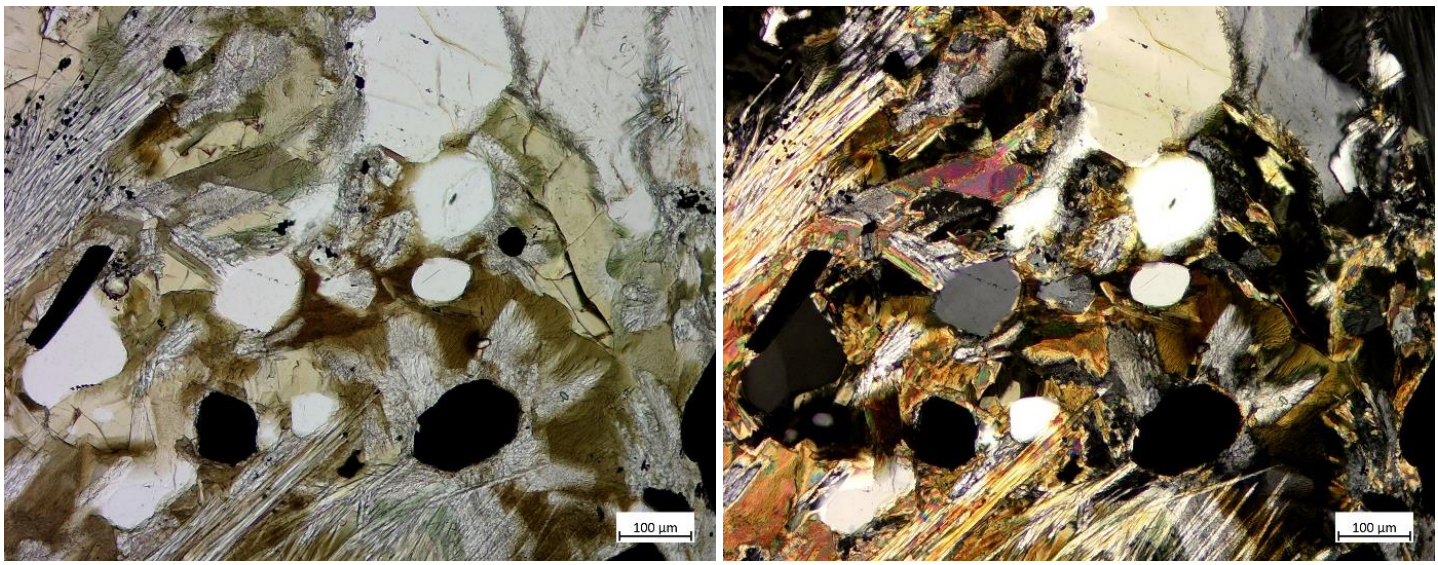

Figure A26: Sillimanite (fibrolite) grown over melanosome1b minerals in 11507. In PPL and XPL.

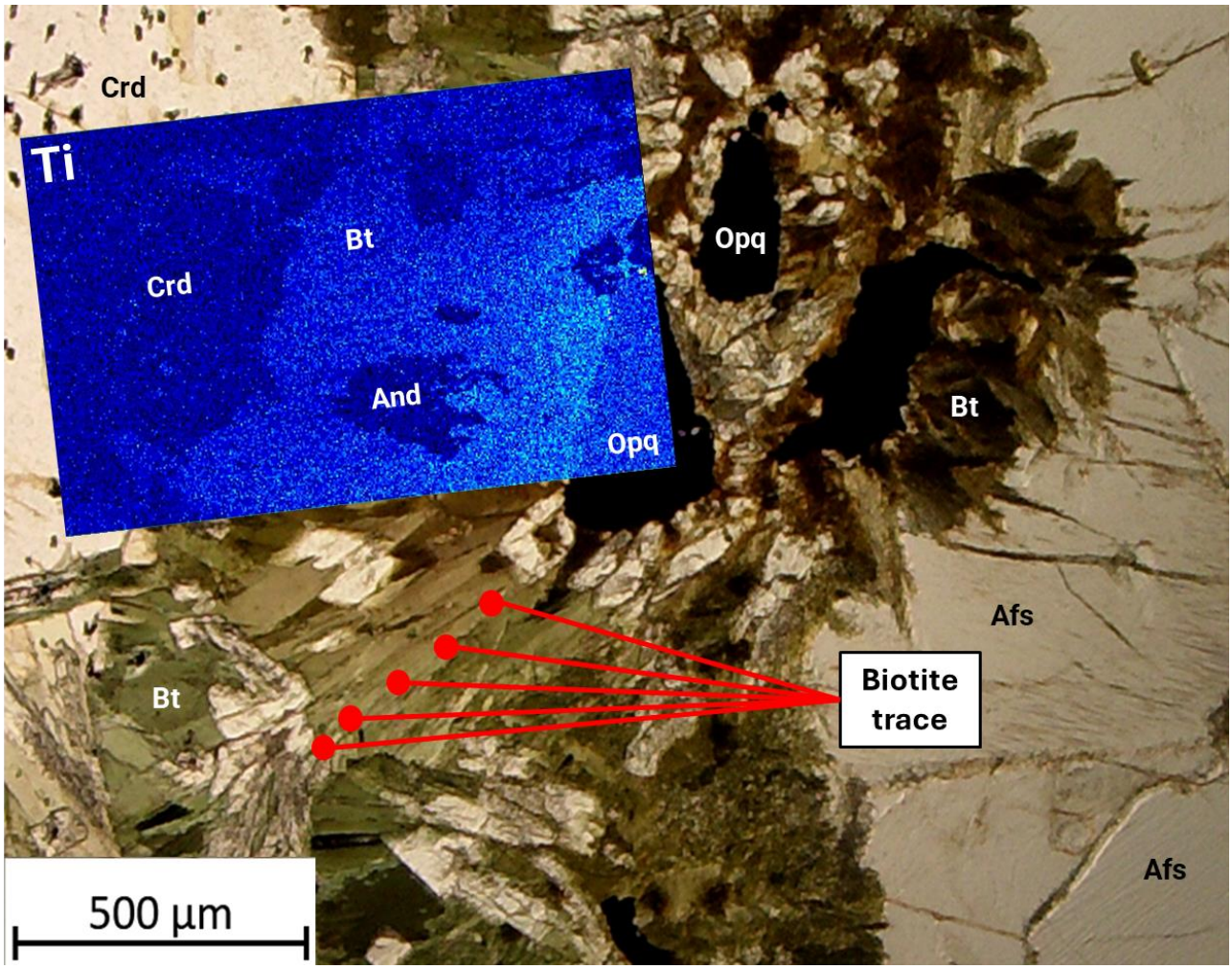

Figure A27: Overview of the melansome1b, bordering the leucosome2 in 11506. In PPL. Indicated is a 5-spot trace over a biotite grain as well as an insert of a Ti chemical map (blue). Lighter blue in this map indicates a higher Ti concentration. Note how Ti in biotite increases towards the iron oxide (Opq) grain.

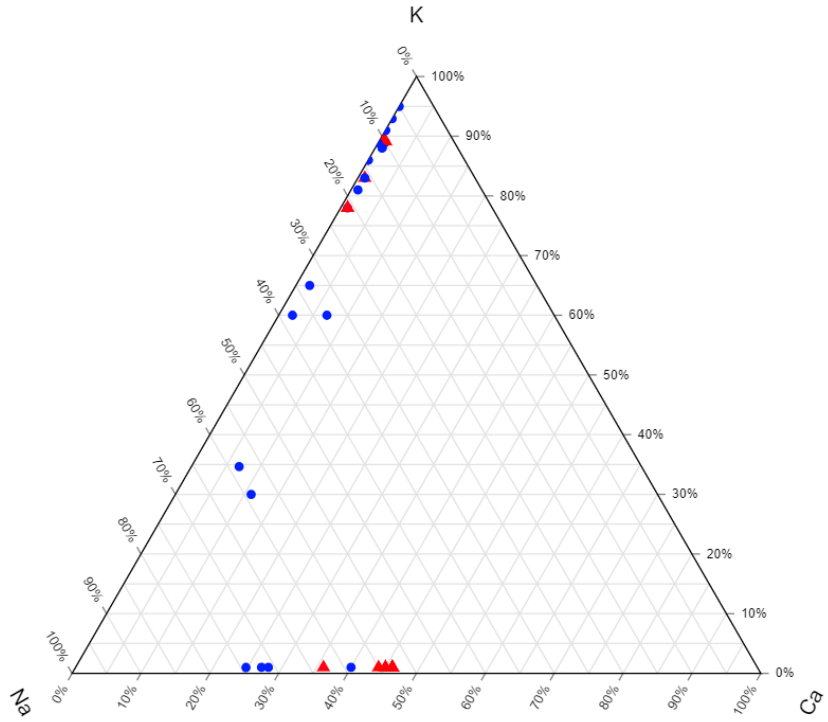

Figure A28: Ternary diagram of all feldspars measured. Red indicates mesosome feldspars, blue indicates leucosome feldspars.

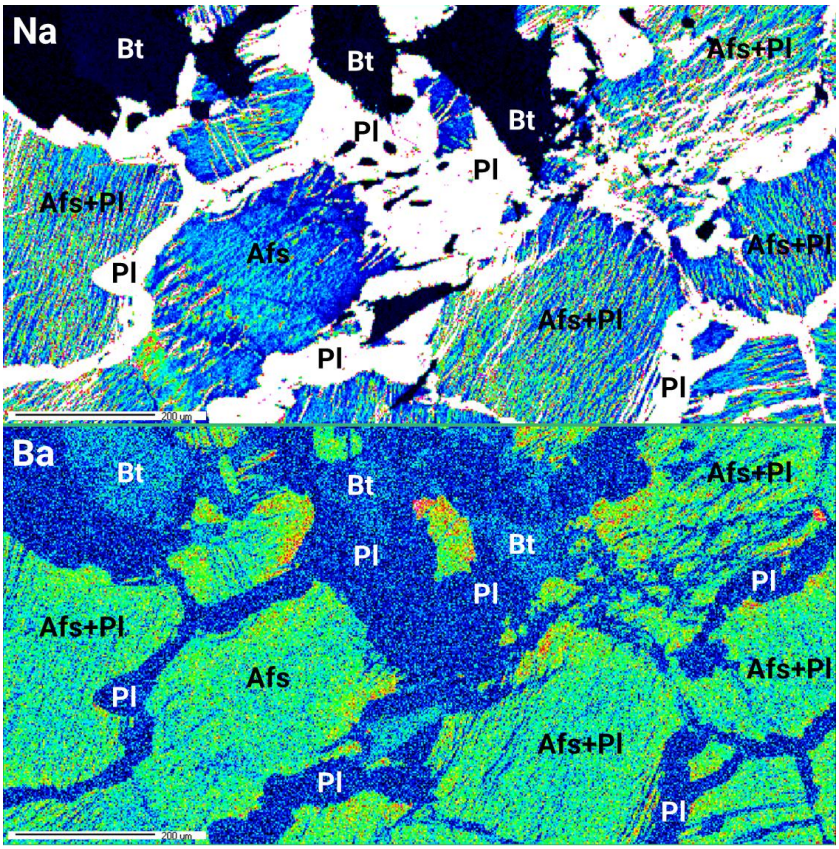

Figure A29: Chemical map of Na (upper) and Ba (lower) in the leucosome2 in 11507. The Na indicates slender grains of Pl (white) surrounding much larger Afs grains (blue). Also visible is albite exsolution in the Afs (green). Black is Qz or Bt. The lower image shows the zoning and enrichment of Ba in Afs grains (green) instead of in Pl (blue).

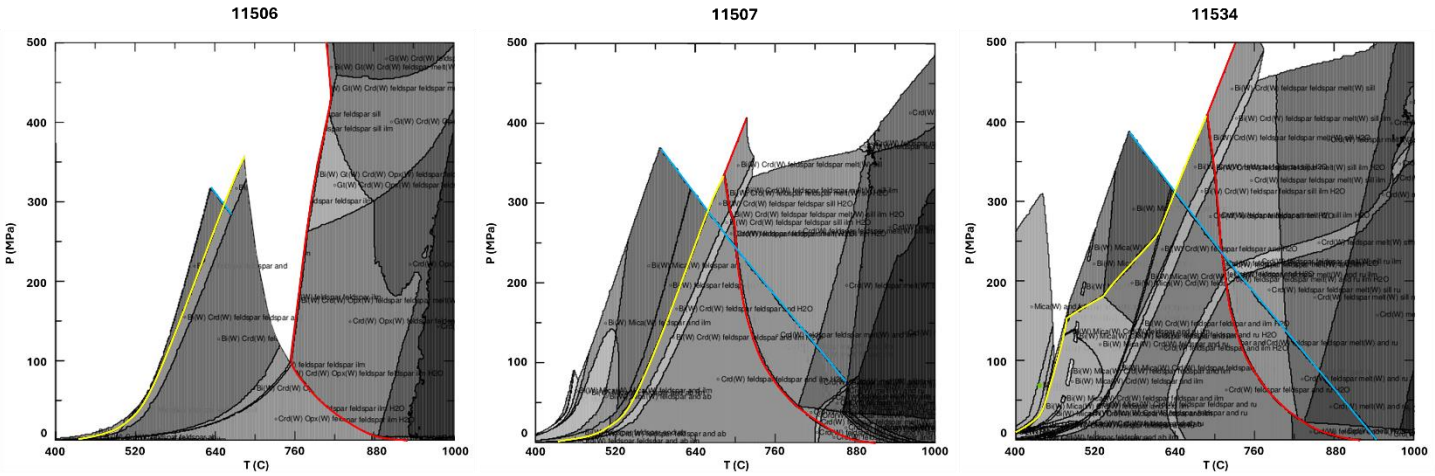

Figure A30: Perple_X P-T models for the compositions of 11506, 11507 and 11534. Yellow indicates the stability curve of Crd, blue indicates the stability curve of And and red indicates the melting curve (solidus). The stability field text is to be disregarded.

Appendix B, Numerical Data

Minerals per thin section (wt.%)		Qz	Pl	Bt	And or Sil	Opq	Crd or Chl	Afs	Green Bt	Domain wt. %
11506	**Mesosome**	6.11 %	7.41 %	5.70 %	0.73 %	1.03 %		4.77 %		25.62 %
	Melanosome	0.97 %		3.07 %	3.78 %	4.65 %	10.38 %		9.03 %	34.68 %
	Leucosome	3.85 %	6.27 %			0.72 %		31.55 %		39.70 %
	Total	**10.92 %**	**13.68 %**	**8.76 %**	**4.51 %**	**6.39 %**	**10.38 %**	**36.33 %**	**9.03 %**	
11507	**Mesosome**	0.88 %	3.15 %	1.91 %	0.10 %	0.34 %		2.03 %		8.41 %
	Melanosome	8.60 %		8.02 %	18.70 %	4.95 %	8.36 %		7.74 %	59.51 %
	Leucosome	10.06 %	7.32 %			0.59 %		17.25 %		32.32 %
	Total	**19.54 %**	**10.47 %**	**9.94 %**	**18.79 %**	**5.88 %**	**8.36 %**	**19.28 %**	**7.74 %**	
11534	**Melanosome**	11.26 %		12.23 %	22.50 %				12.23 %	61.52 %
	Leucosome	14.11 %	8.52 %					19.15 %		38.48 %
	Total	**25.37 %**	**8.52 %**	**12.23 %**	**22.50 %**			**19.15 %**	**12.23 %**	

Table B1: Mineral abundances of the group 1 thin sections in weight percent.

	wt.%	SiO_2	TiO_2	Al_2O_3	FeO	MnO	MgO	CaO	Na_2O	K_2O	P_2O_5	Cl	F	SO_3	BaO	SrO	ZnO	H_2O
11506	Plg meso	60.15	0.03	24.71	0.03	0.02	0.01	6.14	7.98	0.23	0.12	0.00	0.11	0.01	0.01	0.11	0.09	
	Plg leu	66.79	0.02	20.10	0.04	0.01	0.01	1.52	7.55	3.87	0.18	0.04	0.09	0.00	0.00	0.10	0.07	
	Kfs meso	63.88		18.55				0.06	1.15	16.36								
	Kfs leu	63.74	0.04	18.72	0.01	0.02	0.01	0.10	2.06	14.01	0.17	0.01	0.10	0.01	0.41	0.13	0.08	
11507	Plg meso	62.77	0.04	23.37	0.05	0.00	0.00	4.49	8.62	0.24	0.12	0.00	0.06	0.01	0.05	0.09	0.07	
	Kfs meso	63.95	0.04	18.52	0.04	0.02	0.01	0.09	1.90	14.00	0.15	0.01	0.12	0.02	0.32	0.09	0.08	
	Kfs leu	63.64	0.04	18.66	0.04	0.02	0.02	0.08	2.14	13.67	0.17	0.00	0.11	0.02	0.30	0.08	0.08	
11534	Plg leu	63.24	0.02	21.56	0.08	0.02	0.01	2.90	6.90	4.05	0.08	0.00	0.11	0.02	0.10	0.10	0.08	
	Kfs leu	63.74	0.03	18.46	0.02	0.02	0.01	0.03	0.88	15.49	0.16	0.01	0.11	0.01	0.36	0.11	0.08	
11506	Bt meso	34.39	4.03	16.54	21.18	0.07	9.81	0.04	0.08	9.91	0.03	0.81	0.47	0.05	0.15	0.03	0.11	2.29
	Bt mela	35.92	1.35	17.97	16.32	0.06	14.52	0.01	0.10	10.07	0.01	0.18	0.77	0.03	0.02	0.02	0.09	2.56
11507	Bt meso	35.17	3.55	16.53	17.76	0.06	11.15	0.00	0.11	9.78	0.02	0.58	0.80	0.07	0.14	0.03	0.11	4.15
	Bt mela	35.67	2.22	16.70	14.75	0.06	13.86	0.01	0.10	9.59	0.03	0.20	1.04	0.07	0.08	0.01	0.08	5.55
11534	Bt mela	35.19	1.21	18.06	17.91	0.07	11.46	0.01	0.07	9.83	0.01	0.73	0.74	0.06	0.05	0.03	0.09	4.49
11506	Crd	47.94	0.02	33.31	7.69	0.07	9.66	0.00	0.06	0.02	0.00	0.00	0.06	0.02	0.03	0.04	0.07	1.00
11507	Chl	40.98	0.02	35.75	4.67	0.04	1.82	0.60	0.27	1.18	0.01	0.02	0.19	0.03	0.03	0.05	0.09	11.67
11506	Opq	0.54	0.07	0.33	91.57	0.03	0.05	0.00	0.00	0.02	0.01	0.00	0.01	0.01	0.00	0.02	0.11	
11507	Opq	0.05	0.11	0.20	91.82	0.03	0.05	0.00	0.04	0.03	0.00	0.00	0.01	0.02	0.02	0.00	0.11	

Table B2: Average chemical compositions of the minerals measured in weight percent.

Bulk rock	Mesosome		Melanosome			Leucosome		
Wt.%	11506	11507	11506	11507	11534	11506	11507	11534
SiO_2	60.12 %	57.69 %	33.81 %	36.18 %	39.91 %	66.09 %	72.22 %	75.07 %
Al_2O_3	17.33 %	18.34 %	28.81 %	41.15 %	43.82 %	17.13 %	14.21 %	13.48 %
K_2O	5.37 %	5.62 %	3.43 %	2.32 %	3.42 %	11.20 %	7.91 %	8.38 %
FeO	8.84 %	8.10 %	23.69 %	13.25 %	6.23 %	1.80 %	1.88 %	0.03 %
MgO	2.07 %	2.28 %	8.01 %	3.37 %	3.99 %	0.01 %	0.01 %	0.01 %
Na_2O	2.59 %	3.88 %	0.05 %	0.06 %	0.02 %	2.66 %	2.57 %	1.87 %
F	0.13 %	0.22 %	0.28 %	0.26 %	0.26 %	0.09 %	0.08 %	0.08 %
CaO	1.83 %	1.74 %	0.00 %	0.07 %	0.00 %	0.30 %	0.66 %	0.62 %
TiO_2	0.86 %	0.76 %	0.48 %	0.52 %	0.42 %	0.04 %	0.02 %	0.02 %
Cl	0.17 %	0.12 %	0.06 %	0.05 %	0.25 %	0.01 %	0.00 %	0.00 %
BaO	0.04 %	0.13 %	0.02 %	0.02 %	0.02 %	0.31 %	0.18 %	0.20 %
ZnO	0.05 %	0.08 %	0.07 %	0.04 %	0.03 %	0.07 %	0.06 %	0.05 %
SrO	0.04 %	0.06 %	0.02 %	0.01 %	0.01 %	0.11 %	0.06 %	0.07 %
MnO	0.02 %	0.02 %	0.05 %	0.02 %	0.02 %	0.02 %	0.01 %	0.01 %
P_2O_5	0.04 %	0.09 %	0.01 %	0.01 %	0.00 %	0.15 %	0.10 %	0.09 %
SO_3	0.02 %	0.03 %	0.02 %	0.03 %	0.03 %	0.01 %	0.01 %	0.01 %
H_2O	0.48 %	0.85 %	1.19 %	2.65 %	1.56 %			

Table B1.3: Average chemical compositions of the domains of the group 1 thin sections in weight percent.